Comparative analysis on the methods for determination of consolidation and creep parameters using custom software

Master Thesis
Juan Antonio Rebollo Parada
MSc. in Structural and Civil Engineering
Aalborg University
-

The Faculty of Engineering and Science
Aalborg Univeristy
Niels Jernes Vej, 9220 Aalborg Øst
Phone 99 40 99 40
http://www.en.tek-nat.aau.dk

Title:

Comparative analysis on the methods for determination of consolidation and creep parameters using custom software

Project period:

September 2017 - June 2018

Author:

Juan Antonio Rebollo Parada

Supervisors:

Lars Bo Ibsen
Benjaminn Nordahl Nielsen

Editions:-
Report pages: -
Appendix pages: -
Completed -
Front page credit: -

Synopsis:

Study of settlement is of great importance in Denmark, which has great presence of glacial over-consolidated clays with high creep component, an element of importance on long term studies on sensitive structures. Heterogeneous methodology can make consolidation and creep analysis complex and hamper comparative analysis.

An interpretation software, named *MASCoT*, is developed to homogenize the inputs and outputs from different methods and ease the process of comparison and interpretation of parameters from multiple tests and methods.

This program is used to analyse soil data from Danish consolidation tests. Differences, particularities and limitations of the selected methods, as well as the soil samples, are studied and discussed.

Preface

Reading guide

Throughout the project references will be made to source material, which is located in the bibliography at the end of the report. Source references in the report will follow the Harvard method and appear in the text with the name of the author, organisation etc., followed by the year of publication in the form of either "[Name, Year]" or "Name [Year]" depending on the context. The literature in the bibliography is written with author, title and date.

Furthermore figures and tables in the report are numbered in accordance to the respective chapters. This means that the first figure or table in chapter 4 for instance is numbered 4.1 followed by 4.2 etc.

Juan Antonio Rebollo Parada

Table of contents

1 Introduction

Oedometer tests are one of the most relevant tests in soil mechanics since the the beginning of the 20th century. This test, introduced by Karl Terzaghi, allows the simulation of one-dimensional consolidation of soils in a laboratory environment.

Study of time-dependant settlement is of great importance in Denmark, which has great presence of glacial over-consolidated clays. These clays can also display a high component of secondary compression [Grønbech et al.], also known as creep, that can have a relevant influence on long term settlements- Secondary compression is an element of importance on studies of sensitive structures like Limfjord tunnel in Aalborg [Brinch Hansen, 1961b]. Danish geotechnical tradition takes this into account, existing several methods to assess and predict secondary compression settlements, such as Brinch Hansen method [Brinch Hansen, 1961a] and ANACONDA method [Grønbech et al.].

Traditional methodology often relies on the graphical interpretation of settlement curves, like Taylor or Casagrande methods to determine the consolidation parameters. Other methods make use of derivative parameters, studying their evolution to extrapolate information, like Becker of Janbu methods to determine pre-consolidation stress. And some require iterative algorithms and curve fitting to interpret the data, as ANACONDA does. The truth is that interpretation in settlement analysis makes use of a great number of heterogeneous tools and approaches that have evolved since the birth of the discipline to the computer era. This can make the task of interpretation and, especially, the comparison of outcomes from methods with different approaches, quite challenging and difficult to organize.

To tackle this issue, part of this thesis focus on the development of software capable of handling most of the interpretation, from the nuance of drawing tangents at the tail of a curve to determine parameters via multi variable iterative analysis. This allows to homogenize the methodology in terms of user input, reduce the subjective error, and facilitate the output comparison. Additionally, the use of this kind of software bolsters the idea that soil interpretation is an iterative process that requires a trial and error approach to the determination of parameters. By taking most of the calculation and method heterogeneity away from the user, and allowing quick and clear comparison between the outputs of said methods, this process can be greatly optimized.

The objectives of this thesis are:

- To develop a program capable of storing consolidation test laboratory data, perform all necessary analysis to obtain all consolidation parameters normally used in engineering practice and make comparative analysis between the studied tests and methods.
- Use said program to analyse a set of consolidation tests to assess the validity of the studied methods on Danish soils.
- Ascertain the limitations and difference of the methodology used in this thesis, and stablish suitability guidelines for the different methods regarding Danish soils.

This thesis starts with a literature review, assessing the theoretical basis of the methodology used for the separation of strains, consolidation parameters and calculation of pre-consolidation stress. This is done in Chapter 2.

Methodology described in the literature review has been adapted and programmed into the software *MASCoT*, developed as part of this thesis in order to ease the interpretation of the different tests. Description of *MASCoT* and the implementation of the different methods is done in Chapter 3.

The assessment of the different methods has been done using an already existing set of laboratory tests taken from Nørre Lyngby, in Nothern Jutland [Thorsen, 2006]. Chapter 4 describes the origin of these soil samples and reviews the execution of laboratory tests, performed by aalborg UniversityThorsen [2006].

All of these tests have been subjected to analysis to determine their time-dependent properties (i.e. consolidation coefficient, consolidation strains, secondary compression index) using methods from Danish tradition and more widely used methods. Additionally, several methods have been used to determine the pre-consolidation stress of this soils. Description of the analysis is covered in Chapter 5.

Finally, a comparative analysis has been performed, comparing the outcomes of different tests. Discussion on the limitations, particularities and differences between the methods is presented. This discussion covers Chapters 6 and 7 of the thesis.

Literature review 2

2.1 Introduction

This chapter explains the theoretical basis for the methods used in this thesis. Information from the original sources is summarized and presented as a reference for the rest of the thesis. This chapter is divided into two sections. First section refers to the *strain separation methods*, or methods used to study the time rate of consolidation and obtain the consolidation and creep parameters. Next section focus on the methods used to ascertain the pre-consolidation stress, σ_{pc}.

2.2 Strain separation methods

Settlements produced on a saturated soil sample under a certain load increment can be divided in three components:

- Immediate settlements.
- Consolidation settlement.
- Secondary compression settlement or "creep".

While immediate settlements are considered to occur as soon as the load increment is applied, both consolidation and secondary compression are time-dependent processes. Consolidation occurs as a consequence of the dissipation of increment of pore pressure in the soil, depending mainly on its compressibility and permeability. Secondary compression occurs due to the rearrangement of soil particles under the increment of effective pressure. To compute the total deformation, it is necessary to define the contribution of each component.

Usually the main actor of the time-dependent settlement process is the consolidation. However, secondary compression also occurs and can be rather relevant in some types of clays (e.g. Danish Eocene Clays [Grønbech et al.]). The time-strain curve for each stress step in the consolidation test shows the combined effect of consolidation and secondary compression. In order to obtain the parameters that describe both processes, it is necessary to "separate" or isolate the influence of each one on the soil strain.

Along the 20th century, multiple methods have been developed to solve this issue. The classical ones, like Casagrande or Taylor methods [Taylor, 1948] are centered around obtaining the parameters for the consolidation process. This is logical and sufficient for

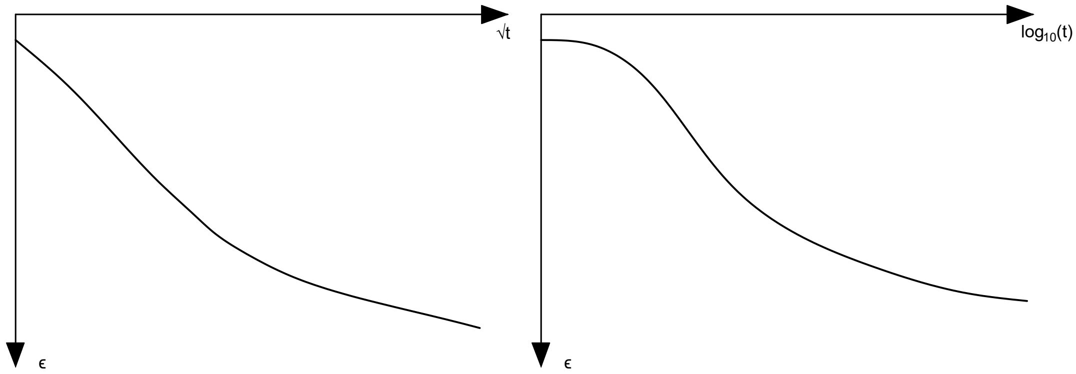

Figure 2.1. Classical $t - \epsilon$ view of a stress step in a consolidation test

most soils, being consolidation the only relevant element. This thesis also uses several methods, based on Danish geotechnical tradition, to ascertain the secondary compression parameters in soil with a relevant influence of creep.

There are several methods that allow the separation of strains, with different levels of complexity, limitations and scopes of usage. As this thesis is written following the scope of methods used in the Danish tradition, two of this methods are chosen; Brinch Hansen's method and ANACONDA method. Additionally, two classical methods for determination of consolidation parameters, such as 24 hour method and Taylor's method are included.

The main parameters studied are:

- Initial consolidation strain, ϵ_0, defined as the strain value at the start of the consolidation process.
- Consolidation strains, ϵ_{100}, defined as the amount of strains occurring between the start and the end of the consolidation process.
- Creep strains, ϵ_{cr}, defined as the amount of strains occurring between the end of consolidation and the time at the end of a given load step.
- Consolidation coefficient, c_v, defined as the average rate of consolidation of a sample under a certain load.
- Secondary compression index, C_α, defined as the rate of secondary compression of a sample under a certain load.
- Tangent modulus, M, defined as the evolution of consolidation strain over a load increment, or the slope of the stress-strain curve.

2.2.1 Taylor

Taylor's method [Taylor, 1948], also known as "square root of time" method uses a graphical approach to evaluate c_v. It works by comparing the experimental curve to the classical theory, using the square root of time as plotting scale. As seen in Figure 2.2, the time-strain curve is straight until about 60 % of the consolidation process, being possible to fit the data to a straight line (A). By using the classical Terzaghi's consolidation theory, it can be determined that the slope of a line (B) intersecting with the consolidation curve at 90 % of the consolidation process is 1.15 bigger that the slope of A.

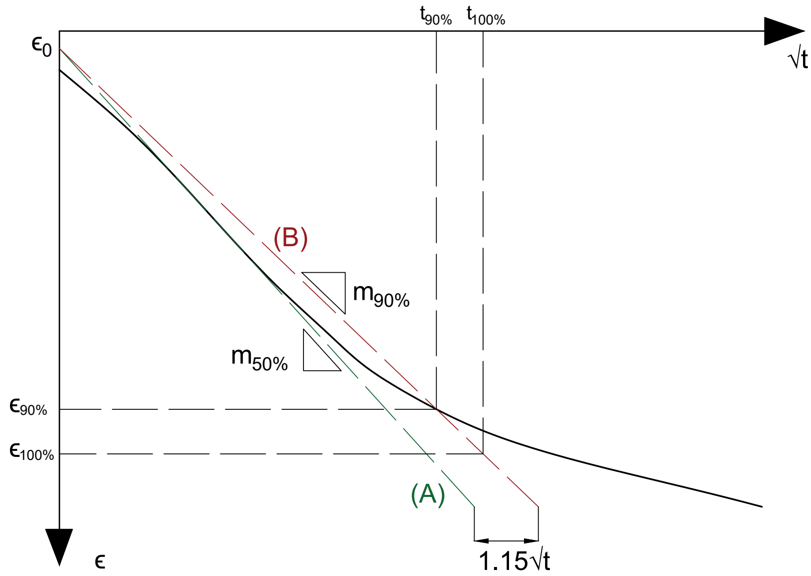

Figure 2.2. Taylor's method applied to a laboratory curve

Thus, by fitting A to the data, $\epsilon_{90\%}$ and $t_{90\%}$ can be determined from the intersection of B and the data curve. Additionally, from A the initial strain, i.e. ϵ_0 can be determined. This, and another value taken from (A), e.g. ϵ_0, t_0 can be used to extrapolate the consolidation strains and obtain the consolidation coefficient c_v.

This method's objective is to determine consolidation parameters, so it gives no insight on secondary compression parameters.

2.2.2 Brinch Hansen

Brinch Hansen's method [Brinch Hansen, 1961a] fits the strain process to an equivalent bi-linear model in a $\sqrt{t}$-$log(t)$ combined axis that describes both the consolidation and the secondary compression, being the consolidation strains at the intersection between the two lines.

Brinch Hansen created a model law describing the whole deformation process. While its derivation its outside the scope of this description, it is used as a base to stablish the bi-linear model by using the tangents to this law in certain points as the slopes for both lines. The chosen points are $t_1 = 0.1t_c$ and $t_2 = 10t_c$, being t_c the "observed time" used to divide the time scale.

By differentiating the general law in these points, the equations for both lines are obtained:

$$\epsilon_1 = \frac{\sigma}{MH_0}\sqrt{\frac{c_v t_s}{A}}\left[(A + log_{10}(e)\sqrt{\frac{t}{t_c}} - \frac{log_{10}(e)}{\sqrt{10}}\right] \tag{2.1}$$

$$\epsilon_2 = \frac{\sigma}{M} log_{10}\left(\frac{t}{t_s}\right) \tag{2.2}$$

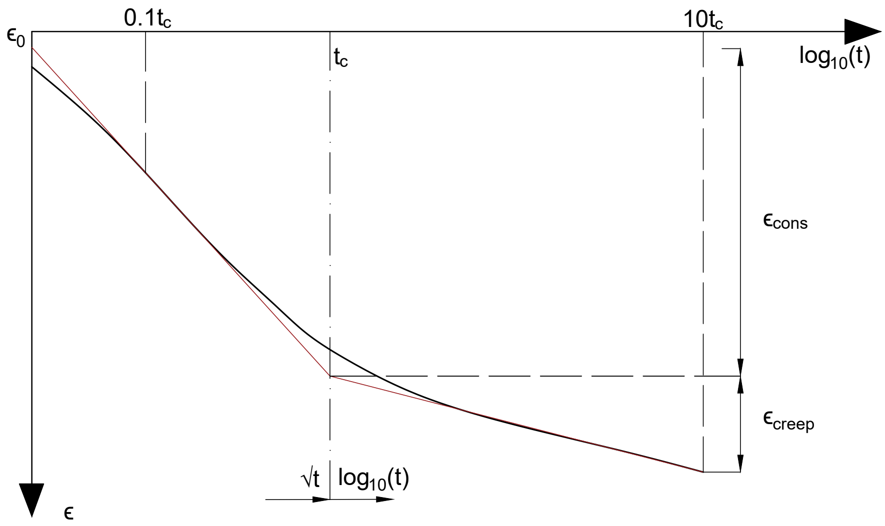

Figure 2.3. Brinch Hansen's method main parameters in $\sqrt{t}$-$log(t)$ axis

Where:

- σ is the current load.
- $A = \frac{t_c+50t_s}{50t_s}$.
- t_s is a characteristic time.
- H_0 is the initial height of the sample.

ϵ_1 and ϵ_2 must intersect when $t = t_c$. Therefore, this system can be solved by iterating t_c until convergence of ϵ_1 and ϵ_2, deriving the characteristic values from the model law.

2.2.3 ANACONDA

Traditional consolidation theory models consolidation and secondary compression processes as separated elements that occur the one after the other. ANACONDA is a method developed by Aalborg University [Grønbech et al.] that works over the assumption that both process occur simultaneously.

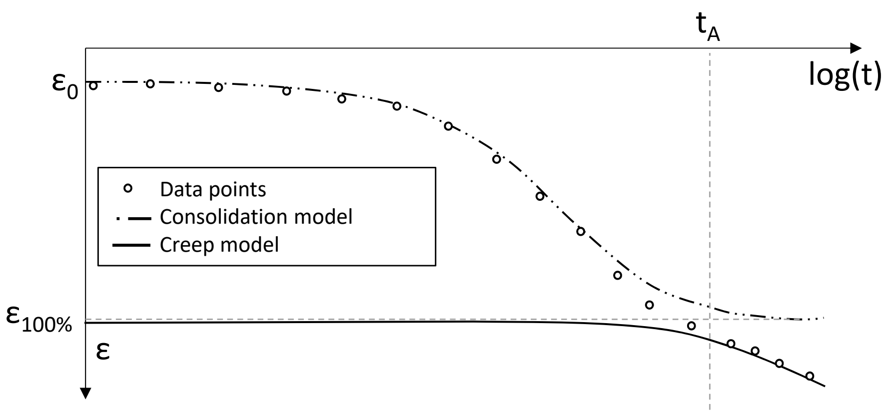

Figure 2.4. Illustration of ANACONDA method

ANACONDA method defines the stress - strain relation for the normally consolidated curve as:

$$\epsilon_{100} = C_c \cdot log\left(1 + \frac{\sigma'}{\sigma'_k}\right) \tag{2.3}$$

Where:

- C_c is the compression index.
- σ' is the effective stress for the load step.
- σ'_k is a characteristic stress.

σ'_k is assumed to be an enough small value, transforming Equation 2.3 into:

$$\epsilon_c = C_c \cdot log\left(\frac{\sigma'}{\sigma'_k}\right) \tag{2.4}$$

Secondary compression is described as:

$$\epsilon_{\alpha,c} = C_\alpha \cdot log\left(1 + \frac{t}{t_b}\right) \tag{2.5}$$

Where:

- $\epsilon_{\alpha,c}$ is the secondary compression strain.
- C_α is the secondary compression index.
- t_b is the characteristic time that governs the instant compression curve.

NOTE: ANACONDA method applies the simplification that $C_\alpha \simeq C_{\alpha,\epsilon}$, being the latest one the modified secondary compression index. Additionally, the assumption that the ratio C_α / C_C is constant [Holtz and Kovacs, 1982] is used here.

Thus, combining Equations 2.4 and 2.5 the total strain can be determined as:

$$\epsilon = C_c \cdot log\left(\frac{\sigma'}{\sigma'_k}\right) + C_\alpha \cdot log\left(1 + \frac{t}{t_b}\right) \tag{2.6}$$

This can be represented in terms of isochrones as parallel curves, being the curve formed by all the points that fulfil $\epsilon(\sigma', t_0)$ the instant compression curve, i.e. the consolidation process. All parallel curves to the instant compression curve, i.e. $\epsilon(\sigma', t = t_i)$ represent different stages of secondary compression.

This process is represented in Figure 2.5:

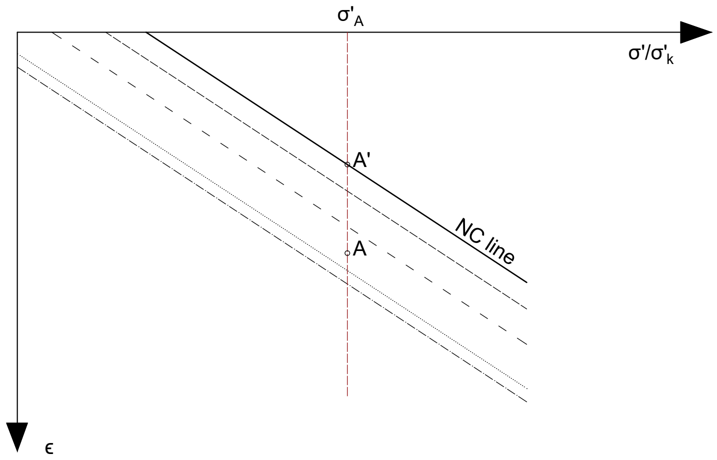

Figure 2.5. Secondary compression isochrones

Time taken by secondary compression to go from point A' in Figure 2.5 (point in which consolidation occurs) to a certain point A is given by:

$$t^* = t - t_A \tag{2.7}$$

Being t_A the time passed before the start of the secondary compression at point A'. During this time, there is an increment of strains, defined as:

$$\Delta\epsilon_{\alpha,c} = \epsilon_A - \epsilon_{A'} = C_\alpha \cdot log\left(\frac{t^* + t_A + t_b}{t_A + t_b}\right) \tag{2.8}$$

Finally, by applying the assumption that t_b is negligible in relation to t_A, 2.8 is simplified as:

$$\Delta\epsilon_{\alpha,c} = C_\alpha \cdot log\left(1 + \frac{t^*}{t_A}\right) \tag{2.9}$$

Equation 2.9 relies on the variables t_A and C_α. Thus, t_A is the time delay that transform the $\epsilon - log\,(t)$ curve into a straight line of slope C_α, as seen in Figure 2.6. Creep strains start as a null value in t_0 and increase logarithmically, tending to the asymptote formed by C_α and $(t + t_A)$.

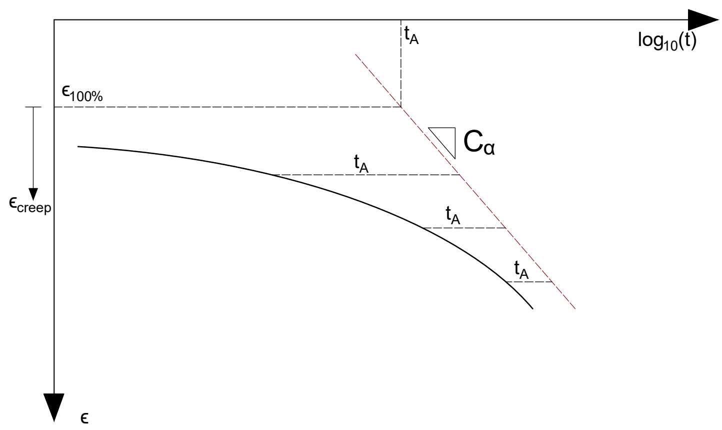

Figure 2.6. Secondary compression curve and straight line fitting

The definition of $\Delta\epsilon_{\alpha,c}$ allows to filter out the secondary compression strains, and allows the consolidation strains to converge to a constant value (i.e. $\epsilon_{100\%}$).

2.2.4 24h measurement

This method is based on the assumption that the consolidation process is usually finished after 24 hours, making this time value the usual standard for duration of consolidation test load steps [ASTM International, 2011]. From this idea, a very simplistic method can be extracted, in which the strains at 24h measurement, $\epsilon\,(t = t_{24h})$, equals the consolidation strains,ϵ_{100}. The rest of the strains, if the test is over 24h, are due to creep.

This method can not be used to obtain the consolidation coefficient, c_v, or the secondary compression index, C_α, as it does not perform an actual analysis of the consolidation curve. It can be used, however, to obtain the consolidation strains and therefore the stress-strain curve. Tangent modulus, M, can also de obtained, as it depends only on the consolidation strains of each load step.

$$M = \frac{\Delta\epsilon_{100}}{\Delta\sigma} = \frac{\Delta\epsilon\,(t = t_{24h})}{\Delta\sigma} \tag{2.10}$$

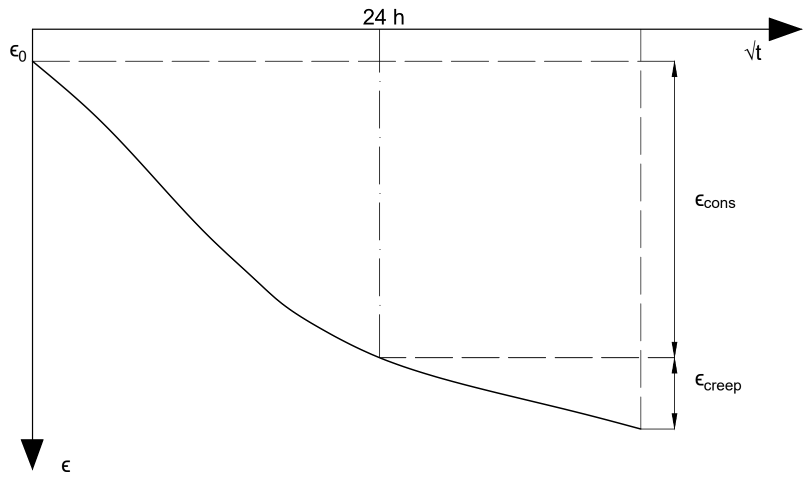

Figure 2.7. 24h method applied to a laboratory curve

2.3 Pre-consolidation stress

Pre-consolidation stress ,also known as overburden or effective yield stress (from now on σ_{pc}), is one of the most essential parameters to determine when assessing terrain settlements.

In soils that have been under higher vertical stresses in past, e.g. pre-glacial soils, σ_{pc} is the value that separates the two main soil states under constant stress; *over-consolidated (OC)* and *normally consolidated (NC)* states. Soil is considered normally consolidated if σ_{pc} equals the in-situ vertical stress σ'_v, while the soil is over-consolidated if σ'_v does not reach σ_{pc}. On a consolidation test, this can be seen in the $log_{10}(\sigma') - \epsilon$ space as a bi-linear model, with the first line corresponding to the over-consolidated state and the second, steeper line to the normally consolidated state.

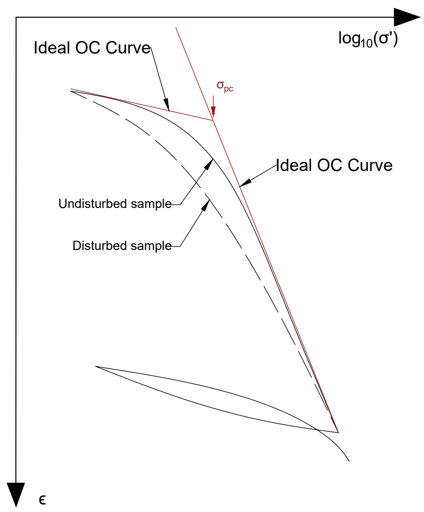

Figure 2.8. Ideal and sample consolidation curves

However, the main issue determining σ_{pc} from laboratory tests is that the border between the OC and the NC curve is usually not clear. Instead of a sharp change of slope in the $log_{10}(\sigma') - \epsilon$ relation, a softer transition appears. This is due to several reasons, being the most common the disturbance of the sample during its retrieval, or the quality of the sample itself. Another common situation is to find soils that yield gradually, or with swelling tendency. All of these situations further complicate an already difficult task.

Since the first studies on soil mechanics at the beginning of the 20th century, numerous methods have been designed to ascertain the value of σ_{pc}, being Casagrande method [Casagrande, 1936] the most famous one. However, most of these methods depend heavily on the quality of the sample and the engineer's interpretation. Therefore, the outcome is usually a range of "probable" σ_{pc} rather than a determinant value.

This situation gets exacerbated by the limitations of each method. Some methods like Casagrane or Pacheco-Silva, are empirical, graphical methods that rely on the ability of the engineer to discern elements like the point of maximum curvature (Casagrande) or the end straight line (Casagrande, Pacheco-Silva) in a curve usually drawn by hand and not assimilable to a theoretical curve. Other methods, e.g. Janbu, Akai, Becker, make use of derivative magnitudes (Tangent modulus, secondary compression index, strain work) to make more objective and unbiased analysis. Still, all of these methods also rely on graphical observation at some point, and are equally subjected to indetermination if the parameter does not adjust ideally to the proposed method [Boone, 2010].

So far, as these methods are the best and only tools to be used by the geotechnical engineer, the best procedure seems to be comparing a set of different methods to discard outliers and find the most "concordant" value. This is the tool that $MASCoT$ offers.

This program collects some of the most popular methods used in the branch, providing computational and graphical support, giving the engineer the possibility of easily obtain and compare the different interpretations. In this section, a brief theoretical definition of the used methods is provided, as well as indications of how the program handles the calculations and graphical solutions. These are the proposed methods included:

- Janbu (1969)
- Akai (1960)
- Pacheco Silva (1970)
- Becker (1987)

- Jacobsen (1992)

The main absent method is the original Casagrande construction. This is due to the fact that this method relies in the concept of maximum curvature to work, as well as the assumption that the $log_{10}(\sigma) - \epsilon$ curve is continuous and soft. This can not possibly be assured with a finite set of data and no mathematical description of the $log_{10}(\sigma) - \epsilon$ curve. In traditional engineering this curve is done by hand and the maximum curvature evaluated by visual observation. As the focus of this thesis is to obtain σ_{pc} with the help of computer software, a decision was made to not to consider a method that relies so heavily on drawing ability and visual inspection.

2.3.1 Janbu

Janbu's method [Janbu, 1963] determines σ_{pc} by comparing the changes in constrained modulus, i.e. M with the applied stress σ in a linear scale. This method is based on the idea that over-consolidated clays suffer a change or collapse on the grain structure when σ_{pc} is reached. This situation produces a stiffness change that is analysed in terms of M.

Constrained modulus is defined as:

$$M = \frac{\delta\sigma}{\delta\epsilon} \tag{2.11}$$

As seen in Figure 2.9, M has relatively large and constant values in the range of low effective stresses (specially in over-consolidated soils), as the deformation produced is small. As σ increases and enters the range of σ_{pc} there is a sudden decrease on M, reaching its minimum. Finally, as the sample approaches the normally consolidated state and tends to follow the line defined by the compression index C_c, the constrained modulus tends to the asymptote m, defined as:

$$m = \frac{log(10)}{C_c}\sigma \tag{2.12}$$

Commonly, σ_{pc} is assumed to be around the minimum value of M. The value around the middle of the decreasing line (i.e. M_1) can be also considered as a safe value of σ_{pc}.

2.3.2 Akai

Akai's method [Akai, 1960] bases the determination of σ_{pc} on how the secondary compression strains ϵ_{cr} develop as the applied stress increases. Secondary compression process increases gradually in the over-consolidated region of the test, tending to stabilize as the sample reaches the normally consolidated state. This can be expressed in terms of the secondary compression index, C_α:

$$C_\alpha = \frac{\Delta e}{\Delta log_{10}(t)} \tag{2.13}$$

Where Δe is the increment of void ratio during the secondary compression process and Δt the increment of time corresponding to $\Delta\epsilon$.

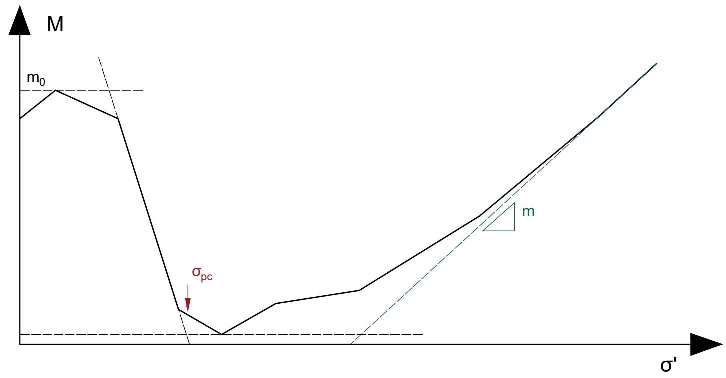

Figure 2.9. Janbu's method applied on a generic $M - \sigma$ relation

As shown in Figure 2.10, σ_{pc} can be found in the stress point where the curve starts to stabilize and flatten.

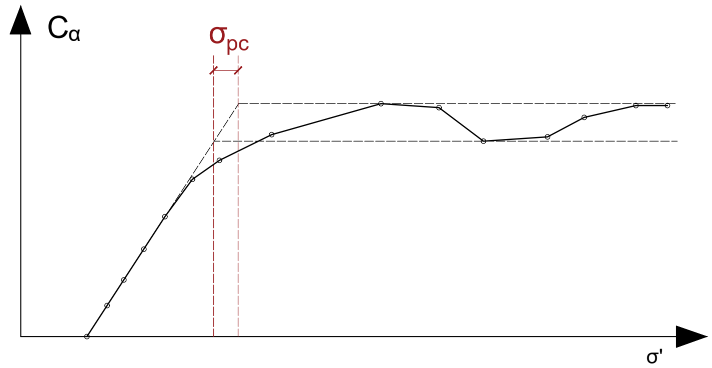

Figure 2.10. Akai's method showing the $C_\alpha - \sigma'$ relation

2.3.3 Pacheco Silva

This method [Pacheco Silva, 1970] determines σ_{pc} in a graphical way, using an empirical construction in the $log(\sigma') - \epsilon$ curve. The method, illustrated in Figure 2.11, works as follows:

1. Draw a horizontal line ($A\breve{}B$) at the initial void ratio (i.e. $\epsilon = 0$) of the sample.
2. Extend the straight line portion of the normal consolidation curve ($C\breve{}D$) until the intersection with $A - B$.
3. Draw a vertical line from the intersection of $A\breve{}B$ and $C\breve{}D$ until it reaches the curve $log(\sigma') - \epsilon$ at the point E.
4. From E, draw a horizontal line until it intersects with $C\breve{}D$ line at F.

The intersection point , F gives the value of σ_{pc}.

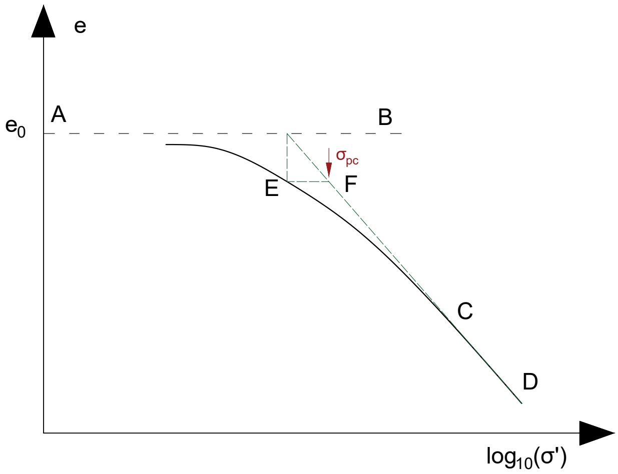

Figure 2.11. Pacheco Silva method applied to a $log(\sigma') - \epsilon$ curve.

2.3.4 Becker

Becker [Becker et al., 1987] uses the concept of work increment to locate σ_{pc}. Work produced by an increment of stress over a material is defined as:

$$W = \int \sum (\sigma_i d\epsilon_i) \tag{2.14}$$

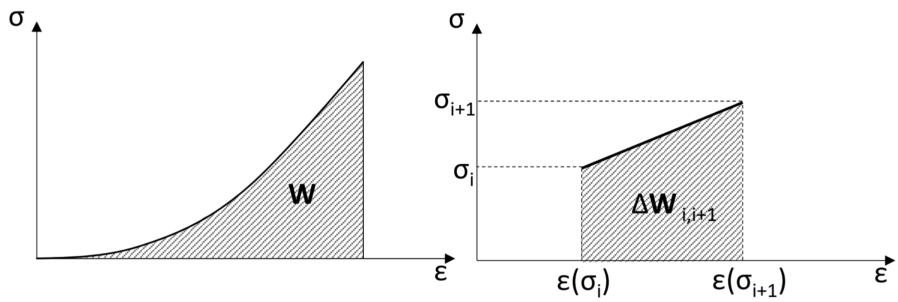

Figure 2.12. Becker's method showing graphical definition of work (left) and work increment for a discrete data set (right).

As the stress-strain relation in soils is non-linear, the only way to describe is through their incremental relation, which holds the linearity. Additionally, work applied to soils is produced by the effective term of the stresses. Finally, as lateral strains are considered null in an oedometer test. Applying these concepts the incremental relation 2.15 for the stress steps $i, i+1$ can be found:

$$\Delta W_{i,i+1} = \left[\frac{\sigma'_i + \sigma'_{i+1}}{2}\right] (\epsilon_{i+1} - \epsilon_i) \tag{2.15}$$

Where σ_i and σ_{i+1} are the effective stress at the end of the steps $i, i+1$, and ϵ_i and ϵ_{i+1} are incremented natural strains.

Interpretation of σ_{pc} comes from the comparison of cumulated work W with σ'. W is redefined as the cumulation of 2.15:

$$W_{i+1} = W_i + \Delta W_{i,i+1} \tag{2.16}$$

As seen in Figure 2.13(b) the relation $W - \sigma'$ shows two different branches with a clear linear behaviour. The first branch corresponds to the over-consolidated region of the test, while the second corresponds to the plastic or normally consolidated region. If these two groups of points are fitted to the corresponding regression lines (defined as pre-yield and post-yield lines), σ_{pc} can be found in their intersection.

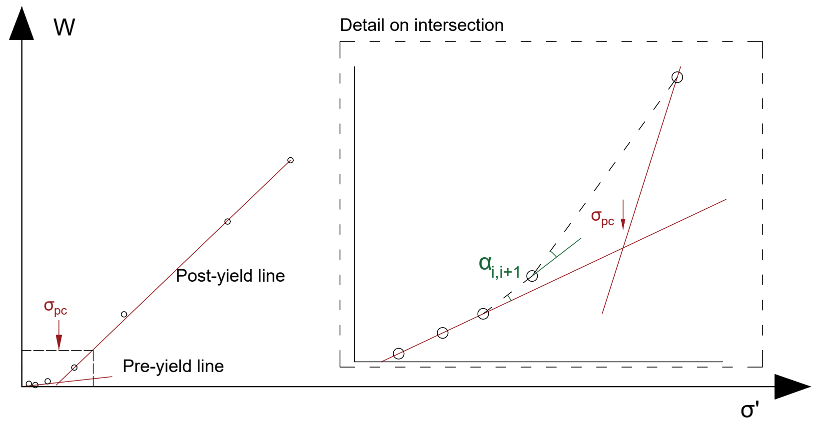

Figure 2.13. Becker's method showing (*a*) stress - void ratio relationship and (*b*) work interpretation

2.3.5 Jacobsen

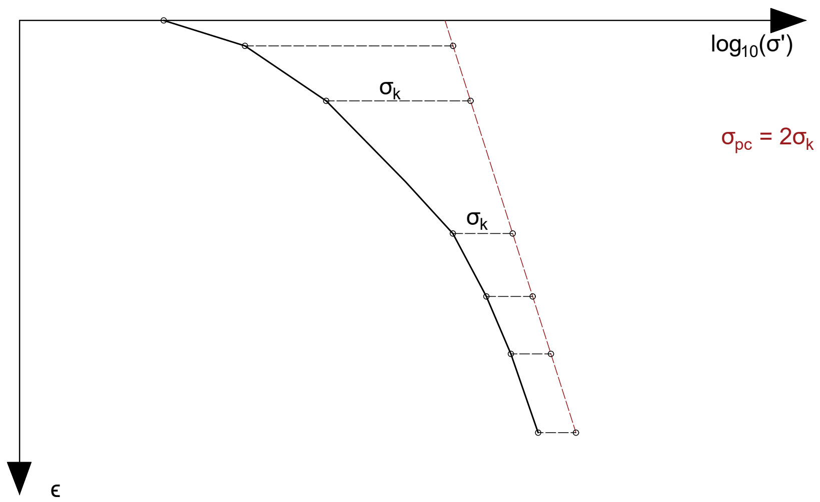

Figure 2.14. Jacobsen's method showing the fitting line for $\sigma' + \sigma_\kappa$

Determination of σ_{pc} is based on the concept of σ_κ. As seen in Figure 2.14,σ_κ is the value that transforms the laboratory data curve in the $log(\sigma') - \epsilon$ space into the ideal virgin compression line. Virgin compression line is defined in the stress-strain chart as:

$$\epsilon = \epsilon_0 + C_{c,\epsilon} \cdot log_{10}\left(\frac{\sigma}{\sigma_\kappa}\right) \tag{2.17}$$

Resolution of Equation 2.17 can be achieved by a least-square fitting optimization of the $log(\sigma+\sigma_\kappa)-\epsilon$ relation. According to [Jacobsen, 1992], fitting should ignore the first points of the data curve, as including them leads to excessively high values of σ_κ.

Once this value is optimized, σ_{pc} is given by [Jacobsen, 1992] as:

$$\sigma_{pc} = 2 \cdot \sigma_\kappa \tag{2.18}$$

3 Software development: *MASCoT*

This chapter describes the software created for this thesis, explaining its basis, objectives and behaviour.

3.1 Introduction

MASCoT stand for *Multi-Analysis Software for Consolidation Tests*. The idea behind *MASCoT* is to provide with a tool capable of both organize a database of consolidation tests and perform multiple analysis on them. This helps to treat each test not as an individual element, but as a part of a group of elements to which it can be compared. Additionally, one of the objectives of *MASCoT* is to allow an easy cross-comparison of multiple interpretation method. This seems essential in a science branch so influenced by subjective interpretation such as soil mechanics. As soils are highly varying, heterogeneous materials, it seems unrealistic to expect that any interpretation methodology can give accurate, mathematical solutions when confronted to completely different soil types, different environments, or even different testing qualities.

In this situation, the most reasonable strategy seems to obtain outcomes from different methods, acknowledge the basis and limitations of each one, and make use of engineering judgement to decide the most probable solution. The objective of creating *MASCoT* is precisely to ease this task by providing all the necessary tools for storage, interpretation and visualization of the raw data and the outcomes from each interpretation.

3.2 On the structure of the program

MASCoT is designed to deal with the necessary steps to obtain all relevant information from raw data in the same user environment.

The program is organized as shown in Figure 3.2. This structure follows the usual procedure to calculate the consolidation parameters in common practice. As each step relies directly on the data obtained from the previous one, the calculation process becomes a linear, one-way path.

As there are different method to solve both the strain separation analysis and the pre-consolidation stress calculation, the program allows the user to calculate all pre-

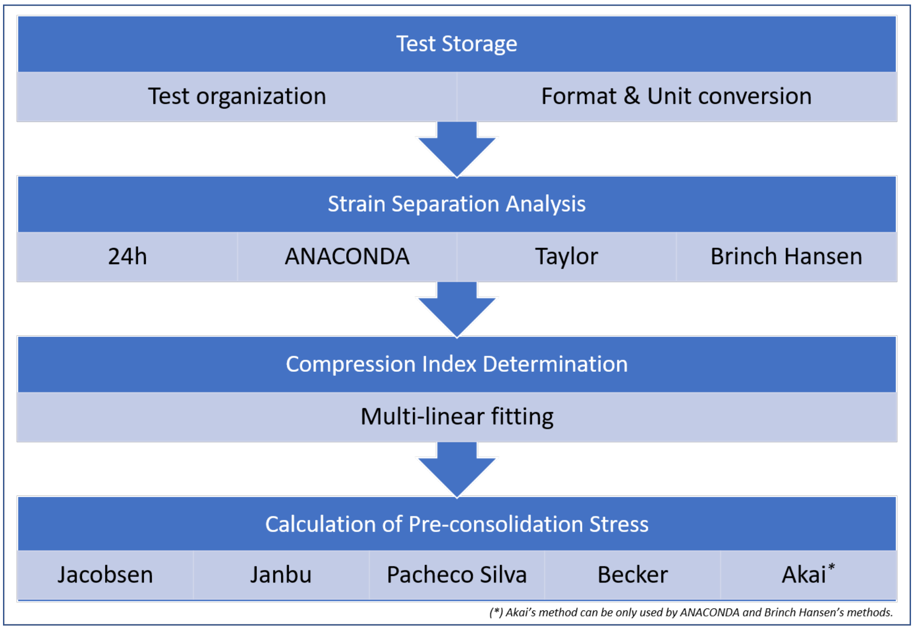

Figure 3.1. *MASCoT* calculation structure

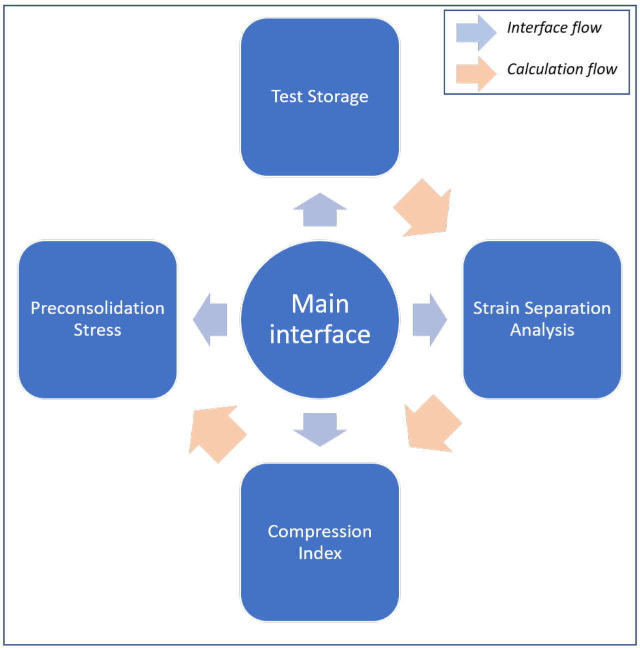

Figure 3.2. *MASCoT* interface structure overlayed and calculation flow

consolidation stress methods for any calculated strain separation method. This means a total of 18 possible values for σ_{pc} for any given test. This feature allows the user to compare results and perform a cross-validation of σ_{pc}, locating and disregarding outliers.

In terms of user interface, the program is organized around a main window that shows all tests and available information. Additionally, the main window serves as a base from which open any method's manager, and store the original data.

3.3 The main window

The user interface of *MASCoT* revolves around its main window, shown in Figure 3.3. This window redirects the user to all the individual analysis tools, besides showing the output obtained for each test at any point of the calculation process.

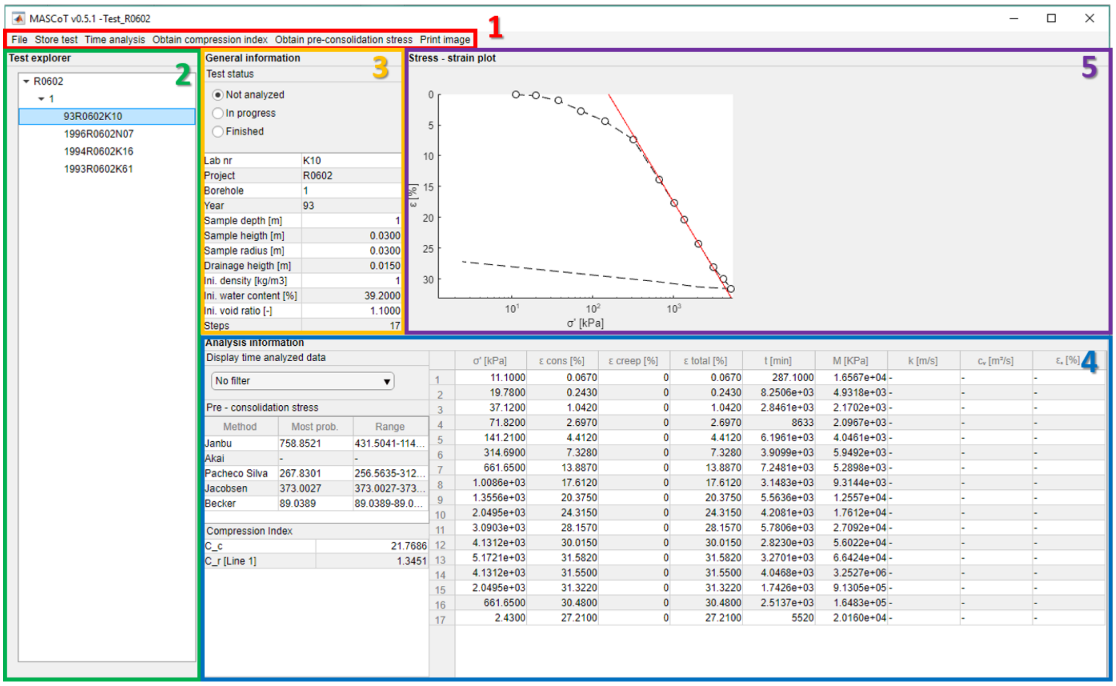

Figure 3.3. *MASCoT* main window displaying: (1) Ribbon options, (2) Test explorer, (3) General information, (4) Analysis information, (5) Graphical information

From this interface the user can create and load test databases, store or edit consolidation tests, and perform all necessary analysis; while being able to compare all information and calculated parameters between the tests.

3.4 Strain separation analysis

3.4.1 Brinch Hansen

Model implementation

While Brinch Hansen original method recommends to fit the two lines to the tangents of $0.1t_c$ and $10t_c$, *MASCoT* allows the user to choose the points to fit the model. This way, the user can avoid or minimize issues such as noise, local errors in measurements, abnormal strain-stress relations, etc.

The linear equations defining the model are:

$$\epsilon_1(t) = m_1 \cdot \sqrt{\frac{t}{t_s}} + n_1 \tag{3.1}$$

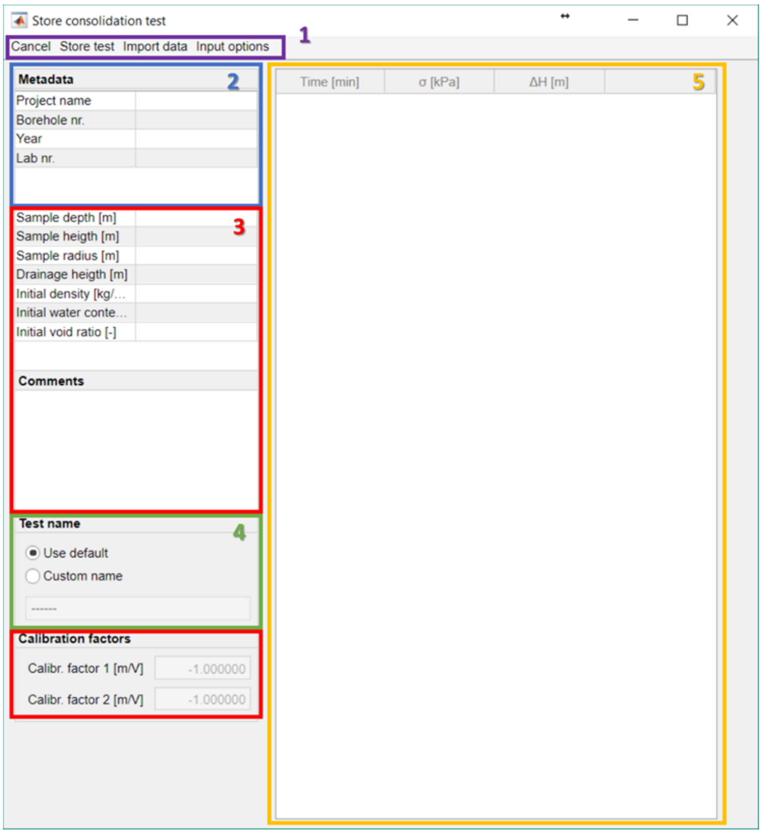

Figure 3.4. Consolidation test storage manager displaying: (1) Ribbon options, (2) Metadata (Indexing), (3) Metadata (Parameters), (4) Test name, (5) Test data

$$\epsilon_2(t) = m_2 \cdot log\left(\frac{t}{t_c}\right) + n_2 \tag{3.2}$$

Where:

- m_1 and m_2 are the slopes of the first and second fit lines.
- n_1 and n_2 are the intercepts of the first and second fit lines.
- t_c is the time at the end of consolidation, i.e. at the intersection of the lines

The objective is to find a value of t_c in which the two lines intersect, i.e.

$$E = \epsilon_1(t = t_c) - \epsilon_2(t = t_c) = 0 \tag{3.3}$$

The main issue, however, is that m_1, m_2, n_1 and n_2 are not constants but values depending of t_c. This is solved with an iterative process. Starting from an initial value, $t_{c,i=0}$, the parameters are refitted to the data points by each i step and the following calculations are performed:

$$\epsilon_1(t, t_{c,i}) = m_{1,i} \cdot \sqrt{\frac{t}{t_{c,i}}} + n_{1,i} \tag{3.4}$$

$$\epsilon_2(t, t_{s,i}) = m_{2,i} \cdot log\left(\frac{t}{t_{c,i}}\right) + n_{2,i} \tag{3.5}$$

$$E = \epsilon_1(t = t_{c,i}) - \epsilon_2(t = t_{c,i}) \tag{3.6}$$

$$t_{c,i+1} = t_{c,i} \cdot \left(1 - \frac{E}{m_{1,i}}\right) \tag{3.7}$$

Finally (usually after no more than 5-10 steps) t_c converges to a constant value.

Parameter calculation

According to Brinch Hansen model, strain parameters are defined from the bi-linear model created. This implies that the initial strain, understood as the strain at the start of the consolidation process is defined in terms of the first line:

$$\epsilon_{0,model} = \epsilon_1(t = 0) = n_1 \tag{3.8}$$

The consolidation strain can be also defined as the value at the end of the consolidation process, this is, the end of the first line. This occurs at $T = 1$:

$$\epsilon_{100\%,model} = \epsilon_1(t = t_c) = m_1 - n_1 \tag{3.9}$$

The increment of creep strains during this step comes directly from the previous equations as the value at the end of the whole process, i.e. the second line, minus the consolidation strain:

$$\epsilon_{creep,model} = \epsilon_2(t = t_{max}) - \epsilon_2(t = t_c) \tag{3.10}$$

Consolidation coefficient is considered as:

$$c_v = 0.2 \cdot \frac{H_D^2}{t_{50\%}} \tag{3.11}$$

Where:

- H_D is the drainage path.
- $t_{50\%}$ is the time when half of the consolidation process occurs.

Secondary compression index is obtained directly as the slope of the second fit line. As the calculations are performed in strains, the modified secondary compression index can be defined as:

$$C_{\alpha,\epsilon} = m_2 \tag{3.12}$$

And the secondary compression index:

$$C_\alpha = (1 + e_0) \cdot C_{\alpha,\epsilon} \tag{3.13}$$

User input

When selecting the *Brinch Hansen* option in the main window, the user access to the manager, as seen in Figure 3.5. This window is divided in several sections, including an input section, a numeric output and several graphic windows.

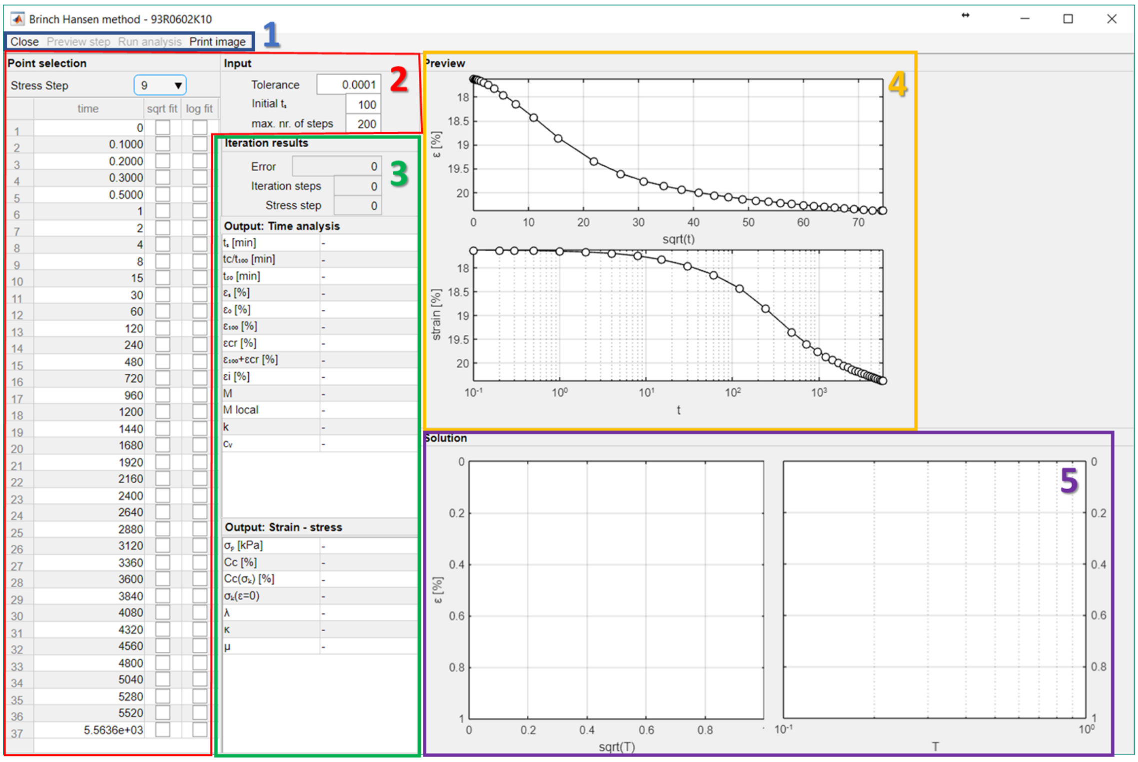

Figure 3.5. Brinch Hansen method manager

The user can assign each of the time points as fitting points to any of the two lines of the model (labelled as $\sqrt{t}$ and $log(t)$). When a point is chosen, the preview graphs update and, if the requirements are met, the calculation options are enabled. In order to be used, this option requires enough data points to fit the bi-lineal model. The minimum amount is two points per column, requisite to generate each line. More points can be used in order to refine the adjustment.

3.4.2 ANACONDA

Model implementation

The model uses as a main input a number of filtering data points to be considered in order to filter the secondary compression strains. Then, t_A and C_α are determined through an iterative process.

First, an initial value of t_A is estimated, Equation 2.9 is fitted to the filtering data points, obtaining a value of C_α and a set of $\Delta\epsilon_{\alpha,c}$ points. This allows to obtain the $\epsilon_{100\%}$ for the filtering data points. $\epsilon_{100\%}$ is fitted to a straight line and its slope is evaluated. The objective is to obtain the minimum possible slope, which means the convergence of $\epsilon_{100\%}$. Thus, depending on this output, t_A is corrected until the slope minimum slope is found.

ANACONDA method does not give an insight to obtain a modelled value of ϵ_0. This means that the procedure relays on obtaining the value externally. *MASCoT* allows several options to overcome this.

- The user can apply the first data point as ϵ_0. This option is only recommended in cases that show low or none elastic deformation, as ϵ_0 is associated to the beginning of the consolidation process only.
- A value from Brinch Hansen method can be imported. This is the most reliable solution, as Brinch Hansen method already separates the consolidation process from the instant compression. However, using this option undermines the independence of the ANACONDA method, as its validity relies on the quality of Brinch Hansen's solution.
- Finally, the user can input a custom value, according to engineering judgement.

Parameter calculation

$$\epsilon_{100\%} = \frac{\sum_{i=1}^{n} \epsilon_{cons,i}}{n} \tag{3.14}$$

Where n the number of filtering data points.

$$\epsilon_{creep} = \Delta\epsilon_{\alpha,c}(t = t_{max}) \tag{3.15}$$

Consolidation coefficient

c_v is calculated according to Equation 3.11. However, this equation required the calculation of t_s to be solved. This is obtained by using the definition of degree of consolidation, U. U is given by:

$$U^{-6} = 1 + \frac{1}{2} \cdot T^{-3} \tag{3.16}$$

In relation to T, the dimensionless time, which in turn is defined as:

$$T = \frac{c_v}{H_D^2} \cdot t \tag{3.17}$$

Applying Equation 3.11 to 3.17, U is defined in terms of t_s. Finally, the classical definition of U is applied to the filtered consolidation strains, meaning:

$$U = \frac{\epsilon(t)}{\epsilon(\inf)} \tag{3.18}$$

If this equation is discretized it can be applied to the data set as:

$$U(t = t_i) = \frac{\epsilon_{cons}(t_i) - \epsilon_0}{\epsilon_{100\%}} \tag{3.19}$$

Where ϵ_{cons} are the strains at any given point when the creep process is filtered out.

Fitting Equation 2.9 and a discretized Equation 3.19 by Least Squares gives the most optimum value of t_s. Finally, c_v is calculated according to Equation 3.11.

User input

When selecting the *ANACONDA* option in the main window, the user has access to the manager, as seen in Figure 3.6.

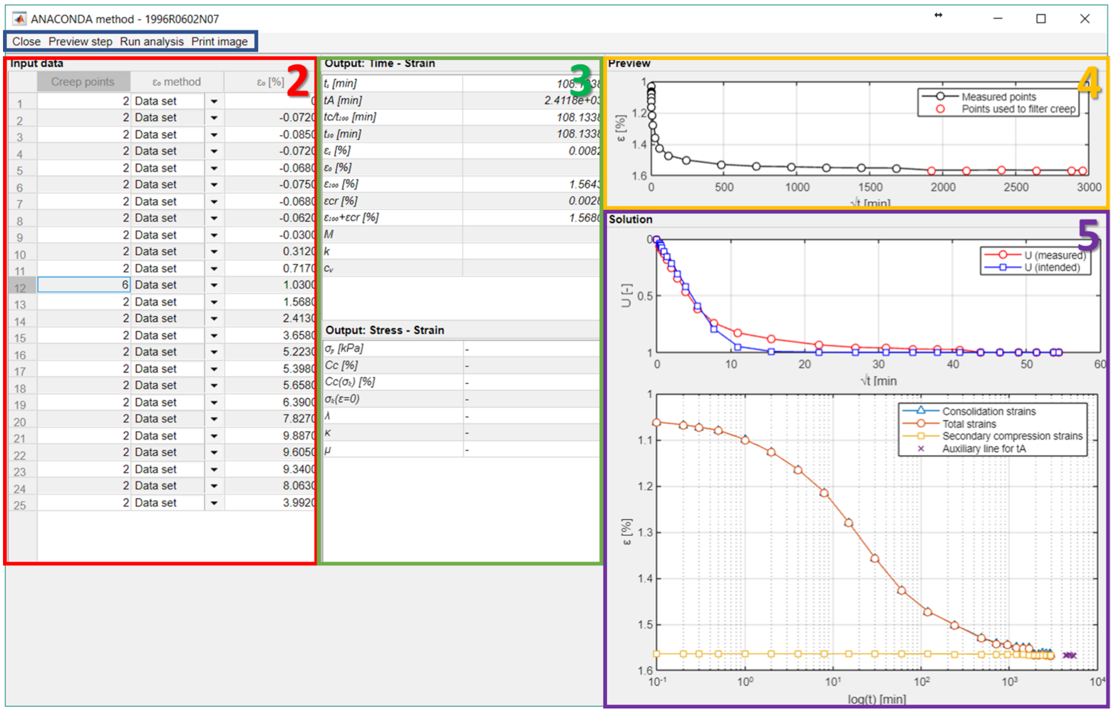

Figure 3.6. ANACONDA method manager

ANACONDA method shows all the input and graphic options in the input table. As it can be appreciated in Figure 3.6, this table is divided in 3 columns and as many rows as loading steps the test has.

- Creep points: This column allows the user to choose how many points will be considered by the user to filter out the consolidation strains.
- ϵ_0 method: This column shows the different options allowed to establish the ϵ_0 value. By default, the program chooses the first data point as ϵ_0. Additional options are a custom value and to import the value from Brinch Hansen method.
- ϵ_0: Third column shows the current value used as ϵ_0.

3.4.3 Taylor

Model implementation

Simplicity of this method makes implementation straightforward. User is required to input the fitting points to determine the line fitting the straight part of the consolidation process.

Once this is done, the slope of the straight line is calculated, leading to the auxiliary line as:

$$\epsilon_{aux} = m_{aux} \cdot \sqrt{t} + n_{aux} = \frac{m_{cons}}{1.15} \cdot \sqrt{t} + n_{cons} \tag{3.20}$$

Finally, intersection of the auxiliary line and the data curve is determined by minimizing their difference, looking for the two points with less increment of strain in respect to the auxiliary line. Then, the line generated by these two points is intersected with the auxiliary line to obtain the value corresponding to $\epsilon_{90\%}$.

As the consolidation test data is usually not precise, specially for the first load steps, there can exist several intersections with the auxiliary line in the region surrounding $t_{90\%}$. As criterion, the algorithm chooses $t_{90\%}$ as the intersection that gives the highest possible value of $\epsilon_{90\%}$.

Parameter calculation

Taylor theory uses the two known points ($\epsilon_{0\%}$ and $\epsilon_{90\%}$) as a base to obtain all consolidation parameters.

Initial deformation is defined from the linear consolidation model, as the intercept of the straight consolidation line at $t = 0$:

$$\epsilon_{0\%} = \epsilon_{cons}(t = 0) = n_{cons} \tag{3.21}$$

Where n_{cons} is the intercept of the model line.

Consolidation strain is obtained according to [Taylor, 1948], as:

$$\epsilon_{100\%} = \frac{\epsilon_{90\%} - \epsilon_{0\%}}{90} \cdot 100 \tag{3.22}$$

Taylor method does not model creep behaviour. However, considering that the deformation process is composed by initial compression, consolidation and creep, it can be concluded that:

$$\epsilon_{creep} = \epsilon_{max,data} - \epsilon_{100\%} - \epsilon_{0\%} \tag{3.23}$$

Consolidation coefficient is defined in base to the 90% consolidation point and Terzaghi's theory. From here:

$$c_v = \frac{T \cdot H_d^2}{t} = \frac{T_{90\%} \cdot H_d^2}{t_{90\%}} \tag{3.24}$$

Where T_{90}, according to Terzaghi's theory, equal to 0.848:

$$c_v = \frac{0.858 \cdot H_d^2}{t_{90\%}} \tag{3.25}$$

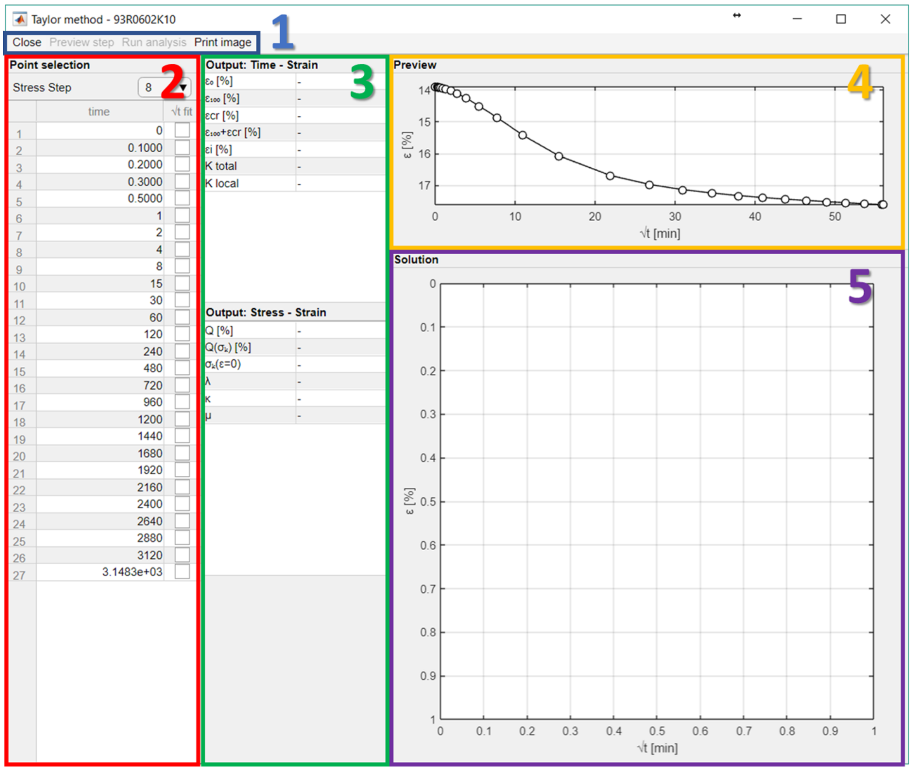

Figure 3.7. Taylor method manager

User input

When selecting the *Taylor* option in the main window, the user access to the manager, as seen in Figure 3.7:

The only input that Taylor's method needs is enough data points to establish the fitting line for the consolidation process up to 60%. This is, to adjust the fitting line to the straight section of the data in the $\sqrt{t}$ scale.

This task is left up to the user in order to avoid the influence of noise, poor measurements, outliers, etcetera.

3.4.4 24h measurement

Model implementation

Implementation of this method is direct and simple. Strain values are taken directly from the data points for each load step. Initial strain is taken as:

$$\epsilon_0 = \epsilon_{data}\left(t = 0\right) \tag{3.26}$$

Consolidation strain is:

$$\epsilon_{100} = \epsilon_{data}\left(t = 24h\right) - \epsilon_0 \tag{3.27}$$

And creep strains:

$$\epsilon_{creep} = \epsilon_{data}\left(t = t_{max}\right) - \epsilon_{100} \tag{3.28}$$

User input

Due to the simplicity of this method, no user input is required. *MASCoT* automatically calculates it when a new consolidation test is stored.

3.5 Evaluation of Compression and Reloading indexes

MASCoT allows the user to evaluate C_c and C_r in a simple and straightforward way, via the Compression Index Manager. When selecting the *Obtain compression index* option, the user will open a window like the one shown in Figure 3.8.

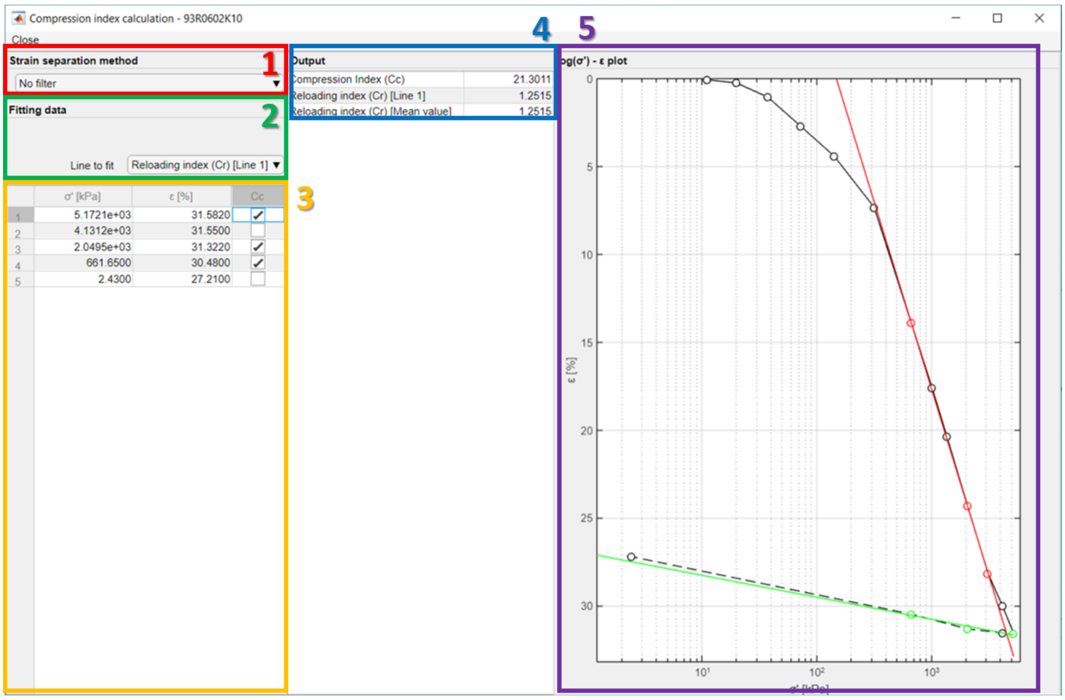

Figure 3.8. Compression Index manager

The calculation procedure is simple. The program calculates C_c and C_r as the slope of the linear fitting (in the log space) of the points decided by the user. This is done by choosing the data points corresponding to the calculated ϵ_{100} for each method. Only the points that can be possibly used are shown as data points. This means that, when calculating C_c, all unloading-reloading points are hidden and vice-versa.

MASCoT automatically calculates the number of unloading-reloading processes existing in the test, so in the event of having more than one (or none), multiple values of C_r can be obtained.

3.6 Pre-consolidation stress analysis

3.6.1 Janbu

Model implementation

Tangent modulus is defined as the variation of deformation over each load increment, in the logarithm scale:

$$M = \frac{\Delta e_{100}}{\Delta log_{10}\left(\sigma\right)} \tag{3.29}$$

Janbu's method is based upon a graphical interpretation of the tangent modulus in a $M-\sigma$ graph, looking for the minimum point before the convergence to the virgin compression line. This point is mathematically easy to find. However, M is a variable that can present a fairly amount of noise, especially in the first steps. This can make an algorithm-based interpretation more complex, with little gain over letting the user interpret the graph by pure visual inspection. For this reason, *MASCoT* relies on showing the $M-\sigma$ graph and the virgin compression line, allowing the user to choose the desired point as σ_{pc}.

User input

As the interpretation is done by pure visualization, the only option given to the user is a slider that can be used to decide the most optimal value for σ_{pc}.

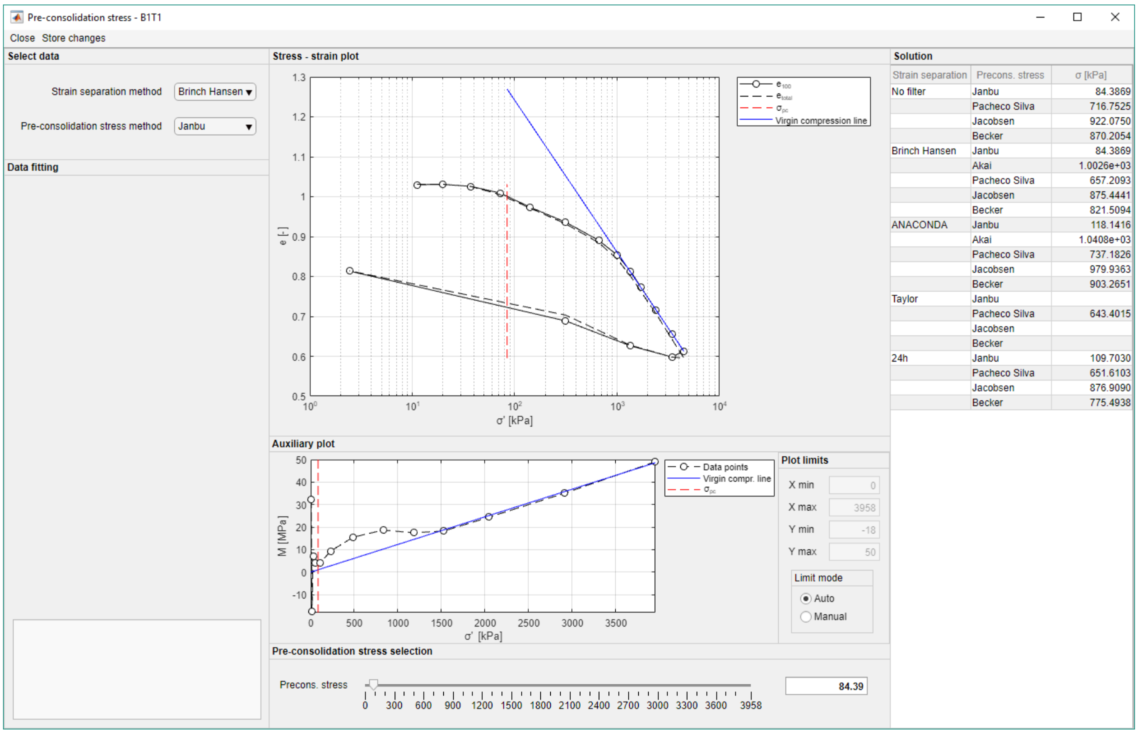

Figure 3.9. *MASCoT*'s pre-consolidation stress manager, showing Janbu's method

3.6.2 Akai

Model implementation

Akai's method is based on the interpretation of the secondary compression index:

$$C_\alpha = \frac{\Delta e_{cr}}{\Delta log_{10}\left(t\right)} \tag{3.30}$$

In a similar fashion to Janbu's, Akai's method is based on the direct, visual interpretation of the secondary compression index. However, as the objective is to find the point in which the value of C_α, interpretation of this method leads to a much larger subjective error than Janbu's.

Akai's method approximates the development of C_α to a linear increase during the over-consolidated phase and a stable value during the normally consolidated phase. *MASCoT* uses this idea by assigning data points to each phase. This is done fitting the corresponding points to a straight line, representing the linear increase; and selecting points that conform the stable, normally consolidated phase. The normally consolidated phase is defined by the maximum and minimum values of C_α assigned to it.

This way, an area can be defined, where the linear increase line intersects the lines defining the stable phase. This gives a small region where the value of σ_{pc} can be found.

User input

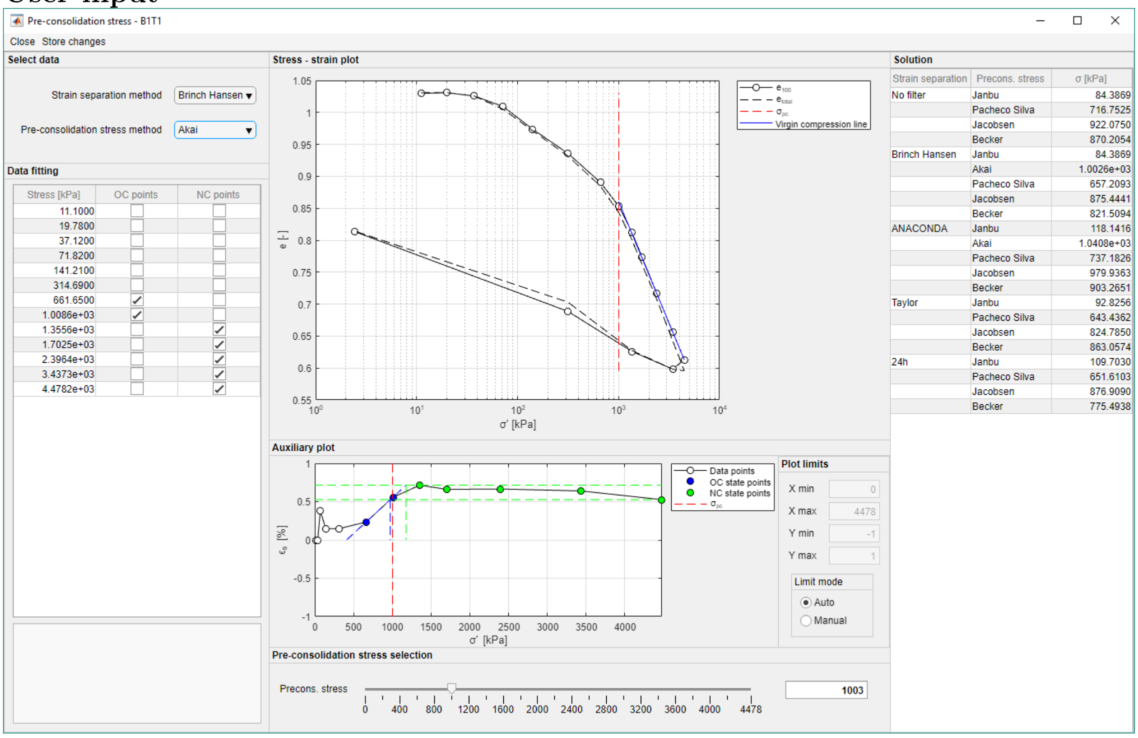

Figure 3.10. *MASCoT*'s pre-consolidation stress manager, showing Akai's method

The user can find the σ_{pc} region by assigning data points to two columns. The first column assigns points to the line that models the over-consolidated phase. The second column assign points to the stabilized normally consolidated phase. C_α on the normally consolidated phase is considered to be between the maximum and minimum values associated to the data points chosen by the user.

These inputs serve to delimit the probable σ_{pc} region. The user still needs to specify σ_{pc} using the slider found in the lower part of the screen, as seen in Figure 5.12.

3.6.3 Pacheco Silva

Model implementation

Pacheco Silva's method is based upon a purely graphical construction, taking the virgin compression line as a starting point. As this graphical construction is performed over the Casagrande construction, using one of the most stable parameters as reference, it seems fair to think that this method offers a consistent methodology for any given consolidation test. As the virgin compression line is already defined by the user in Section , this method can be fully automatized.

The value of $\sigma_p c$ is determined by solving a series of equations illustrated by Figure 3.11.

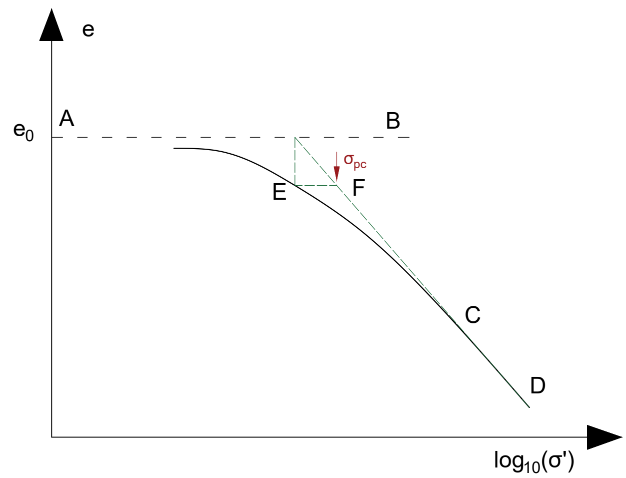

Figure 3.11. Pacheco Silva method applied to a $log(\sigma') - \epsilon$ curve.

First, the intersection of the line defined by C_c:

$$e = C_c \cdot log_{10}(\sigma) + n_{C_c} \tag{3.31}$$

And the horizontal line:

$$e = e_0 \tag{3.32}$$

Give the first intersection point and the following σ value:

$$\sigma = 10^{\frac{e_0 - n_{C_c}}{C_c}} \tag{3.33}$$

By interpolating the data set corresponding to the Casagrande construction of the consolidation test, the intersection point F can be obtained as:

$$F\left(\sigma_F = 10^{\frac{e_0 - n_{C_c}}{C_c}}, e_F = e_{data}\left(10^{\frac{e_0 - n_{C_c}}{C_c}}\right)\right) \tag{3.34}$$

Finally, σ_{pc} can be obtained from Equation 3.31 and Point F as:

$$\sigma_{pc} = 10^{\frac{e_F - n_{C_c}}{C_c}} \tag{3.35}$$

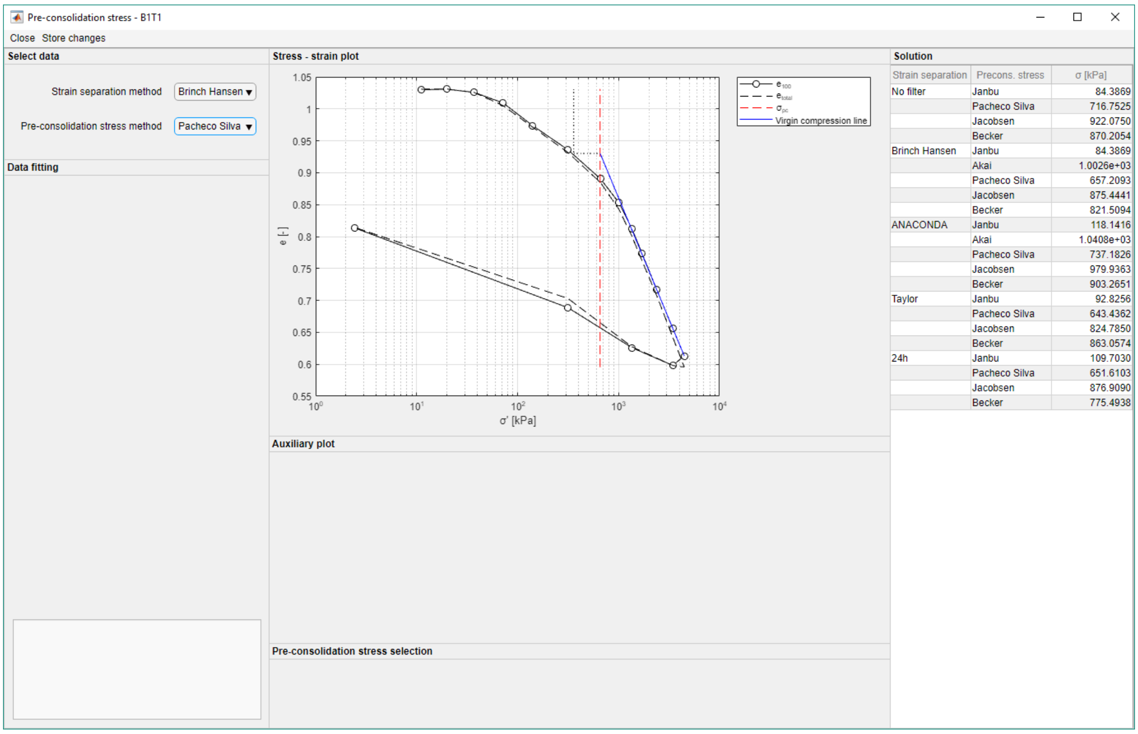

Figure 3.12. *MASCoT*'s pre-consolidation stress manager, showing Pacheco Silva's method

3.6.4 Jacobsen

Model implementation

Jacobsen's method defines σ_{pc} in terms of an added stress level, σ_κ that transforms the Casagrande construction into a straight line, in the logarithmic scale. The objective, then, is to find a σ_κ that, when added to the $\sigma - \epsilon$ data set allows a linear fitting, giving the minimum possible error.

This optimization problem is solved by *MASCoT* using a numerical iteration algorithm combined with a linear fitting via Least Square Regression. The numerical root-finding algorithm used is the bisection method. Bisection method requires two starting points, with smaller and bigger stress, (respectively σ_S and σ_B), than the objective point. This is achieved with a starting point of $\sigma_S \simeq 0$ for the smaller value and $\sigma_B >>> max(\sigma_{data})$.

User input

The algorithm used to solve Jacobsen's method is an automatized process that requires no additional intervention, in theory. However, due to multiple factors, it can occur that some stress steps do not adjust ideally to the rest of the logarithmic curve. This affects specially to points from the first steps, that are usually affected from sample crushing, swelling, sample remodelling, etcetera. These values can alter the fitting process and the resulting σ_{pc}. To help overcome this issue, *MASCoT* allows the user to choose the points to be used in the fitting process, as seen in Figure 3.13.

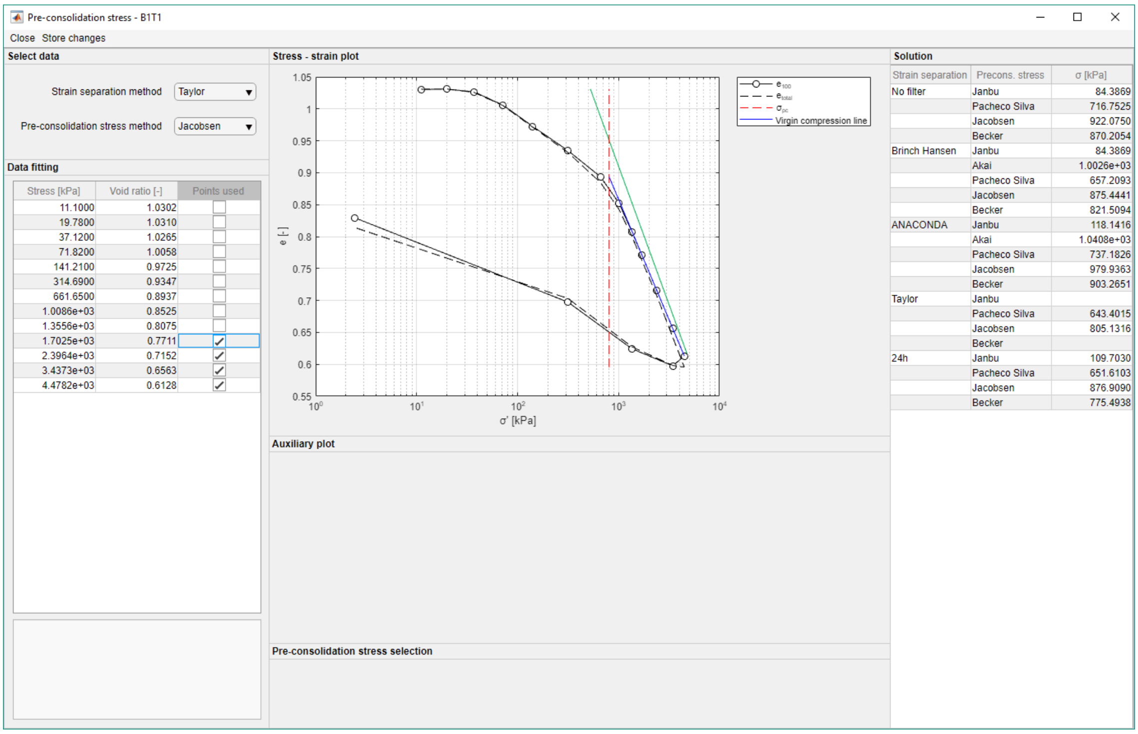

Figure 3.13. *MASCoT*'s pre-consolidation stress manager, showing Jacobsen's method

3.6.5 Becker

Model implementation

As with other methods, like Akai's or Janbu's, Becker's method obtains σ_{pc} by a graphical study of a derived parameter, in this case, the strain work. Strain work is defined for each load step i as:

$$W_{i+1} = W_i + \left[\frac{\sigma'_i + \sigma'_{i+1}}{2}\right](\epsilon_{i+1} - \epsilon_i) \tag{3.36}$$

Interpretation of this method is based upon the idea that W can be fitted into two lines, and that the pre-consolidation stress can be found in their intersection. Consequently, *MASCoT* implementation of Becker's method is limited to the selection of the points that conform each line.

This point selection can be fully automatized. If the curvature of the curve is studied, this is, $\delta^2 W/\delta\sigma^2$, it can be deduced that the point of maximum curvature is the inflexion point that separates the points belonging to each line.

However, there is still the issue of local deviations and outliers occurring in specific data points. Points that suffer sample crushing, swelling, sample remodelling, etcetera, can alter the fitting lines and deviate the resulting σ_{pc}. For this reason, *MASCoT* relies directly on engineering judgement and works by letting the user selecting the fitting points.

User input

An example of the user interface for Becker's method can be seen in Figure 3.14. The only input required is the manual selection of the points for each fitting line. To help with the interpretation, there is an auxiliary plot showing the $W - \sigma$ graph with the selected points and, if possible, the fitting lines.

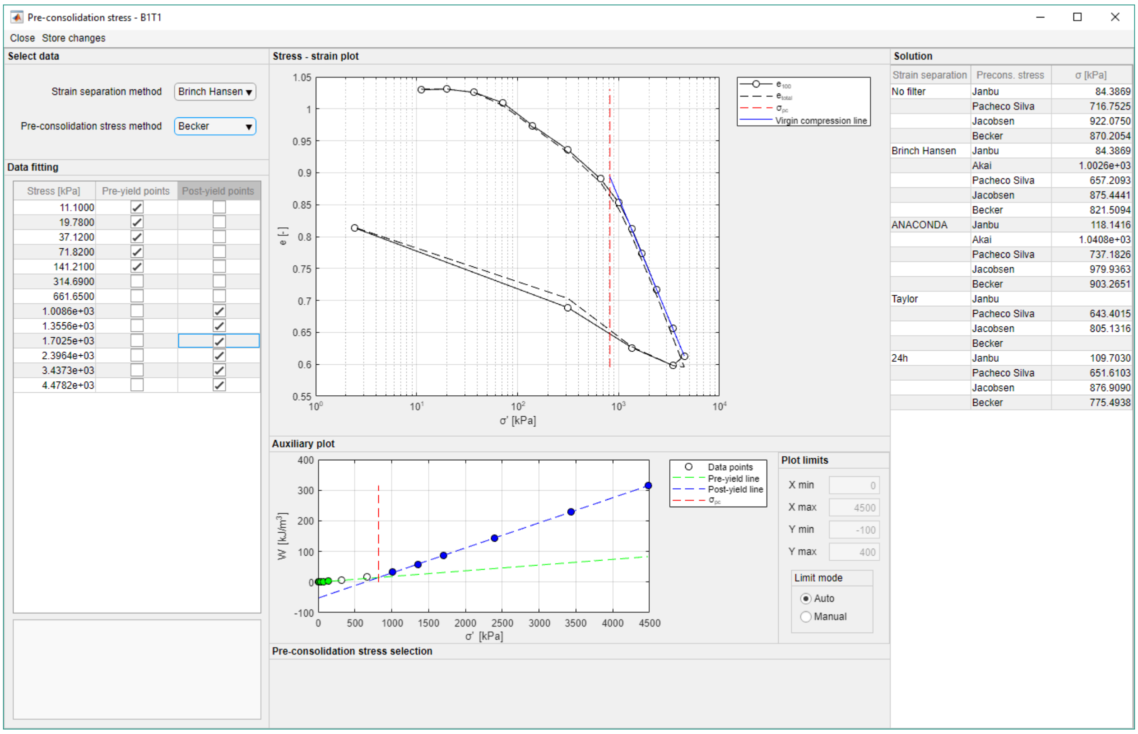

Figure 3.14. *MASCoT*'s pre-consolidation stress manager, showing Becker's method

3.7 Comparative Analysis

One of the main capabilities of *MASCoT* is the possibility to perform post-calculation comparative analysis between different tests, or compare the parameter differences between two calculation methods.

MASCoT has two different comparative analysis: The *Parameter vs Parameter* comparison (labelled as P/P), and the *Method vs Method* comparison (labelled as M/M).

3.7.1 P/P analysis

P/P analysis makes a comparison of two parameters for any given number of methods and tests. This has multiple utilities, e.g. compare different strain separation methods for a consolidation parameter depending on the load step, or study the evolution of a parameter in a certain soil with tests in different depths.

In the example in Figure 3.15, the evolution of the compression modullus, M over the load stress can be appreciated. Values of M correspond only to Brinch Hansen's method, and two different tests have been included in the analysis. Additionally, this test's unloading process is not interesting, so it has been removed from the analysis via the outlier treatment tools.

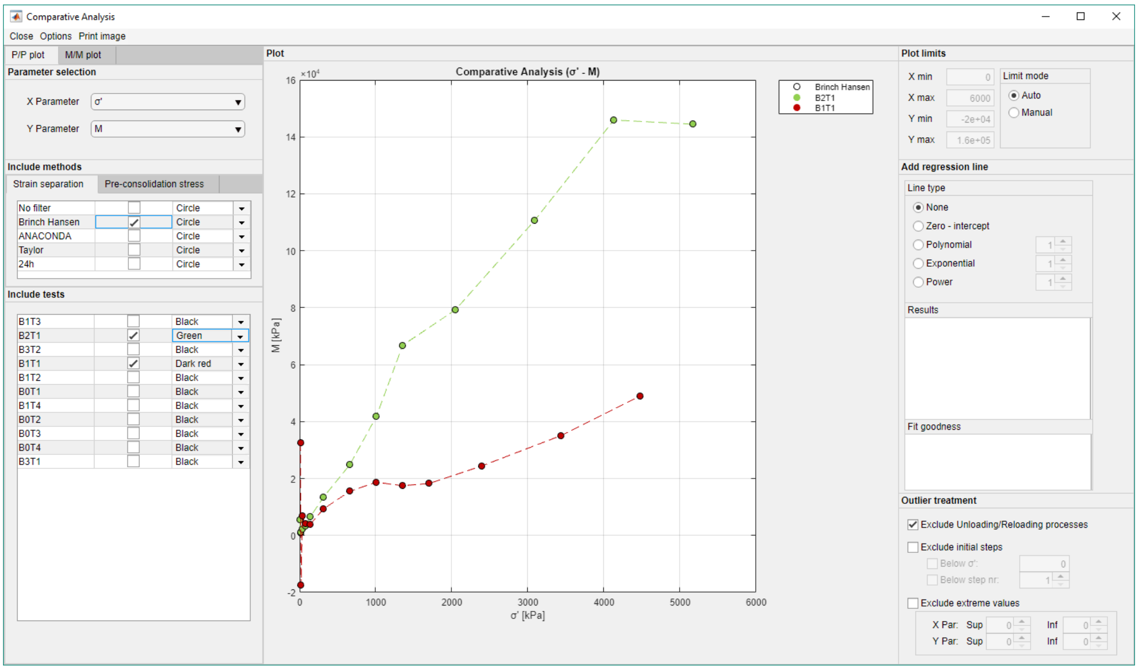

Figure 3.15. *MASCoT*'s comparative analysis tool, showing the P/P analysis options

3.7.2 M/M analysis

M/M analysis compares a parameter as the outcome from two different methods. This analysis is useful to cross-compare different methods and look for bias between the results, or study the dispersion of a parameter and its reliability.

As an example, in Figure 3.16 the parameter $C_{\alpha,\epsilon}$ is being compared for Brinch Hansen and ANACODA method for four different tests. In the graph, both the dispersion and the bias of between the methods can be appreciated.

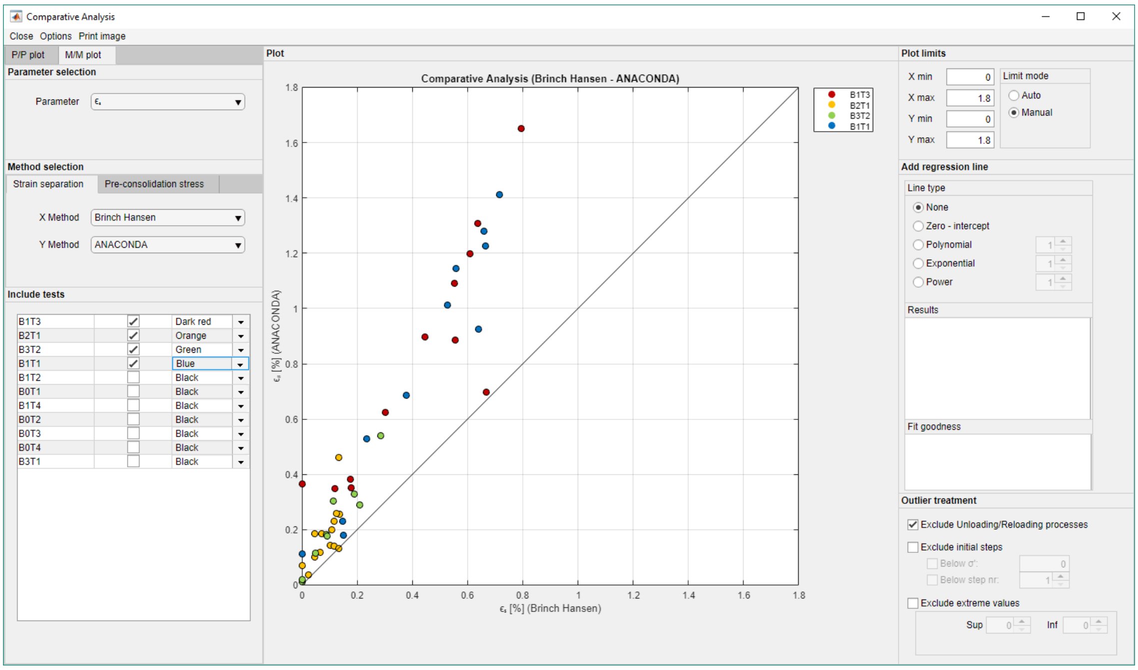

Figure 3.16. *MASCoT*'s comparative analysis tool, showing the *M/M* analysis options

Soil data 4

In this chapter, the data used in this thesis is presented. The data used comes from a geotechnical study performed by the Geotechnical Department of Aalborg University [Thorsen, 2006].

This study is based on data extracted at Nørre Lyngby (North Jutland, Denmark). The study comprised the retrieval of eleven samples from several boreholes, which were tested in oedometer test machines. The information obtained in this study serves as base data for the purpose of the present thesis.

In Sections 4.1 and 4.2 the information from [Thorsen, 2006] is summarized.

4.1 Source of soil data

Figure 4.1. Location of study site in Denmark [Google, 2018]

According to [Thorsen, 2006], soil data consists of eleven samples taken from three main boreholes and four shallow boreholes. The main boreholes are placed two distinct areas known as point A (for boreholes 1 and 2) and B (for borehole 3), as seen in Figure 4.2, while the shallow ones were performed between point A and B, as shown in Figure 4.3.

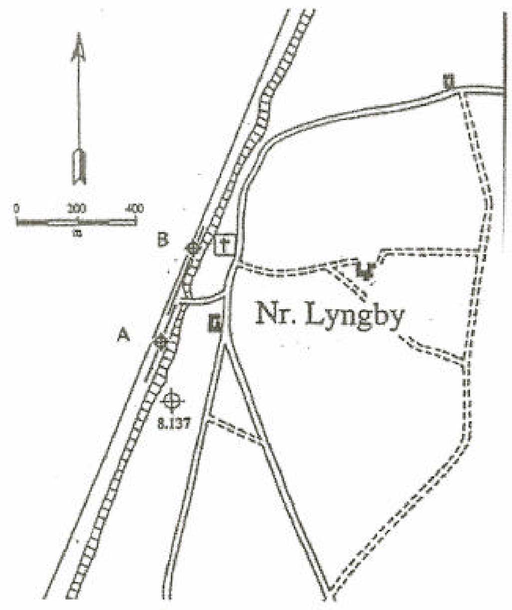

Figure 4.2. Borehole locations in Nørre Lyngby [Thorsen, 2006]

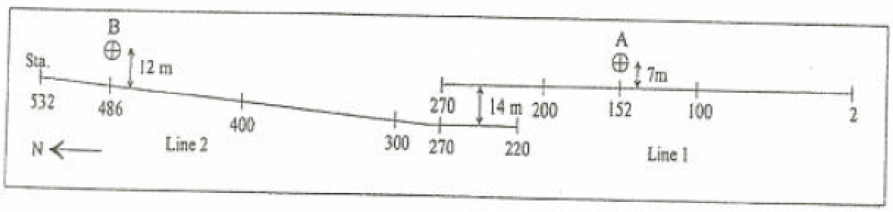

Figure 4.3. Seismic profiles in Nørre Lyngby [Thorsen, 2006]

Samples were retrieved from these sites in two different ways:

- Directly taking the samples via 70 mm diameter thin-wall sampler.
- Extracting material from intact core samples.

In all cases, all samples were trimmed to obtain cylinders of 60 mm diameter and 30 mm height.

Samples were taken from a variety of points in the field survey, focusing on the different types of clays present. A detailed graph on the location of these samples can be seen at Figure 4.4. To summarize, the samples are arranged as follows:

- Nine samples are taken from post-glacial silty clays with presence of sand stripes.
- One sample is taken from an Eem inter-glacial clay.
- Another sample is taken from a section of glacial, Weichsel sandy clay.

Originally, samples are labelled according to the laboratory code assigned to them. However, to make easier to the user the location of these samples, a re-labelling process has been performed. The new denominations for the tests can be seen at Table 4.1. Samples

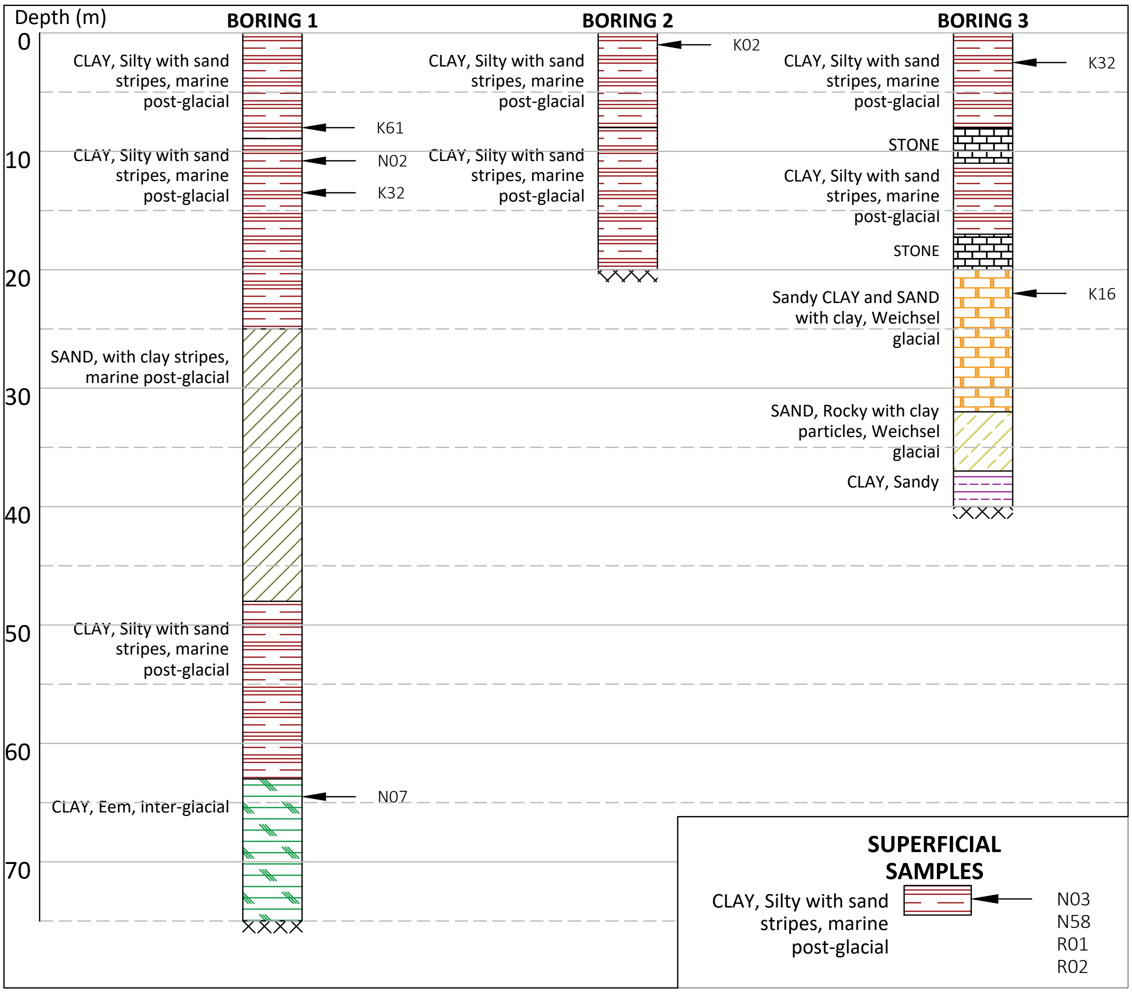

Figure 4.4. Location of test samples in the different boreholes [Original labeling]

from the different shallow boreholes between the main ones have been grouped under the denomination "B0".

Borehole	Original test name	New test name	Retrieving method
-	N03	B0T1	Thin wall sampler
-	N58	B0T2	Thin wall sampler
-	R01	B0T3	Thin wall sampler
-	R02	B0T4	Thin wall sampler
1	K61	B1T1	Extracted material
1	N02	B1T2	Thin wall sampler
1	K10	B1T3	Extracted material
1	N07	B1T4	Thin wall sampler
2	K02	B2T1	Extracted material
3	K32	B3T1	Extracted material
3	K16	B3T2	Extracted material

Table 4.1. Consolidation tests re-labelling

According to the borehole distribution, it seems that the samples can be grouped as:

1. Samples from shallow boreholes (B0), B1T1, B2T1 and B3T1.
2. Samples B1T2 and B1T3, could present slightly different properties to group 1.
3. Sample B1T4.
4. Sample B3T2.

4.2 Laboratory test program

Consolidation tests were performed on the soil samples. According to [Thorsen, 2006], oedometer devices had a single drainage interface, in the lower surface. This drain was composed of a small filter stone of a diameter smaller than the apparatus. This increases the drainage path, which is considered as:

$$H_d = 0.7 \cdot D = 42\ mm \tag{4.1}$$

Testing was performed as Incremental Load (IL) tests. Load steps duration was extended to allow the sample to dissipate the excess water pressure, isolating the effect of the secondary compression process in the later time stages.

Prior to the start of the test program, the initial state parameters of the samples are obtained, as seen in Table 4.2:

	Year	Depth $[m]$	Water content [%]	Bulk density $[t/m^3]$	Grain density $[t/m^3]$	Void ratio $[-]$	Current stress $[kPa]$
B0T1	1997	2.2	16.4	2.06	2.7	0.53	30
B0T2	1996	2.2	19.7	2.01	2.7	0.61	30
B0T3	1996	2.2	28.9	1.96	2.7	0.78	30
B0T4	1995	2.2	22.5	2.05	2.7	0.61	30
B1T1	1993	8	37.4	1.87	2.76	1.03	110
B1T2	1996	10.8	32.9	1.89	2.7	0.9	145
B1T3	1994	13.5	39.2	1.8	2.7	1.1	160
B1T4	1996	64.5	27.7	1.94	2.72	0.79	650
B2T1	1993	1	23.9	1.99	2.7	0.68	20
B3T1	1994	2.5	32.7	1.9	2.7	0.89	30
B3T2	1994	22	17.3	2.11	2.71	0.51	220

Table 4.2. Initial state parameters

The outcome of the test program can be seen in Figures 4.5 and 4.6. Tests have been arranged for display according to both the borehole they were taken from, and the retrieving method.

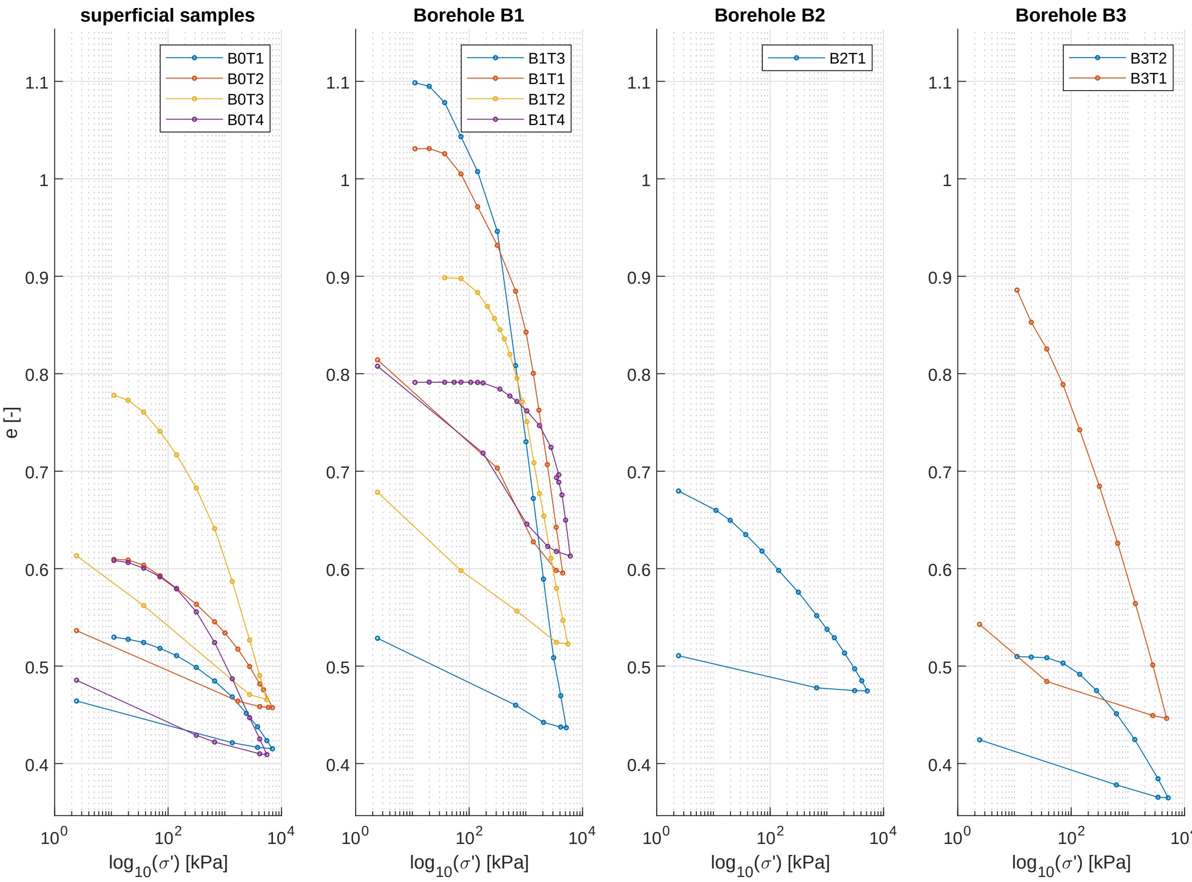

Figure 4.5. Consolidation tests divided by boreholes and superficial samples

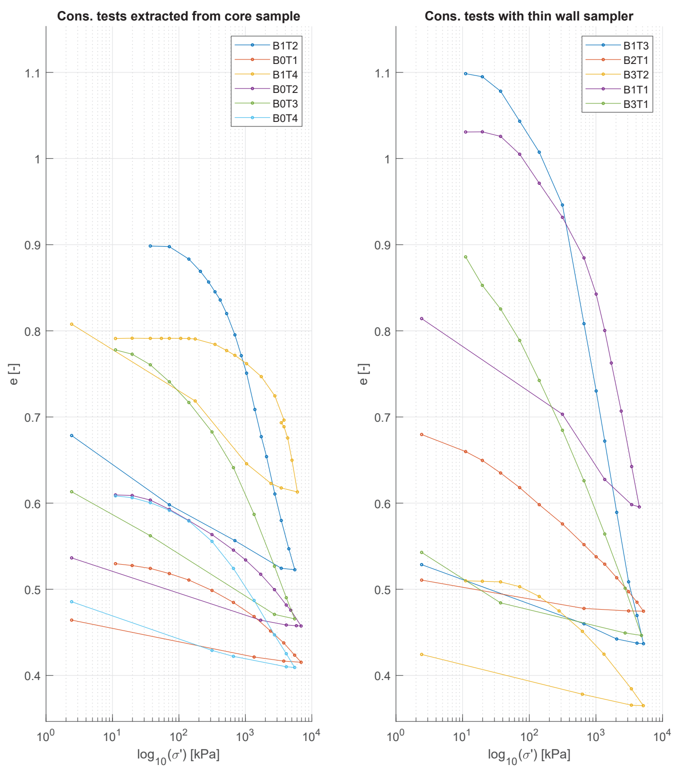

Figure 4.6. Consolidation tests divided by retrieving method

Soil data analysis 5

This chapter covers the analysis procedure done in this thesis on the eleven soil samples.

5.1 Introduction

All eleven tests were interpreted by using the custom software MASCoT, specifically developed along this master thesis to analyse the data and compare the results. The objective of this analysis was to obtain the defining parameters of the consolidation and creep processes, as well as the value of the compression index C_c and pre-consolidation stress σ_{pc}.

To achieve this, tests were subjected to a 3-stage analysis:

1. Individual load steps were analysed using several methods to obtain the parameters defining consolidation and creep parameters:
   - Brinch Hansen
   - ANACONDA
   - Taylor
   - 24h

   This process is known as the "strain separation analysis".
2. Compression index was obtained for each outcome of the strain separation analysis.
3. Pre-consolidation stress is calculated for each outcome of the strain separation analysis. σ_{pc} was obtained by using the following methods:
   - Janbu
   - Akai*
   - Pacheco Silva
   - Becker
   - Jacobsen

   Akai method being calculated only for the strain separation methods allowing the calculation of the secondary compression coefficient, c_α.

All methods discussed here were applied to every stress step of every sample. All the strain separation results are shown in Appendix A, while the pre-consolidation stress results are shown in Appendix B. This chapter follows specific analysis to one of the tests, in order to exemplify the whole process.

5.2 Strain separation

In this section, there is a brief description on the calculation procedure for the strain separation methods in order to interpret the soil data, by making use of the options given by *MASCoT*. As 24h method is fully automatized, it is not included here.

5.2.1 Brinch Hansen method

Following the implementation on *MASCoT* of Brinch Hansen's method, the data points of each step were used to fit the bi-linear model in two areas: the straight line in the $\sqrt{t}$ scale, and the end tail in the $log(t)$ scale. An example of this procedure appears in Figures 5.1 and 5.2.

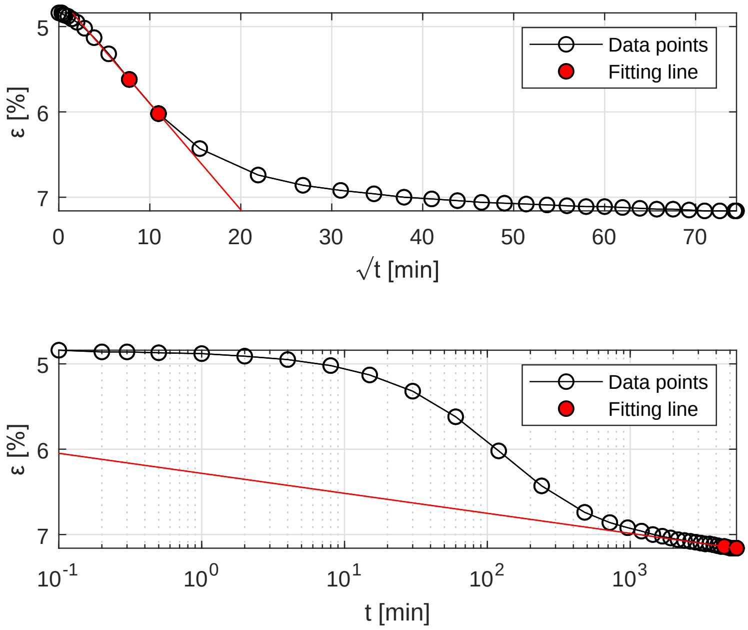

Figure 5.1. Determination of fitting lines for sample B1T1, step 7, via Brinch Hansen method in *MASCoT*.

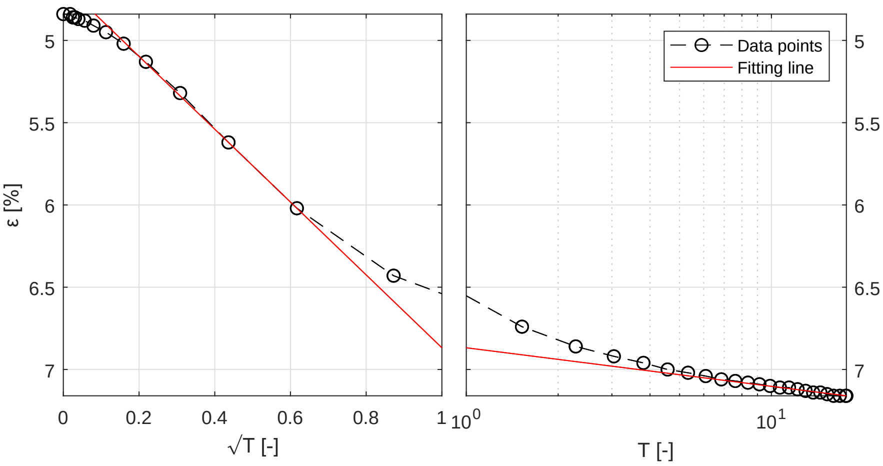

Figure 5.2. Convergence of the Brinch Hansen bi-lineal model for sample B1T1, step 7, in *MASCoT*.

For the most part of the analysis, this method presented no issues. However, the method became problematic in two cases. The first one consists of the first steps in almost every test. These steps present high inaccuracy, as the sample is still adjusting to the testing machine. As a consequence, the curve obtained resembles nothing similar of the expected "S" curve. This was expected, and the procedure followed was to fit the lines in order to obtain $\epsilon_{100} = \epsilon_{total}$. Parameters in these steps are usually not in line with the rest of steps and therefore ignored in the interpretation.

The second issue is that, as a consequence of the use of low load increment ratios (LIR) during the execution of some consolidation tests, there are steps that present curves that can not be analysed via Brinch Hansen's method. This issue is discussed in detail in Section 6.1.1.

5.2.2 ANACONDA method

As included in $MASCoT$, use of ANACONDA is based upon the number of points used to define the creep process. To obtain the most accurate solution, a trial-and-error process was used. The objective was to find the value that gives the minimum error between the experimental and theoretical U, as well as getting a horizontal tail in the consolidation process.

As for the value for the initial strain at the beginning of each step, the following criterion was followed:

$$\epsilon_{0,ANAC} = max\left(\epsilon_{0,Data\ points}, \epsilon_{0,Brinch\ Hansen}\right) \tag{5.1}$$

An example of how the calculation options for ANACONDA method were set up can be seen in Figure 5.6.

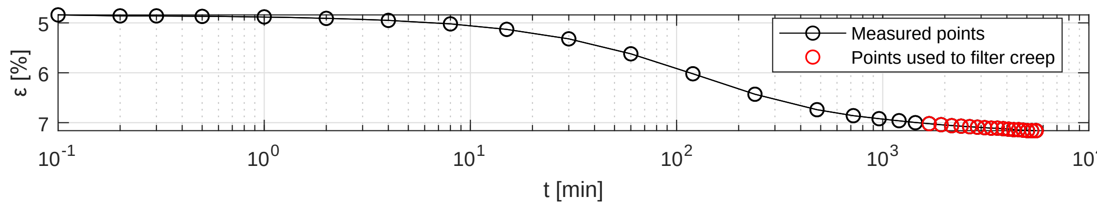

Figure 5.3. Determination of creep points for sample B1T1, step 7.

In Figure 5.4 there is an example of how the calculated degree of consolidation matches the one extracted from experimental data. Therefore, the consolidation coefficient c_v properly defines the consolidation process.

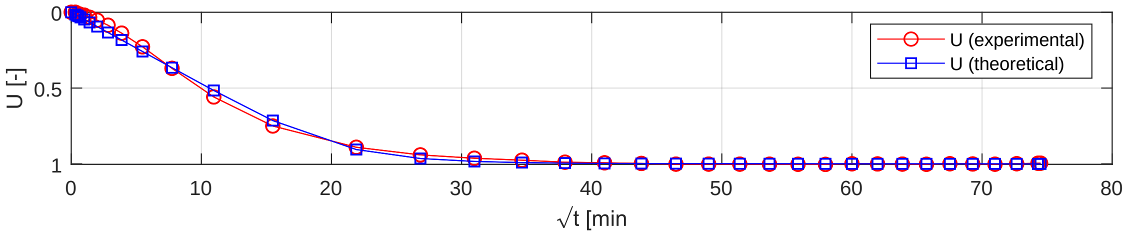

Figure 5.4. Adjustment of theoretical and experimental degree of consolidation for sample B1T1, step 7

Finally, Figure 5.7 shows the results of the analysis. It can be seen that consolidation strains tend to a horizontal line, adjusted to Terzaghi's theory. This confirm that the amount of creep strains subtracted from the total strains is not excessive, and that the time for the end of consolidation not insufficient (which would lead to the tail of the consolidation strain curve to "rise" instead of being horizontal).

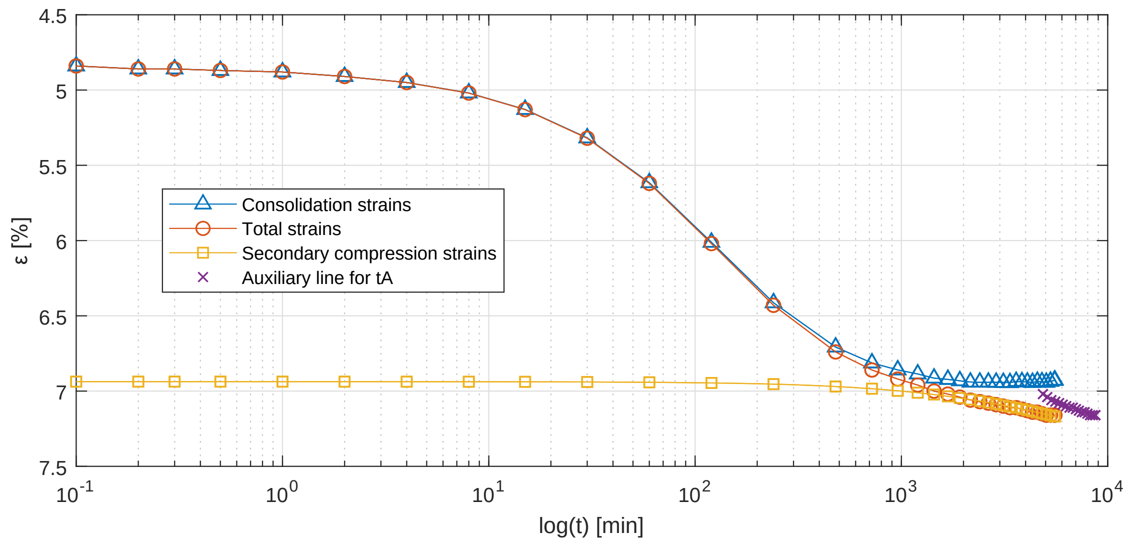

Figure 5.5. Consolidation and secondary compression strains filtered out for sample B1T1, step 7

5.2.3 Taylor method

Input for Taylor method is similar to the first part of Brinch Hansen's method. Points from the data set were chosen in order to fit the straight line in the $\sqrt{t}$ scale, allowing the program to interpolate the ϵ_{100} value and the rest of the parameters.

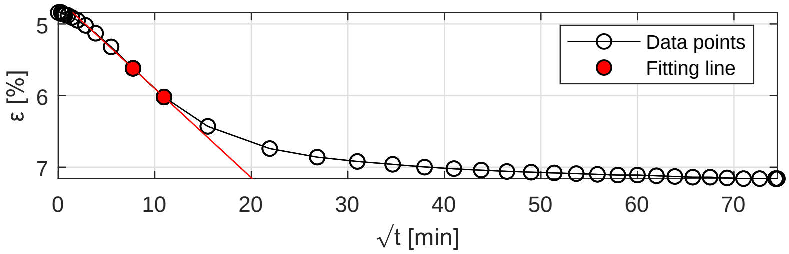

Figure 5.6. Adjustment of the straight consolidation line in Taylor's method for sample B1T1, step 7

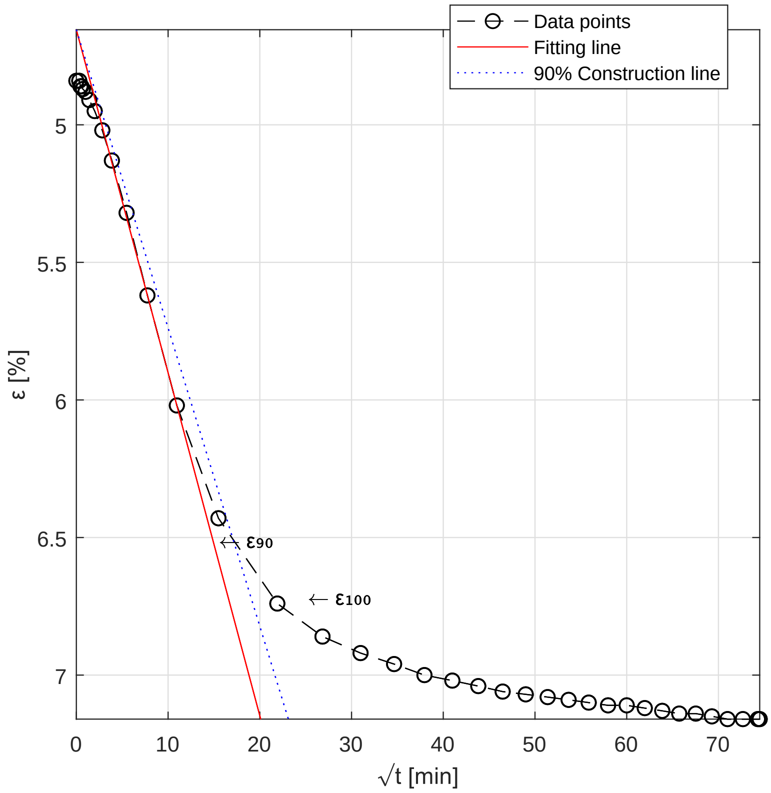

Figure 5.7. Calculation of consolidation parameters in Taylor's method for sample B1T1, step 7.

5.3 Compression Index

Compression index was calculated individually for each strain separation method using *MASCoT*. The program allows to do that by manually choosing the points corresponding to the straight line in the virgin compression part of the curve.

Criterion to fit the virgin compression line was to select the points that allowed a line that adjusted to the majority of the straight section in the presumed normally consolidated line. For some tests, like Test B1T1 in Figure 5.8, this is an easy task, as the virgin compression like is clear. Other tests, like Test B1T3, present a divergence in the last points, which were ignored in the fitting.

Some tests, like Test B2T1 in Figure 5.9, presented curved transitions from the over-consolidated to the normally consolidated state. In these cases, only the last points were chosen.

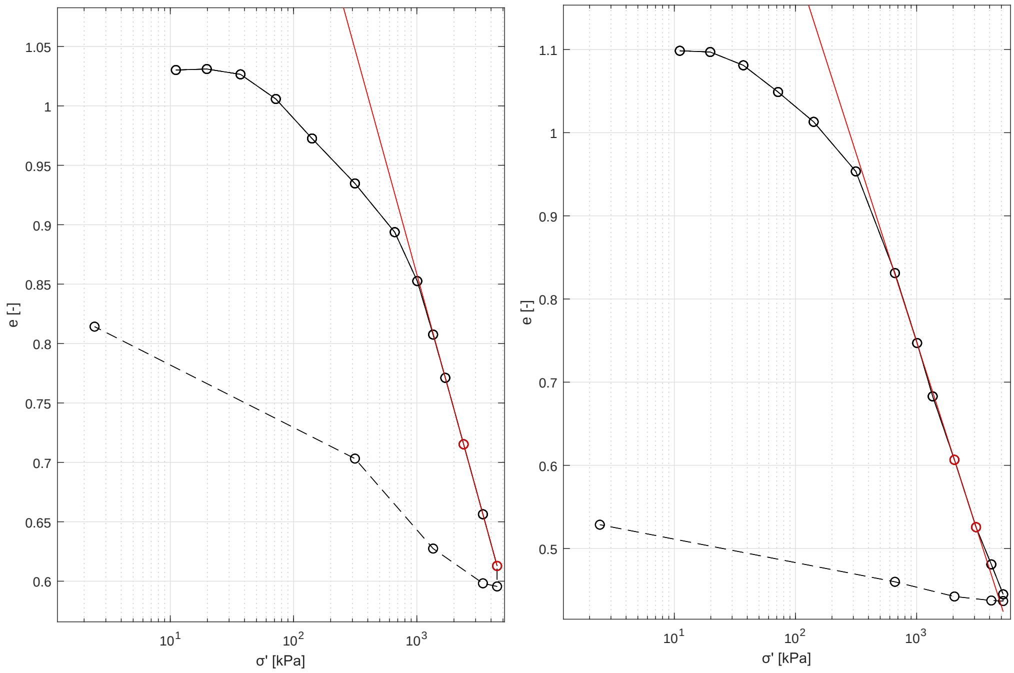

Figure 5.8. Calculation of compression index for samples B1T1 (left) and B1T3 (right)

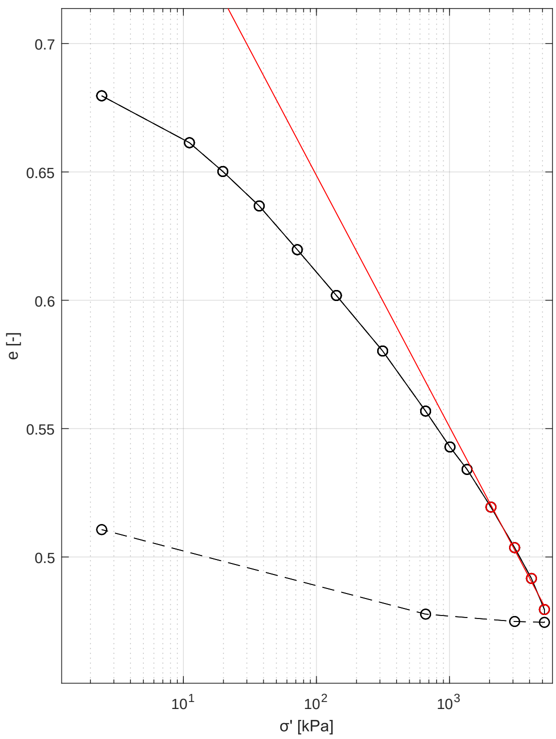

Figure 5.9. Calculation of compression index for sample B2T1

5.4 Pre-consolidation stress

In this section, there is a brief description on how the pre-consolidation stress methods were used to interpret the soil data and obtain the pre-consolidation stress, σ_{pc}, by making use of the options given by *MASCoT*. As Pacheco Silva's method is fully automatized, it is not included here.

5.4.1 Janbu method

Janbu's method is calculated in *MASCoT* by manually selecting the optimal point in the $M - \sigma'$ graph given by [Janbu, 1963]. This was done in the analysis by looking the minimal point reached before the curve tends to the virgin compression line. However, most of the tests presented atypical curves, remarkably different that the graphic examples in [Janbu, 1963]. This led to extremely low values for σ_{pc} in almost every test. In Tests B1T1 and B1T3, as shown in Figures 5.10 and 5.11, it can be seen that after an initial peak, both tests achieve the minimum value in points close to $\sigma_{pc} = 0$ before trending to the virgin compression line.

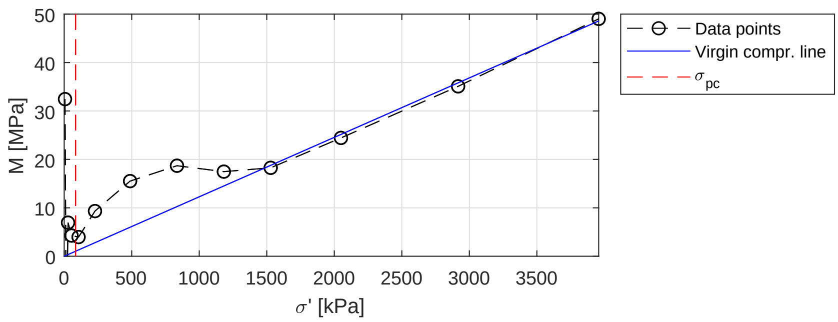

Figure 5.10. Janbu's method applied to Test B1T1

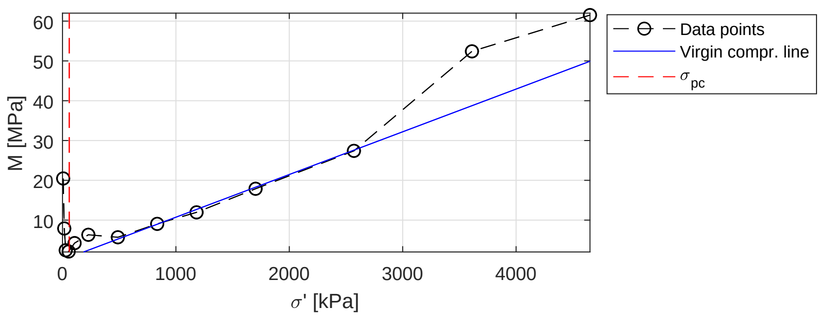

Figure 5.11. Janbu's method applied to Test B1T3

5.4.2 Akai method

Akai's method was obtained for every outcome of Brinch Hansen and ANACONDA methods, as these are the only ones that provide results for the secondary compression index, C_α.

In Figure 5.12 it is possible to see an example of Akai's method applied to Test B1T1. Over-consolidated and normally consolidated states are well defined by the data points, and the range for σ_{pc} is usually narrow.

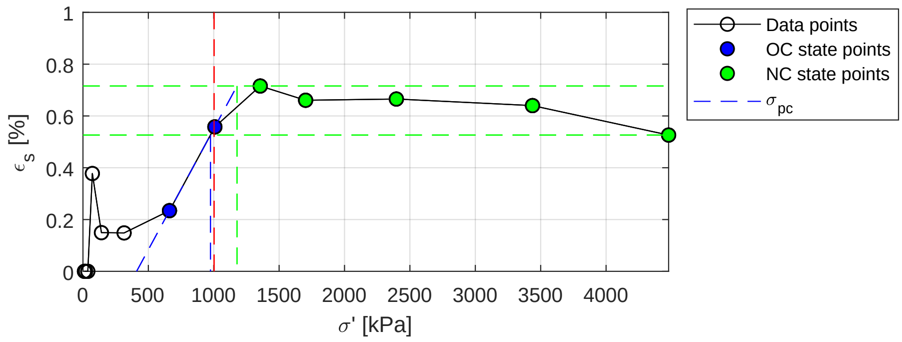

Figure 5.12. Akai's method applied to Test B1T1

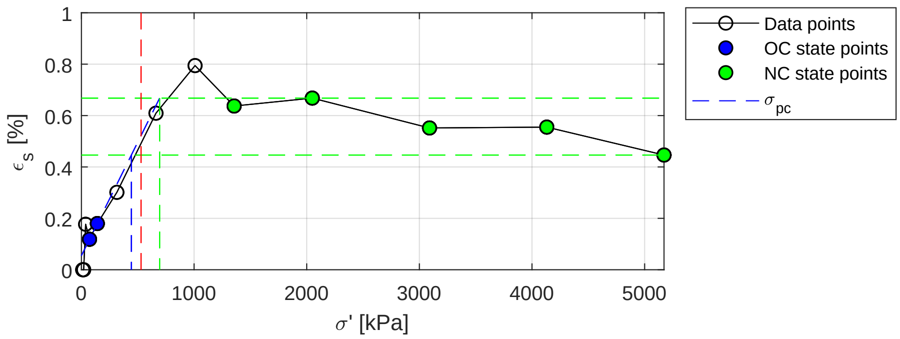

Figure 5.13. Akai's method applied to Test B1T3

5.4.3 Jacobsen method

Jacobsen's method was applied by fitting most points of the curve, except the first points, i.e. the ones that do not successfully consolidate due to sample remodelling and other factors; and outlier points that did not fit to the rest of the experimental curve. An example is presented in Figure 5.14.

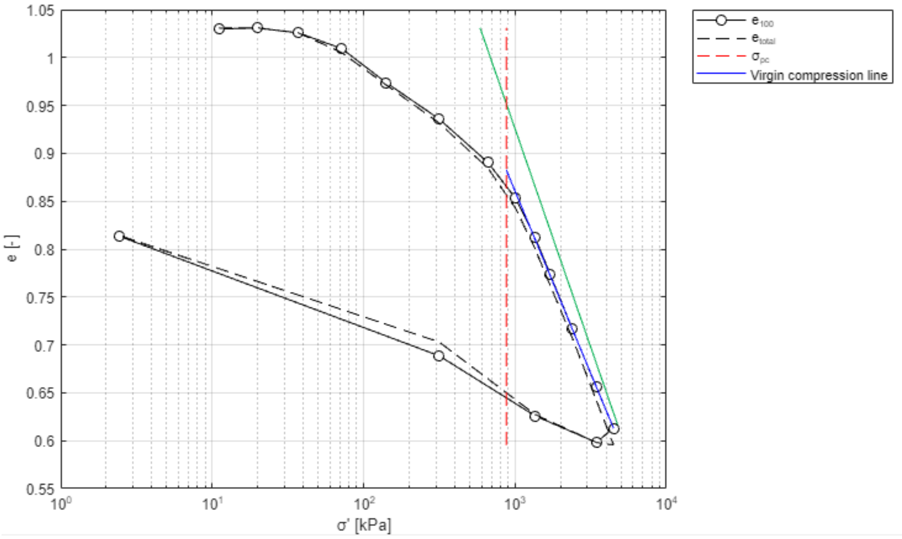

Figure 5.14. Jacobsen's method applied to Test B1T1

5.4.4 Becker method

Becker's method required visual verification that the points were valid for the fit, as this was not always the case. For example, some of the points with higher stresses did not properly fit with the post-yield line as, for example, Figure 5.16. Likewise, points close to the intersection of the pre and post-yield lines were left out of the fitting, as these points tend to form a transition curve [Becker et al., 1987]. Finally, initial points that did not develop consolidation properly were left out of the fitting process.

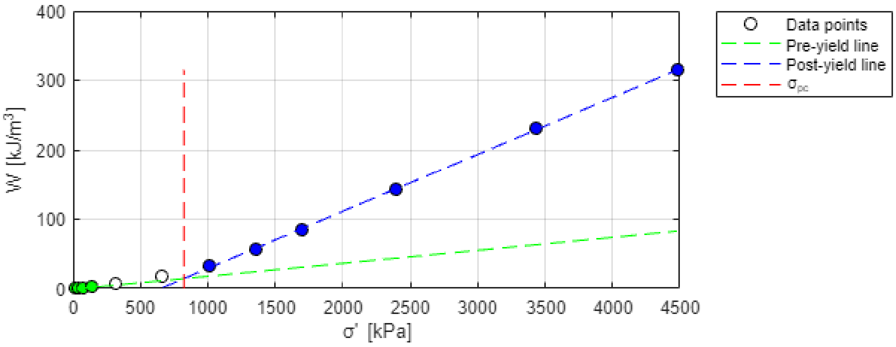

Figure 5.15. Becker's method applied to Test B1T1

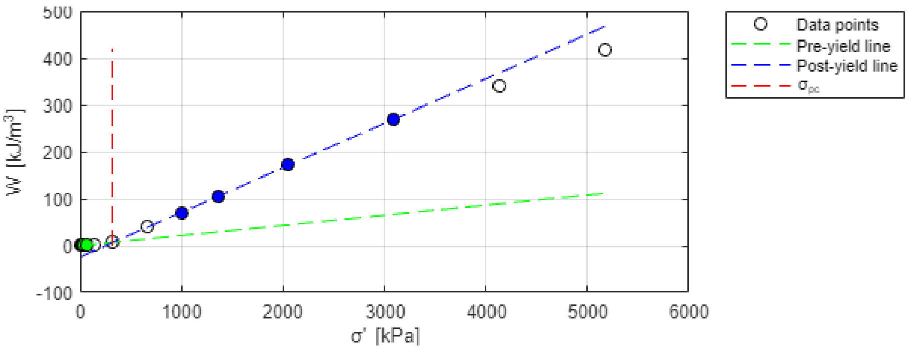

Figure 5.16. Becker's method applied to Test B1T3

5.5 Results

All numerical results from the strain separation analysis are presented in the Appendix A, while results from pre-consolidation stress are presented in Appendix B. In Figure 5.17 a graphic example can be appreciated for Test B1T1, showing the results for the different strain separation methods in the stress-strain chart.

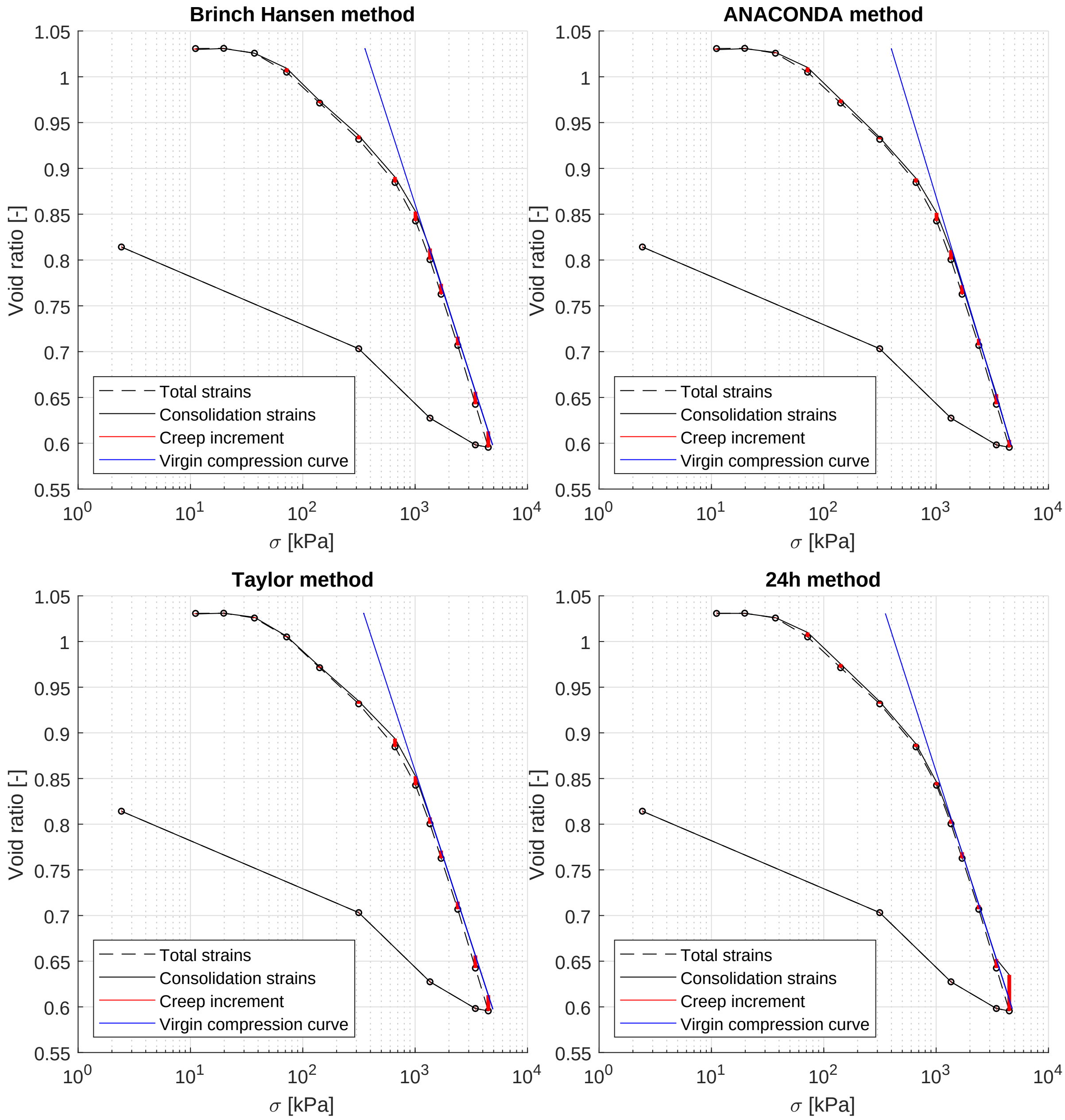

Figure 5.17. Results from analysis of test B1T1.

Likewise, Figure 5.18 displays the outcome of all pre-consolidation stress methods applied on Test B1T1.

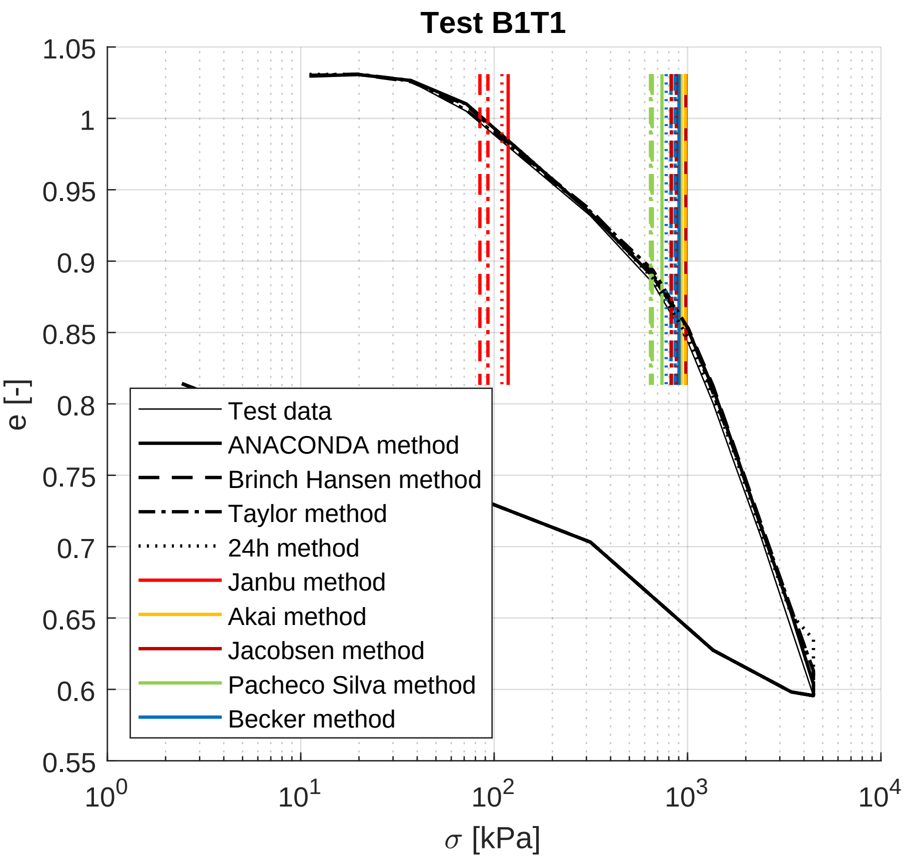

Figure 5.18. Results from pre-consolidation stress analysis of test B1T1. Each vertical line represents a value of σ_{pc}. Line style represents the strain separation method used, e.g. all vertical dashed lines are outcomes of Brinch Hansen's method. Colour represents outcomes for each pre-consolidation stress independently of the strain separation method used.

6 Discussion on strain separation methods

This chapter focus on the limitations and particularities of the different strain separation methods, using as a reference the analysis performed to the soil data described in Chapter 4.

6.1 Limitations in the execution of the different methods

6.1.1 Intersection of Brinch Hansen fitting lines in cases with low load increment ratio

Parameters from Brinch Hansen's method were obtained by using the *MASCoT* corresponding tool. To run the analysis, the points which best represent the requirements given by [Brinch Hansen, 1961a] were chosen, i.e. the points that linearly align in the square root of time plane, and the end points in the logarithm of time plane. A proper example is shown in Figure 6.1.

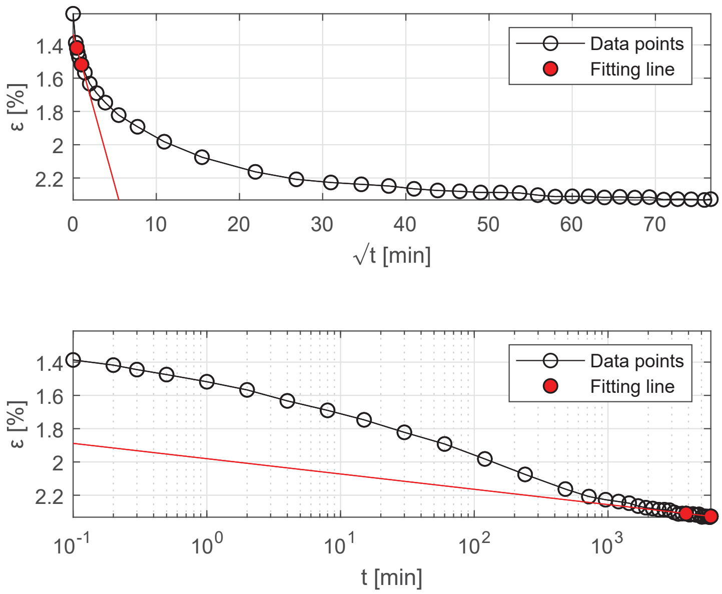

Figure 6.1. Point selection for test B3T2, step 6

As explained in Chapter 2, these points are used to create a bi-linear model in which intersection the transition from consolidation to creep process can be found. This method, however, presents a several limitation in this aspect. Based on a graphical adjustment to the time-strain curve, Brinch Hansen's method is highly sensitive to the shape of said curve.

A typical issue can be seen in Figure 6.2. In this case, the creep process effect seems to be relatively high during the end of consolidation. The consequence is that the curve (which, disregarding creep in Terzaghi's theory, should end in a horizontal tail) has a steep slope. The slope of the logarithmic creep component (C_α) ends up being higher than the slope of the square root of the consolidation component.

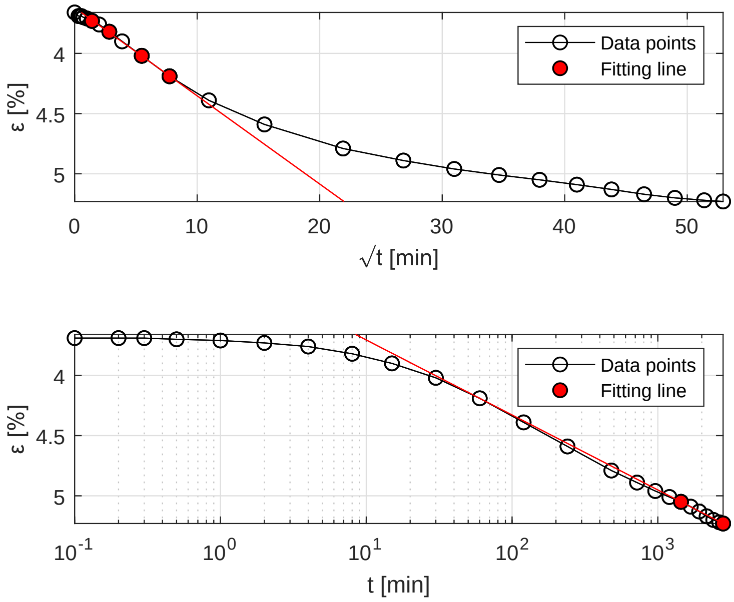

Figure 6.2. Point selection for test B1T4, step 15

This situation can prevent intersection at all between the two lines, producing a failure in the method. This can be unintuitive at first because, at first sight, two straight, non parallel lines, should always intersect. However, the lines shown in Brinch Hansen construction are not lines but curves, as seen in Equations 6.1 and 6.2:

$$\epsilon_{\sqrt{t}} = a_{\sqrt{t}} \cdot \frac{\sqrt{t}}{t_s} + b_{\sqrt{t}} \tag{6.1}$$

$$\epsilon_{log_{10}} = a_{log_{10}} \cdot \frac{log_{10}(t)}{t_s} + b_{log_{10}} \tag{6.2}$$

Given the previously stated conditions, these two curves can fail to intersect. This is clearly seen in Figures 6.3, 6.4 and 6.5. These figures represent the data points and fitting lines from the Brinch Hansen's construction. However, instead of using the bi-scaled construction the data in directly displayed into a single scale (linear and logarithmic).

These plots are complicated to interpret if the objective is to obtain the consolidation parameters in a graphical way. Nevertheless, they show clearly the limitation of Brinch Hansen method.

Figure 6.3 shows the step 12 of the B1T4 test, which presents a classical consolidation shape, such as the one in Figure 6.1. Figures 6.4 and 6.5 correspond to the step 15 of the same tests, i.e. the curve seen in Figure 6.2. The only difference is the that the points used for the fitting are not exactly the same (although all of them taken from the linear tail).

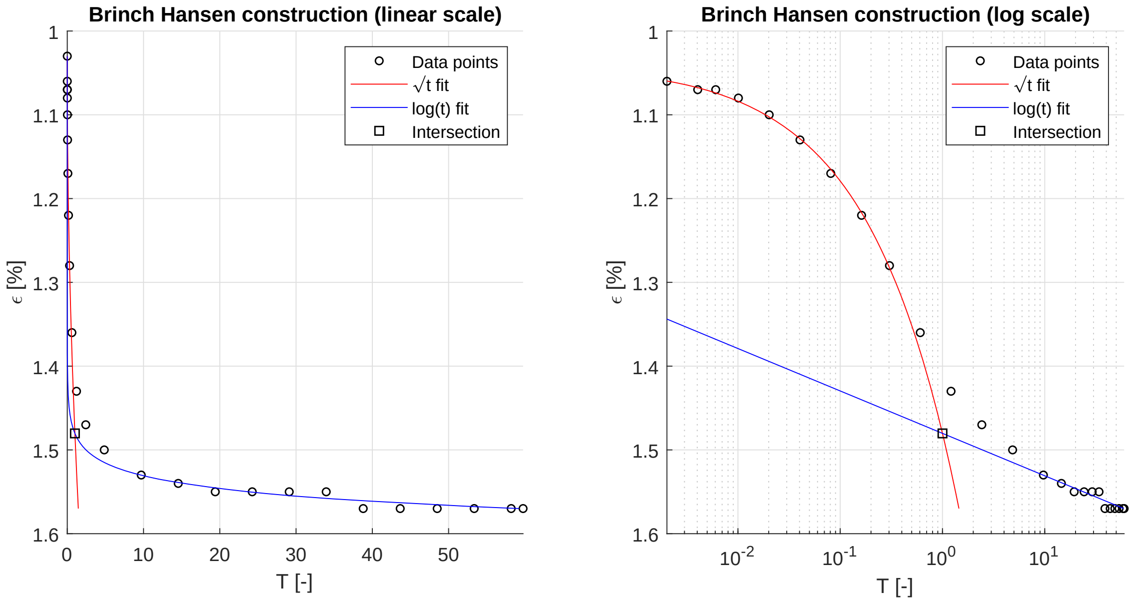

Figure 6.3. Point selection for test B1T4, step 12

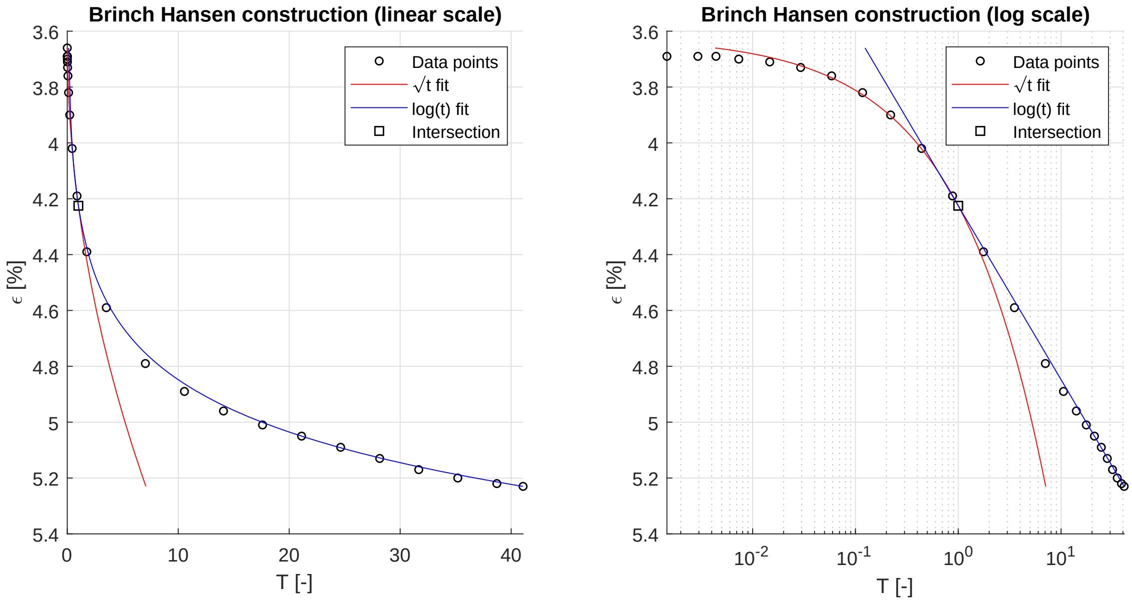

Figure 6.4. Convergent point selection for test B1T4, step 15

In the first case, the two fit curves provide with a clear intersection in T=1. However, in the second one the consequence of the high creep can be seen. the logarithmic fitting

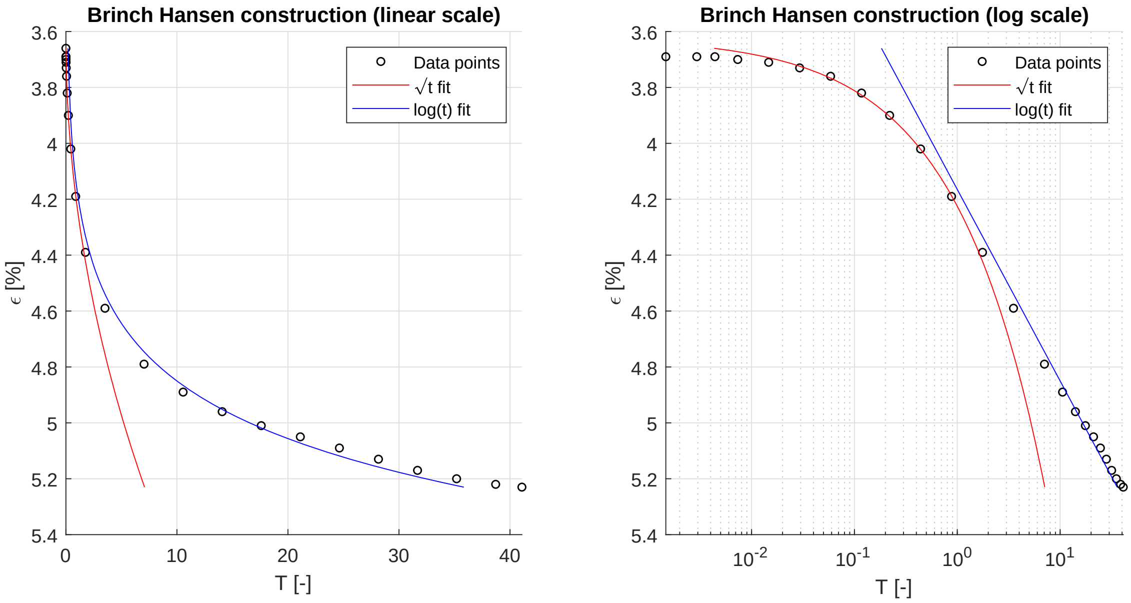

Figure 6.5. Non convergent point selection for test B1T4, step 15

curve becomes steeper and rises above the points where the consolidation process rises. This case shows a fringe situation in which the intersection becomes a tangent.

If the creep has higher presence, the curves have no contact at all and the method fails. This is what it can be seen in Figure 6.5, where intersection is not longer possible.

This criterion followed to avoid the failure in cases like the one shown in step 15 stays limited to an almost arbitrary pick-and-choose process until a possible combination of selected points can be found. In some cases, it seems entirely impossible to achieve a solution.

The most probable cause for this behaviour can be attributed to how the testing was performed in the laboratory. Specifically on the load increment applied for each new step. Load increment ratio ($LIR = \Delta\sigma/\sigma$) for each test should be, according to the geotechnical standard [ASTM International, 2011], equal to the existing stress, this is $LIR = 1$. LIR values smaller than 0.7 may "preclude evaluation for the coefficient of consolidation, c_v, and the end-of-primary consolidation" [ASTM International, 2011].

As seen in Figure 6.6, a significant quantity of the load steps done do not follow this recommendation. Some of the tests reach values of $LIR \simeq 0.15 - 0.5$.

This deviation in the LIR has a direct influence on the shape of the consolidation curve. This is clearly seen on Figure 6.7. In this figure there are three examples of tests with different LIR management along the testing process. Test B2T1 has values around 1 until step 8, at which point the LIR drops to less than 0.5. Test B3T1 maintains values fairly around 1, while test B1T2 presents very low values for almost the whole test.

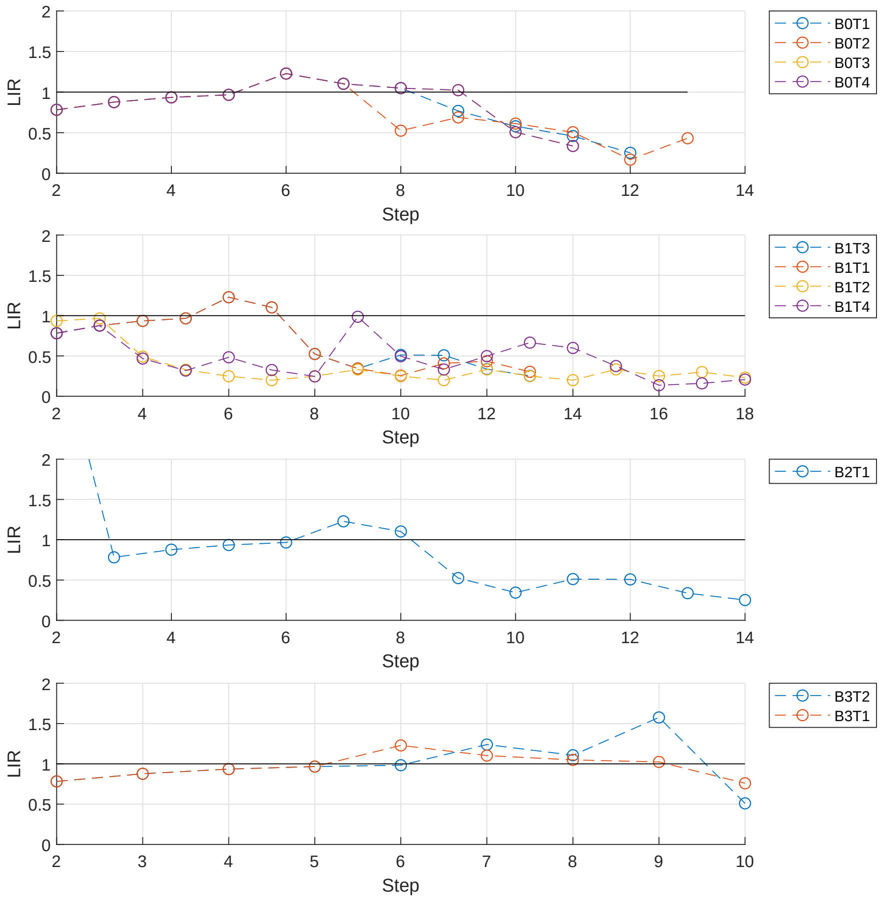

Figure 6.6. Step load increment in all studied tests

For all three tests, steps with a LIR around 1 show typical S shaped curves. As the LIR value drops below 1, the tail of the curves tends to a straight line. Consequently, it seems safe to assume that the studied clays are highly sensitive to the use of small LIR values. For these cases, the consolidation process may not be fully occurring.

While this situation should not affect the creep process, it can clearly affect the determination of the consolidation coefficient c_v and consolidation strains, ϵ_{100} for all methods studied here. As per Brinch Hansen's method, this situation can lead to consolidation curves that can not be solved at all.

6.1.2 Influence of criteria for selection of ϵ_0

Following Terzaghi's consolidation theory, it can be stated that there are three main components when subjecting clays to a load increment; initial settlement, consolidation and secondary compression.

In a theoretical process, the consolidation starts right after the load is applied, obtaining a curve that starts at t_0 with the first strain value taken when applying the new load,

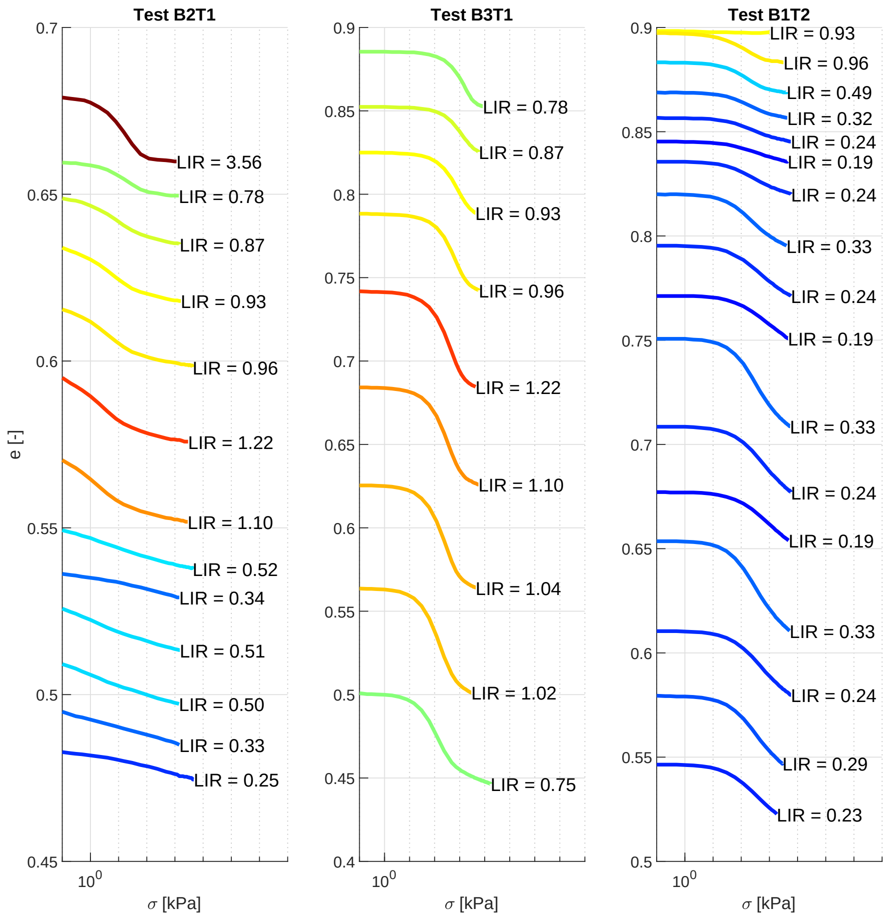

Figure 6.7. Comparison for all loaing steps for tests B2T1, B3T1 and B1T2, showing the shape of each consolidation curve and the LIR value associated to it. Colour of each time curve is associated to its LIR value to clarify visual comparison

$\epsilon(t = 0)$.

However, Terzaghi's theory is based, among others, on the principles of soil homogeneity and complete saturation. This is usually not true, and due to air bubbles being present, or soil grains initial crushing, an additional instant settlement can occur [Taylor, 1948]. Thus, the initial value of the strain-time curve is usually discarded as the initial consolidation strain and, instead, another value is devised as part of the method in different ways.

For example, Taylor's method (and Brinch Hansen's, which works in a similar way to this respect) makes use of the fitting line used in the $\sqrt{t}$ space. In these cases, the value of , $\epsilon(t = 0)$ is taken as the intercept of the line with the ordinate axis.

This can be seen at Figure 6.8, where the initial deflection is taken as the model value d_s instead of the data point d_0 (using his original terminology). And, as a consequence,

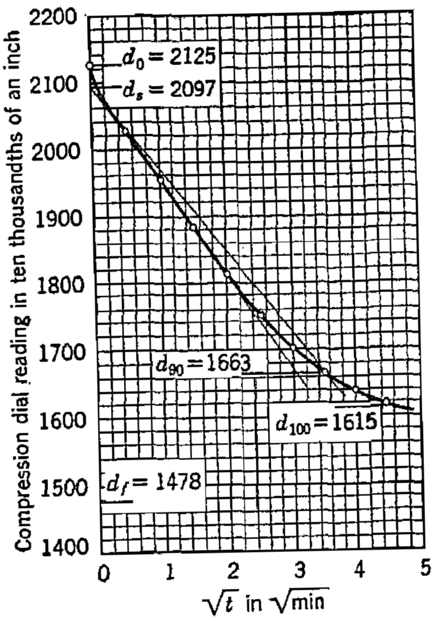

Figure 6.8. Square-root method example [Taylor, 1948]

Taylor definition of consolidation strain is:

$$d_{100} = \frac{10}{9} \cdot (d_s - d_{90}) \tag{6.3}$$

Which corrects out of the consolidation process the initial additional compression.

Casagrande's method also disregards the value given by the data points. In fact, being this method based on a logarithmic scale, the initial value can not been represented for this graphic method to use. Instead, Casagrande uses a mathematical construction that iterates an idealized $\epsilon(t = 0)$ from the consolidation curve and the theoretical degree of consolidation equation, U.

ANACONDA method, on the contrary, has no direct indications on this regard in [Grønbech et al.]. For this case, the software *MASCoT* gives the option to use the first data value as $\epsilon(t = 0)$, or the model value from Brinch Hansen method. The software tool *MASCoT* is based upon [Vestergaard, 2007] uses only the later option.

It is important to notice that, normally, this discussion has little significance, because methods already solve this strain lag successfully, and its influence does not affect the most relevant parameter c_v.

However, some soils studied in this thesis are rather particular in this regard. As shown in Figure 6.9, some soils take a long time to start consolidating. This translates into an almost horizontal start in the logarithmic scale and a concave curve in the square-root scale (as opposed to the convex or linear start of most soils). The consequence of this is that, when fitting a line to the straight part of the curve, the model $\epsilon(t = 0)$ rises above the data point value, as seen in Figure 6.10.

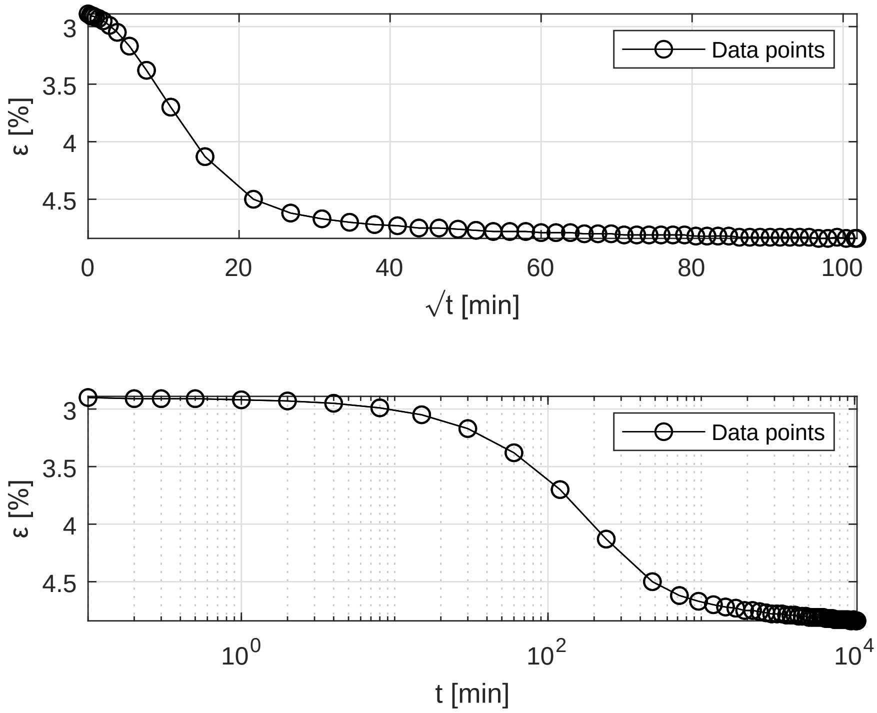

Figure 6.9. Strain-time plot of test B1T1, step 7

Conceptually, if Equation 6.3 is applied, the potential consequence is that the magnitude of the consolidation strain exceeds the total strain increment and the consolidation model starts with less deformation than the end of the previous load step. In the specific case of Figure 6.10, the previous step ends its consolidation around $\epsilon = 2.77\%$ and the creep ends at $\epsilon = 2.89\%$. The current step, however, starts with a corrected $\epsilon_0 = 2.6\%$. This model leads then to an impossible situation.

This difference between initial strains can be significant, being for this step up to 14.5% of the consolidation strain. When applying this parameter to field settlement calculation, this difference could have an influence when calculating the time it takes to reach a certain degree of consolidation U. This can be seen by comparing experimental and theoretical U curves, as seen in Figure 6.11. Here it can be seen a comparison of the consolidation process obtained in laboratory, and the one calculated by applying the parameters extracted from using Brinch Hansen method on the same sample (value named as *corrected* initial strain).

The model $\epsilon - \sqrt{t}$ curve is obtained as:

$$\epsilon(t) = \epsilon_{100} \cdot U\left(\frac{c_v t}{H_d^2}\right) \tag{6.4}$$

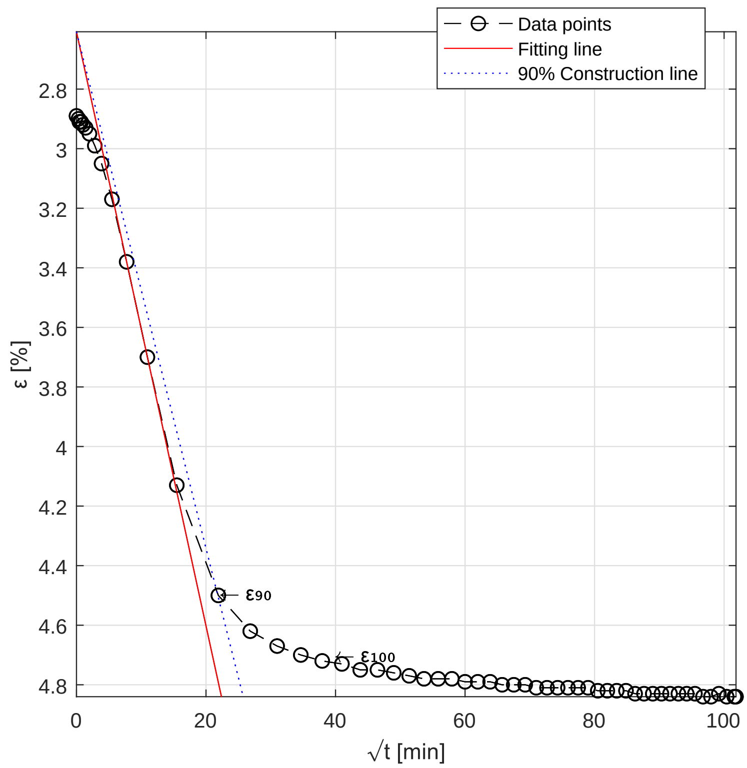

Figure 6.10. Taylor method used in test B1T1, step 7

Being U:

$$U\left(\frac{c_v t}{H_d^2}\right) = 1 - \frac{8}{\pi^2}\sum_{m=0}^{\infty}\frac{1}{(2m+1)^2}e^{-\frac{(2m+1)^2\pi^2}{4}\frac{c_v t}{H_d^2}} \tag{6.5}$$

Equation 6.5 shows the theoretical degree of consolidation, the one normally used when calculating settlements. However, if the total consolidation settlement is known, as it is for a consolidation test, the degree of consolidation can be obtained as an experimental value, U_{exp} from the existing data points:

$$U_{exp} = \frac{\epsilon_{data}(t) - \epsilon_0}{\epsilon_{100}} \tag{6.6}$$

Note that, in Equation 6.6 the value for ϵ_0 can be obtained from the first data point or corrected from the model, as explained before.

In an usual laboratory test, $U_{exp} \simeq U$ up to the point in which the creep starts to appear. This can be seen in Figure 6.12. Here U_{exp}, when using the corrected value for ϵ_0, fits properly for the whole consolidation process. With the exception of the initial points not fitting to the linear consolidation curve. If U_{exp} is calculated using the original value for ϵ_0, i.e. including the initial compression as part of the consolidation process, U_{exp} does not match the theoretical consolidation.

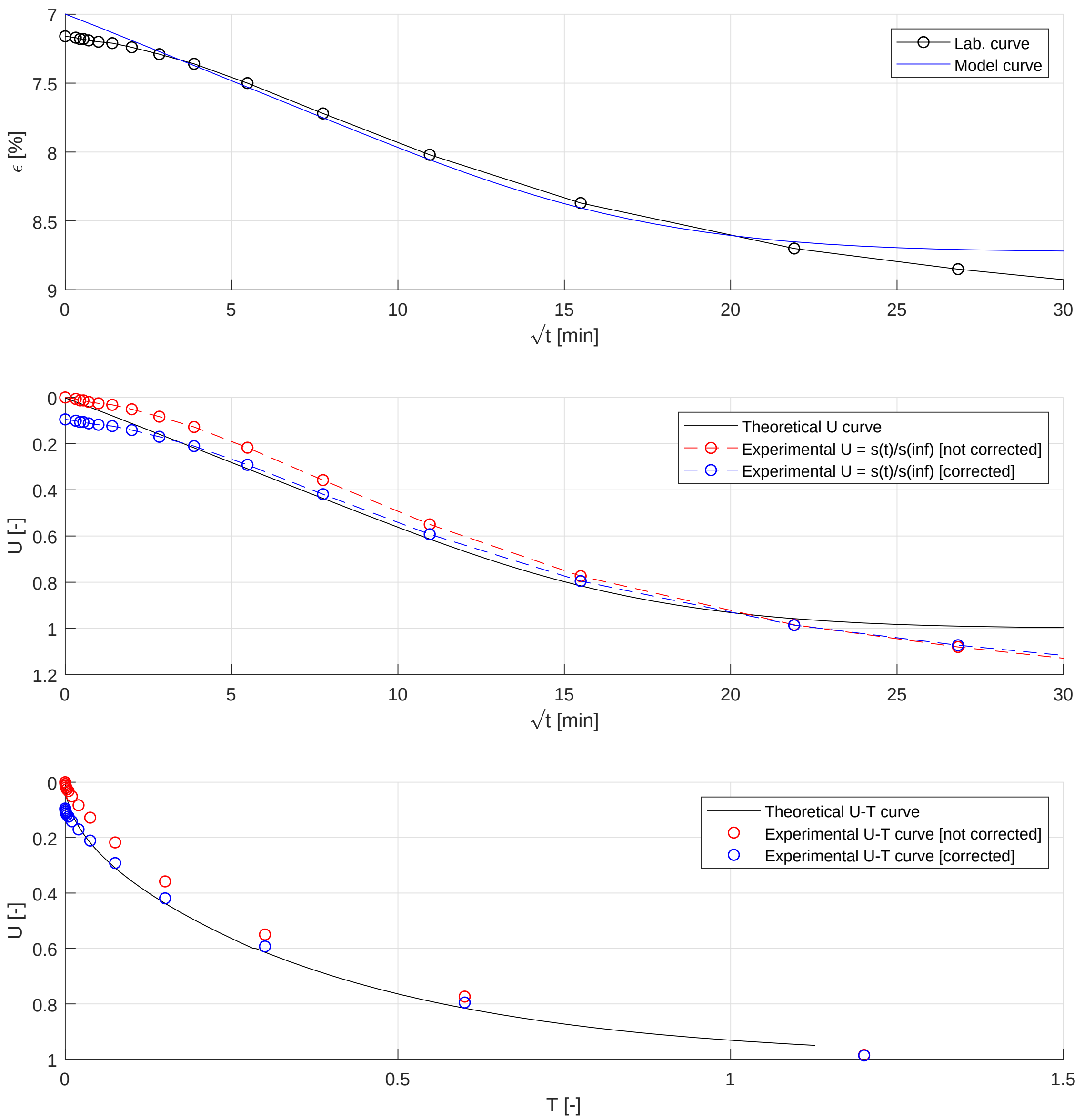

Figure 6.11. Set of plots from test B1T1, step 7 showing: a) $\epsilon - \sqrt{t}$ plot of the laboratory curve and the model curve obtained from Terzaghi theory; b) $U - \sqrt{t}$ plot showing the theoretical U curve and the curves obtained from experimental data, adjusted according to the definition of ϵ_0; c)$U - T$ plot of the same curves in plot b.

However, this is not true for Figure 6.11. As it can be seen in the $U - \sqrt{t}$ plot, using the corrected value ϵ_0 results in a curve that adjusts properly to the consolidation process, but resulting in an initial degree of consolidation bigger than zero, $U(T = 0) > 0$, which is not possible according to the consolidation theory. This situation makes sense taking into account that using a corrected ϵ_0 creates non-existent additional strains in this case, that would occur before the theoretical consolidation starts.

If the not corrected ϵ_0 value is used, the relation $U(T = 0) = 0$ in maintained, and there is a delay in the time the consolidation process occurs. During the first instants, the experimental consolidation starts with an almost horizontal slope and then converges to a line parallel to the theoretical U. As the relation $U - T$ is altered, the settlements in field

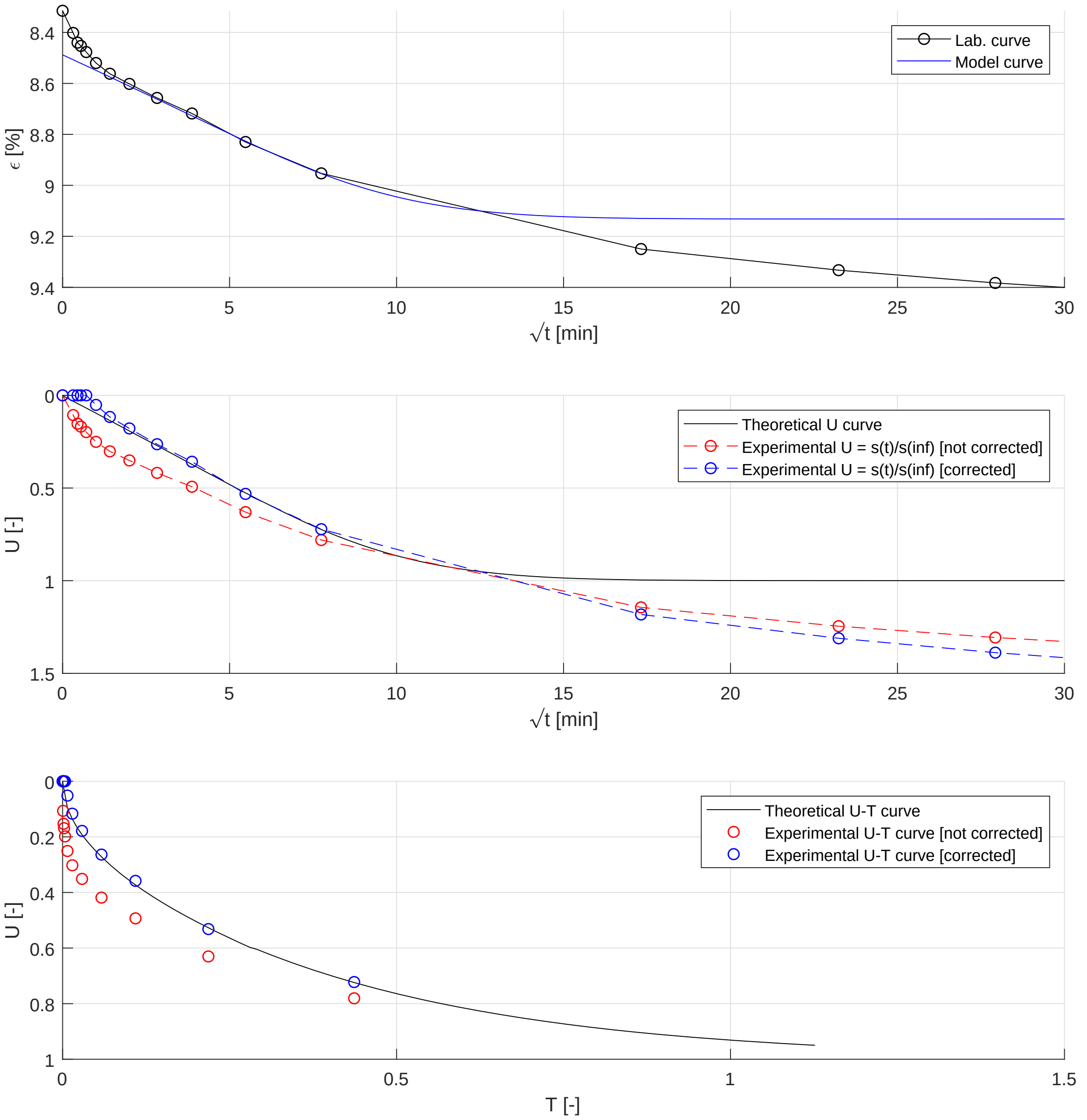

Figure 6.12. Set of plots from test B3T2, step 10 showing: a) $\epsilon - \sqrt{t}$ plot of the laboratory curve and the model curve obtained from Terzaghi theory; b) $U - \sqrt{t}$ plot showing the theoretical U curve and the curves obtained from experimental data, adjusted according to the definition of ϵ_0; c)$U - T$ plot of the same curves in plot 'b'.

would occur later than expected, if Terzaghi's theory is used.

Two conclusions can be drawn from this analysis:

1. Use of corrected values of ϵ_0 above the one given by the data set should not be used to obtain ϵ_{100}, as it simulates a false initial settlement due to instant consolidation in experimental curves. Of course, to obtain the rest of the parameters (e.g. c_v) it can be necessary to assume a corrected value to obtain the mean consolidation values.
2. This type of clays does not exactly follow Terzaghi's consolidation theory, so a time lag can be expected when using it to predict settlements.

6.2 Crossed comparison of the methods used

6.2.1 Consolidation strains

Consolidation strains are highly consistent in all tests, with constant correlation between the different methods. For almost every situation, there is a situation as $\epsilon_{100,Taylor} > \epsilon_{100,BrinchHansen} > \epsilon_{100,ANAC.} > \epsilon_{100,24h}$. An example can be seen in Figure 6.13.

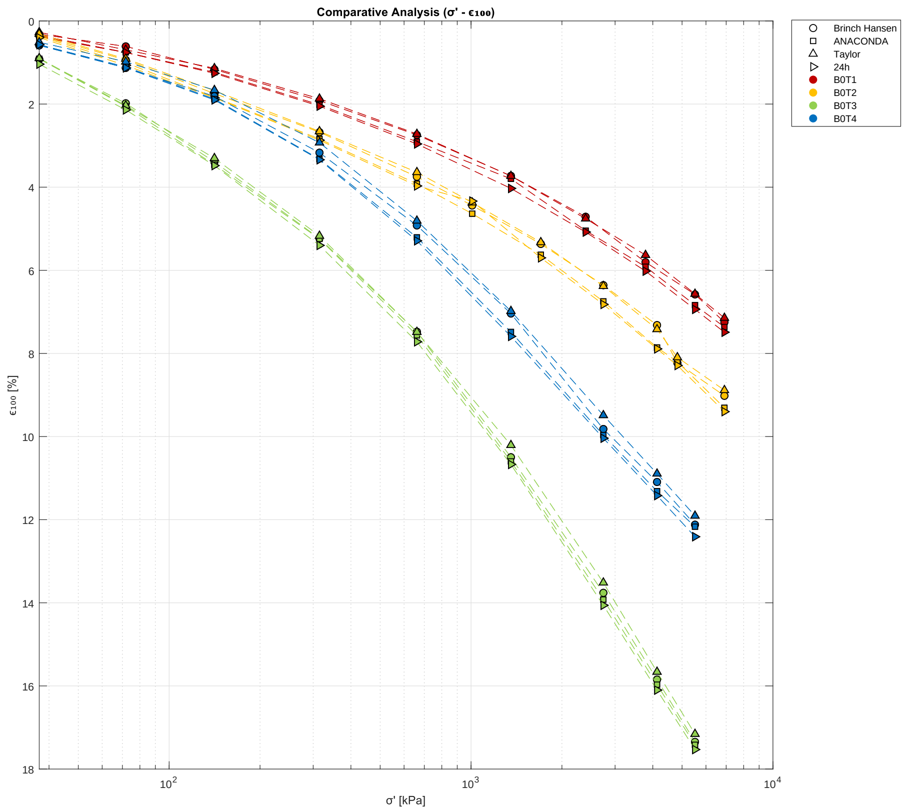

Figure 6.13. Consolidation strains for superficial samples.

6.2.2 Consolidation modulus

The consolidation modulus presents a high correlation for all tests in the correlation ANACONDA-Brinch Hansen-Taylor. However, values for 24h method are less consistent and present higher dispersion. This can be seen in Table 6.1. Examples are shown in Figures 6.14 and 6.15. It can be concluded that the consolidation modulus is a stable parameter, independently of the chosen method.

	bias	r^2
Taylor/Brinch Hansen	1.0095	0.926
Brinch Hansen/ANACONDA	1.0712	0.951
ANACONDA/Taylor	1.0187	0.931
ANACONDA/24h	1.0029	0.71
Taylor/24h	1.1466	0.675
Brinch Hansen/24h	0.7558	0.37

Table 6.1. Consolidation modulus correlation factors for the different methods, using the whole data set.

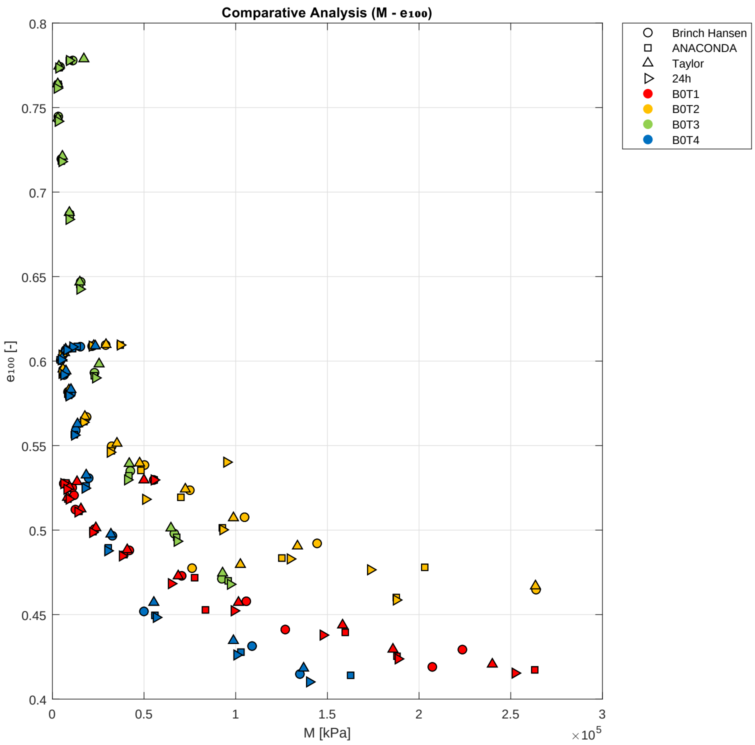

Figure 6.14. Consolidation modulus values, superficial samples

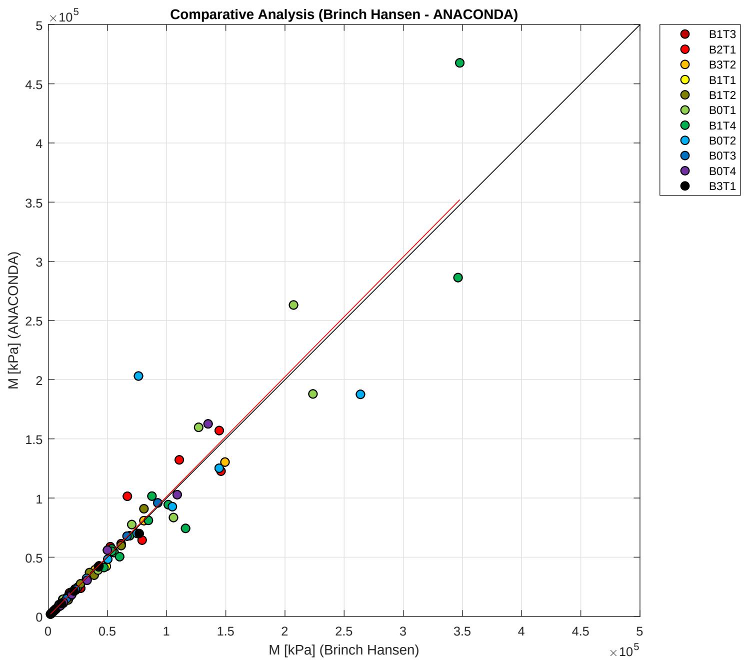

Figure 6.15. Consolidation modulus correlation between ANACONDA and Brinch Hansen methods

6.2.3 Consolidation coefficient

Consolidation coefficient values are compared for ANACONDA, Brinch Hansen and Taylor methods. As seen in Table 6.2, there is a high dispersion for almost every test, and low correlation. In general it appears that Brinch Hansen's method gives higher values of c_v, followed by ANACONDA and Taylor.

As explained before, this could be a an outcome of the majority of extremely low LIR values. Even if it falls out of the scope of this thesis, more tests with standard LIR should be performed in order to confirm or dismiss this hypothesis.

	Brinch Hansen / ANAC.		Brinch Hansen / Taylor		ANAC./Taylor	
	bias	r^2	bias	r^2	bias	r^2
B0T1	0.84532	-0.17889	0.14891	-0.60798	0.24499	-0.25708
B0T2	0.42293	-0.50898	0.13699	-0.59312	0.15151	-1.7909
B0T3	0.58867	0.56728	0.23212	0.15798	0.39066	-0.13672
B0T4	1.1406	-0.95636	0.24932	-0.84323	0.19983	0.16441
B1T1	0.53517	0.87759	0.19167	0.87489	0.35501	0.88943
B1T2	0.45408	0.41834	0.2097	0.85336	0.42386	0.64941
B1T3	0.53805	0.94838	0.2036	0.94407	0.37772	0.96981
B1T4	0.067089	0.42695	0.096671	0.2908	1.1237	0.29949
B2T1	0.54846	0.51678	0.3441	0.28528	0.49584	-0.05689
B3T1	0.54935	0.61494	0.20692	0.97711	0.35876	0.75383
B3T2	0.27743	0.23775	0.12067	0.071315	0.36165	-0.30311

Table 6.2. Consolidation index correlation factors for the different methods and tests.

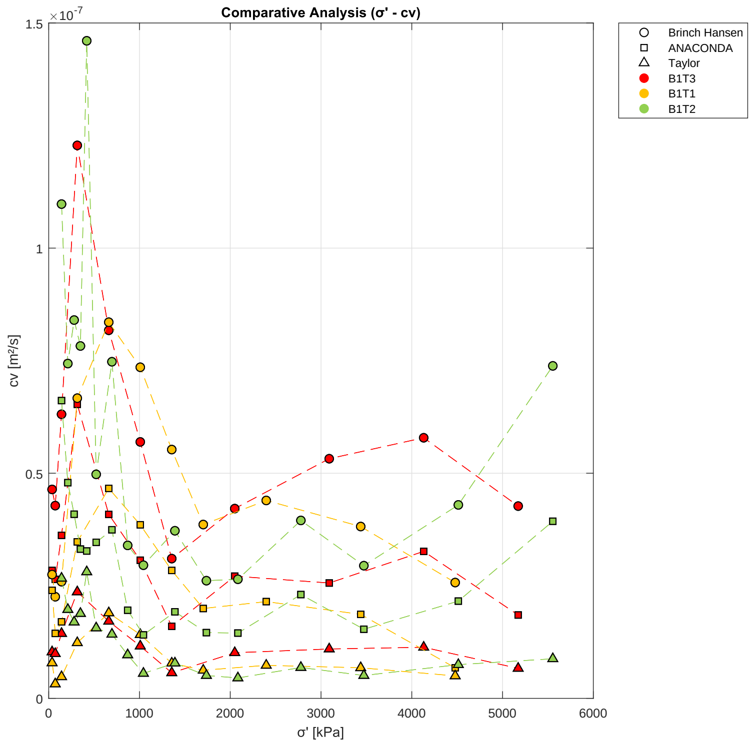

Figure 6.16. Consolidation coefficient values for tests B1T1, B1T2 and B1T3.

6.2.4 Secondary compression index

For the secondary compression index c_α, the analysis is limited to the two methods that give an insight on this parameter; ANACONDA and Brinch Hansen.

If the two methods are compared, as seen in Figure 6.17, there is a clear tendency occurring. ANACONDA method gives values higher than Brinch Hansen in a consistent and very defined way. The correlation has a bias of 1.927 and a r^2 of 0.9.

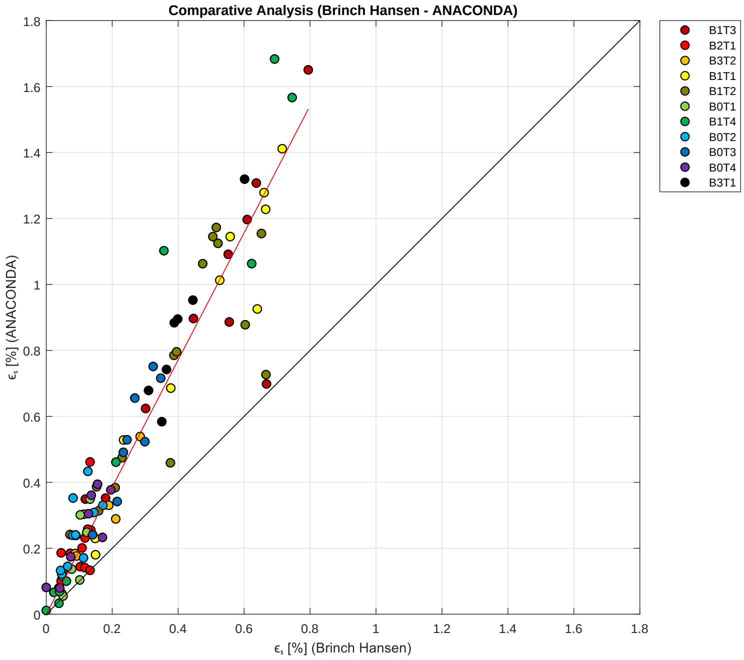

Figure 6.17. Secondary compression index correlation between ANACONDA and Brinch Hansen methods

It is important to notice that each method calculates c_α in a different way. Brinch Hansen's method considers this value directly as the slope of the creep tail, while ANACONDA has a more complex approach. ANACONDA method input it is not as intuitive as Brinch Hansen's. The requirement to specify the number of data points affected by creep leads to an manual, iterative process that requires experience to discern.

To ascertain if misinterpretation of the method is the cause of this difference, a sensitivity analysis has been performed for the whole test set. For this analysis, ANACONDA method has been used in every load step, varying the main input: the number of creep points. This number changes from 2 points, the minimum, until half of the data set. This is enough to reach the consolidation curve and include all possible creep points.

The outcome can be seen in Figure 6.18. It can be seen that, even if there are points around 1, the most frequent values occur around 2. It could be argued that, even if the stable value tends to be 2, each load step could give the value corresponding to 1 when the optimum value of points is reached. However, when looking at plot a) of individual tests, in Figure 6.18 it remains clear that these values happen only in several load steps and have the same value for different amounts of creep points. The conclusion is that, even if user input does in fact affect the value of c_{alpha}, there is a clear tendency for this parameter to be around 2 times the value from Brinch Hansen's method.

Going back to the theoretical basis of both methods, an explanation can be found for

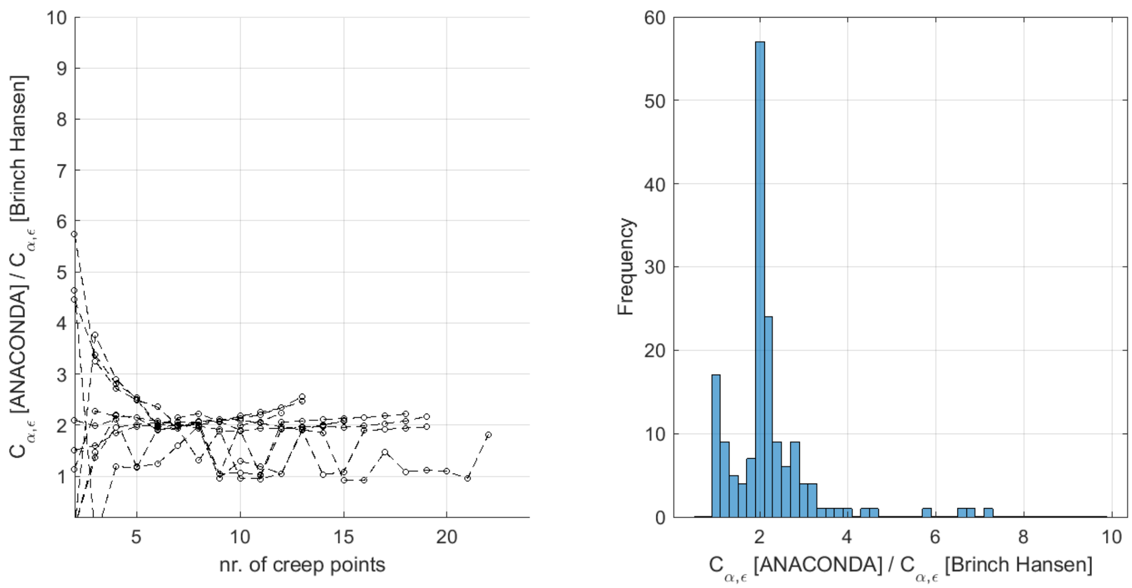

Figure 6.18. Set of plots from test B1T3, showing: a) Inididual outcomes of $c_{\alpha,\epsilon,ANACONDA}/c_{\alpha,\epsilon,BrinchHansen}$ for a variation of creep points in ANACONDA method; b) Histogram of values from plot 'a'.

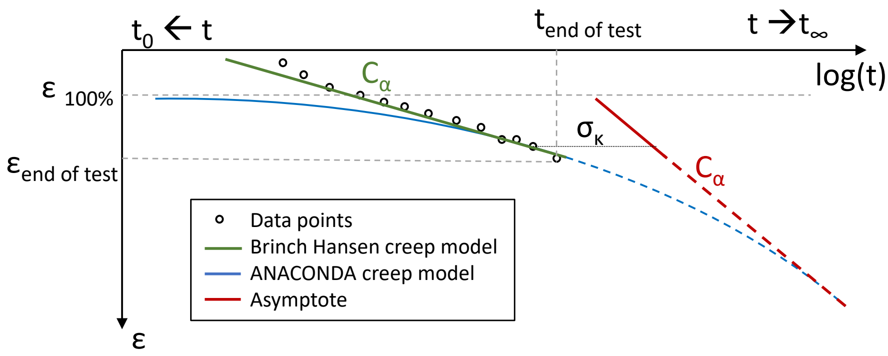

Figure 6.19. Comparison of creep models by Brinch Hansen and ANACONDA

this behaviour. Each method has a different concept of what defines C_α. On one hand, Brinch Hansen's method assumes that creep behaves linearly once the tail of the test has been reached. Being consolidation non-existent, C_α can be obtained as the slope of the points that conform such tail. On the other hand, ANACONDA treats creep as a non-linear process that *tends* to an ideal state that can never be reached. Instead of obtaining C_α from the actual data, ANACONDA tries to predict the final state of creep strains by defining its asymptote.

An example is shown in Figure 6.19, where Brinch Hansen's method uses the current data to obtain C_α while ANACONDA tries to fit the asymptote. If the test duration was prolonged, the value from Brinch Hansen would slowly tend to the one given by ANACONDA.

The conclusion from this comparison is that, even if Brinch Hansen accurately describes the creep process occurring in the short term after the consolidation process, ANACONDA would describe long term creep more accurately and, in general, be more conservative.

However, the only way to actually confirm or dismiss this idea is to perform consolidation tests with extremely high duration or compare the outcome from each model with on-site data from monitored structures. Both options remain out of the scope of this thesis, and remain as a suggestion

Discussion on pre-consolidation stress methods 7

7.1 Janbu method

From the analysis performed on the test samples, the most clear conclusion is that Janbu's method outcomes are consistently diverging from the rest of the methods.

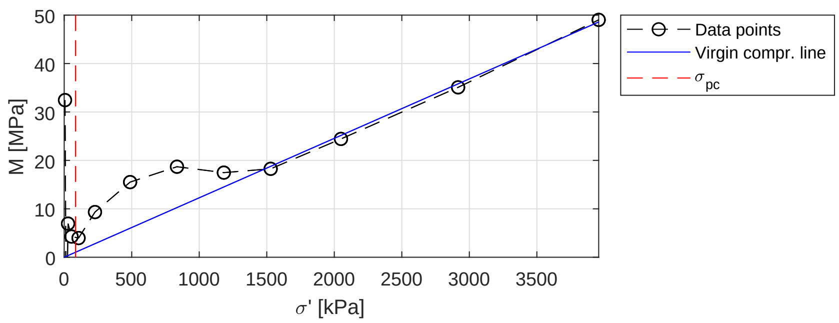

Figure 7.1. Janbu's method applied to Test B1T1

When applying Janbu's method, as for example in Figure 7.1 for Test B1T1, the minimum value for the tangent modulus M is achieved at extremely low loads, leading to significantly low values of σ_{pc}. When compared to the rest of the methods, the divergence seems clear, as seen in Figure 7.2. Not only Janbu's method offers different results, but a simple visual evaluation of the stress-strain curve indicates that the intersection between the virgin compression line and the re-compression line occurs in the proximity of the σ_{pc} values given by the rest of the methods.

The example given is for Test B1T1, but this behaviour repeats itself for all tests in a consistent way. If the outputs from all tests are compared against other methods, e.g. Pachecho Silva and Akai in Figure 7.3, a clear and well defined tendency can be appreciated.

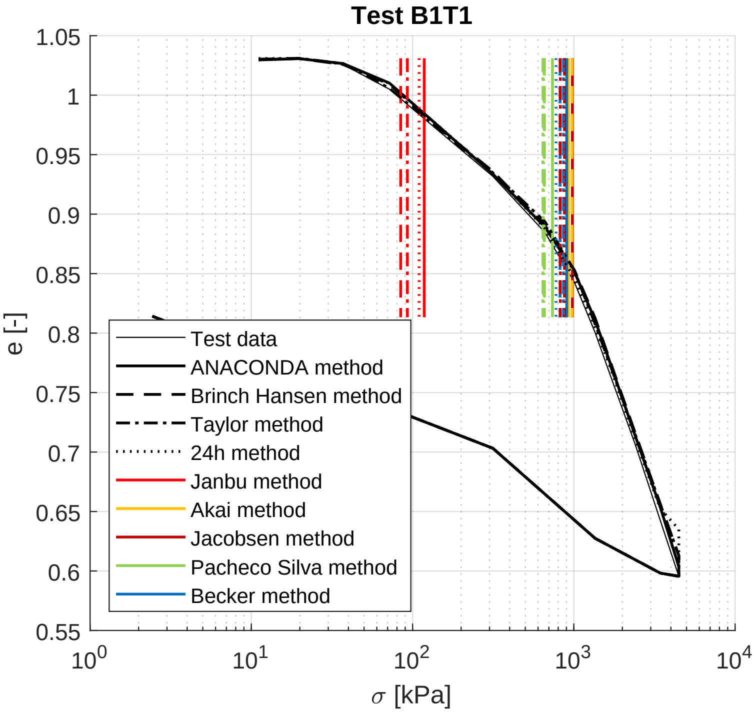

Figure 7.2. Results from pre-consolidation stress analysis of test B1T1.

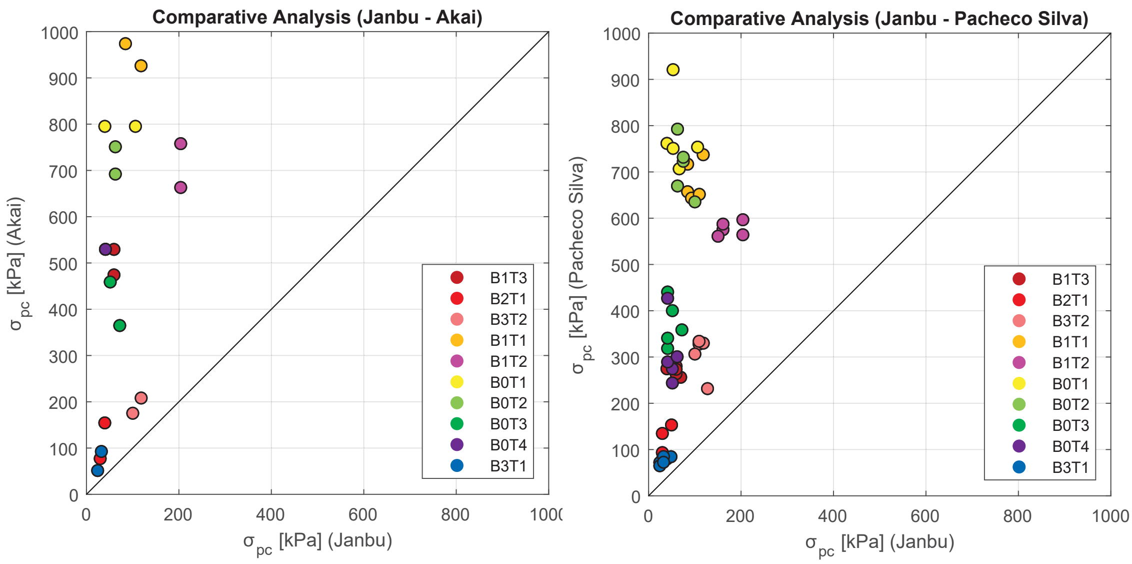

Figure 7.3. Brinch Hansen method main parameters in $\sqrt{t}$-$log(t)$ axis

Observing the tangent modulus curve presented in 7.1, it seems that the outcome of the tests does not follow the indications given by [Janbu, 1963]. According to [Kjell Karlsrud and Hernandez-Martinez, 2013], this shape may be a consequence of sample disturbance. Karlsrud suggests that poor sample quality can be appreciated by a reduction of the initial horizontal line defined by the initial tangent modulus M_0, and an increase of the minimum tangent modulus, M_L, before converging to the virgin compression line. An example can be appreciated in Figure 7.4, where the sample labelled as "Block" is undisturbed, while sample labelled as "54mm" is highly disturbed. Curve from Figure 7.1 is shaped like the disturbed sample from Figure 7.4, rather than the undisturbed one.

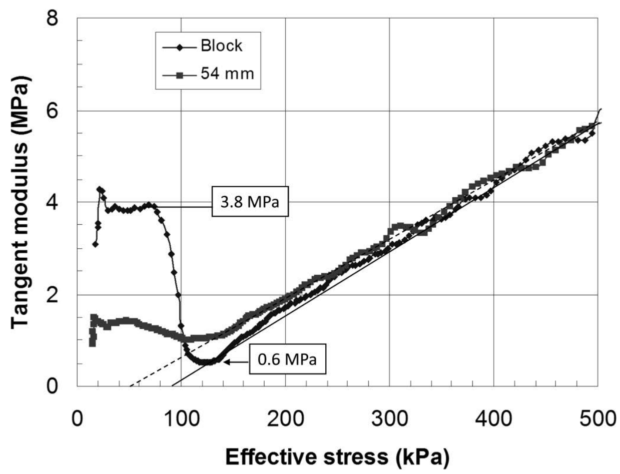

Figure 7.4. Example of triaxial test results on block sample versus 75 and 54 mm samples, Onsøy clay [Kjell Karlsrud and Hernandez-Martinez, 2013].

The consequence of this is that the whole analysis performed in Chapter 5 regarding Janbu's method is not correct, as the minimum tangent modulus was not properly identified. Following the indications from Figure 7.4, σ_{pc} should be found, for B1T1, around 1000 kPa, as displayed in Figure 7.5.

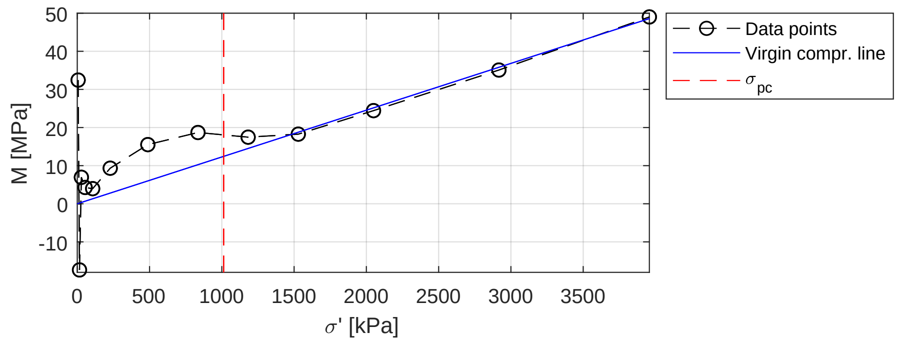

Figure 7.5. Janbu's method applied to Test B1T1, following the indications from [Kjell Karlsrud and Hernandez-Martinez, 2013].

This correction leaves the output from Janbu's method closer to the rest of the methods. However, it does not seem possible to accurately interpret σ_{pc} from Figure 7.5, as there is only two values to define M_0,M_L, and the critical area between both points. All studied tests suffer this situation. Some tests, e.g. Test B0T3 in Figure 7.6 do not even present any resemblance with the curves shown Figure 7.4, making impossible the identification of M_0 or M_L and misleading the interpretation.

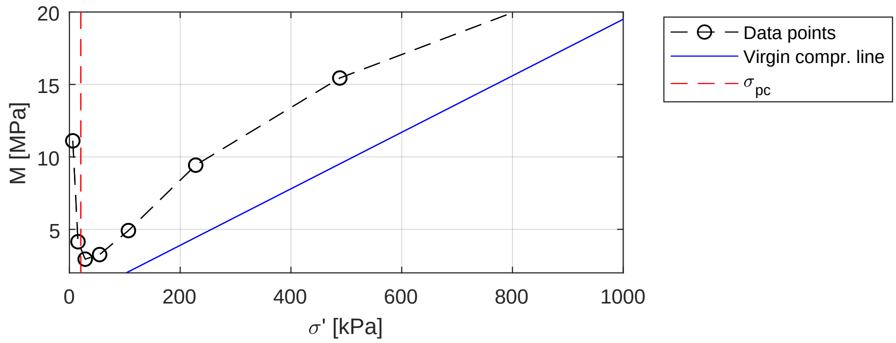

Figure 7.6. Zoom of Janbu's method on Test B0T3, displaying the area prior to convergence with the virgin compression line. σ_{pc} can be found around 400-450 kPa according to other interpretation methods.

7.2 Akai, Pacheco Silva, Jacobsen and Becker methods

Leaving out Janbu's method from the comparison, results seem satisfactory when studying the correlations between methods, with the exception of several outliers. Graphical comparisons can be seen in Figures 7.7, 7.8 and 7.9.

		Janbu	Akai	Pacheco Silva	Jacobsen	Becker
Janbu	b	-	-	-	-	-
	r^2	-	-	-	-	-
Akai	b	0.191	-	-	-	-
	r^2	0.171	-	-	-	-
Pacheco Silva	b	0.154	0.831	-	-	-
	r^2	0.187	0.823	-	-	-
Jacobsen	b	0.142	0.965	0.836	-	-
	r^2	0.415	0.866	0.786	-	-
Becker	b	0.107	0.997	0.794	0.888	-
	r^2	0.012	0.58	0.867	0.44	-

Table 7.1. Correlation factors of all σ_{pc} methods

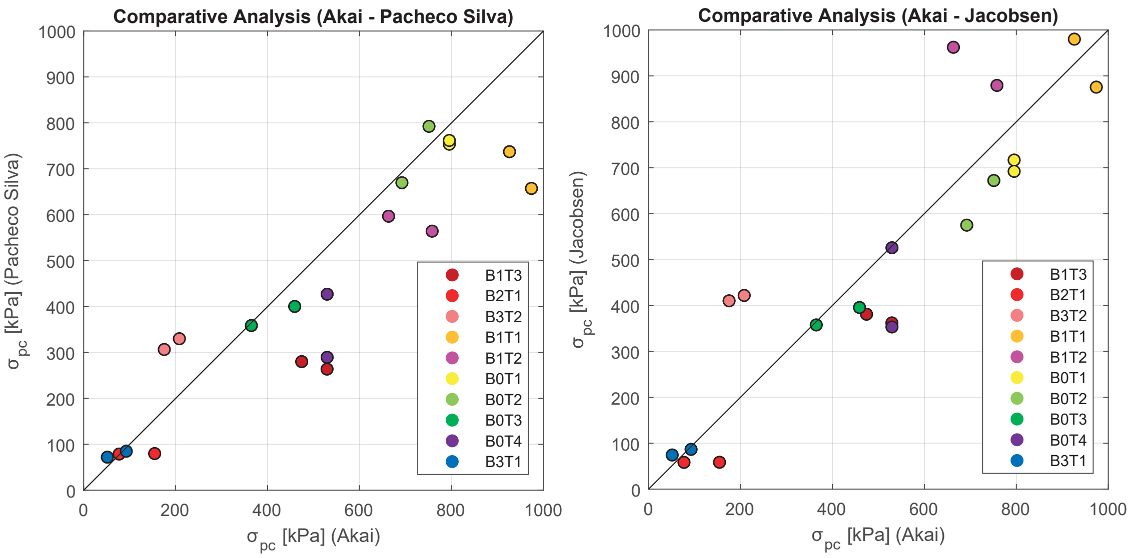

Figure 7.7. Comparison of Akai-Pacheco Silva methods (left) and Akai-Jacobsen methods (right)

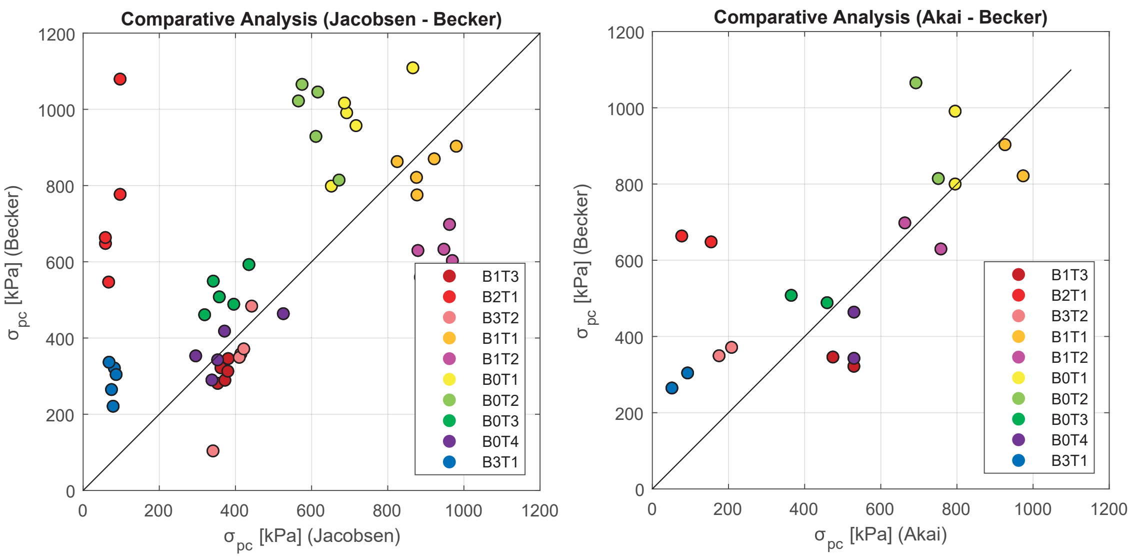

Figure 7.8. Comparison of Jacobsen-Becker methods (left) and Akai-Becker methods (right)

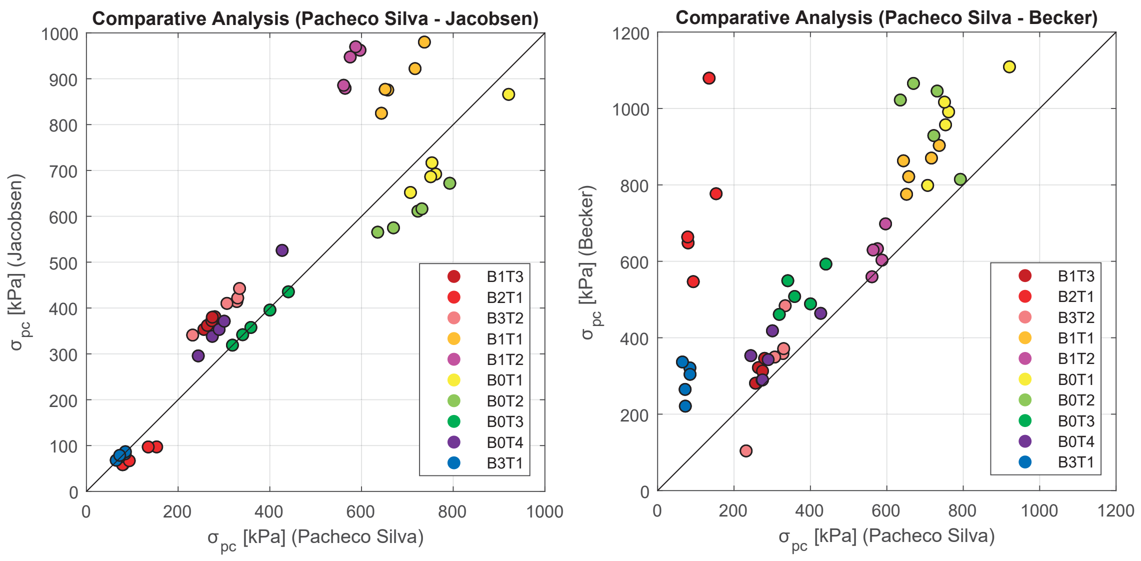

Figure 7.9. Comparison of Jacobsen-Becker methods (left) and Akai-Becker methods (right)

There are two particularities to notice in this comparison, corresponding to Tests B2T1 and Tests B3T1 (marked in the graphs in blue and red, respectively) for Becker's method. In these cases, the σ_{pc} predicted by this method results in a extremely high value compared to the rest of the methods. This can be seen in Figure 7.10. Here, it can be appreciated that Janbu's method is still giving low values, while Akai, Jacobsen and Pacheco Silva give similar values and Becker's method presents higher value. A particularity of these curves is that they present a slow transition from the presumed reloading curve to the virgin compression curve. Transition that seems to occur in a point of low stress,around 100 kPa, in accordance with the results from Akai, Jacobsen and Pacheco Silva methods.

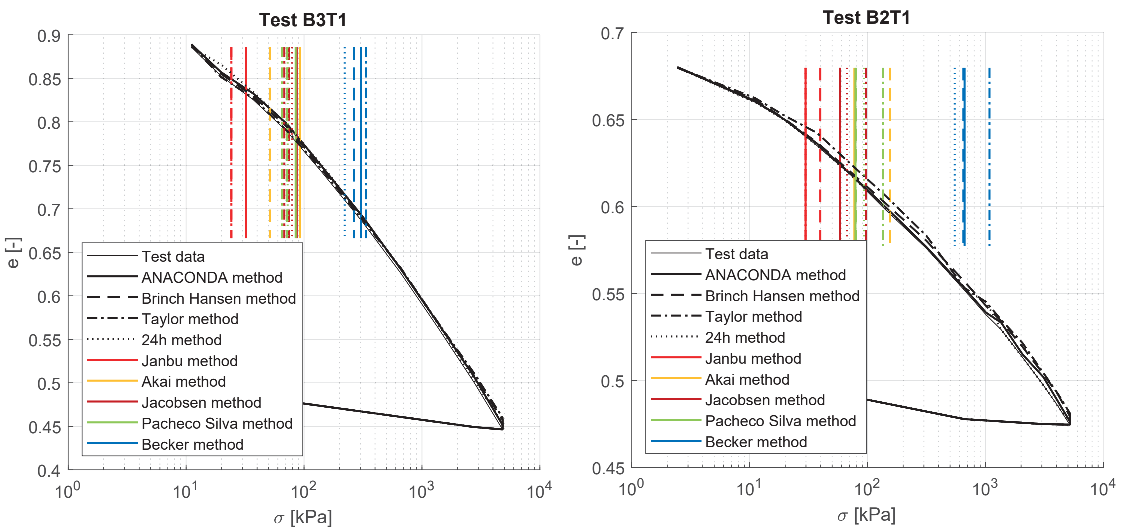

Figure 7.10. Results from pre-consolidation stress analysis of Tests B3T1 (left) and B2T1 (right)

Observing the work curve for Test B3T1, as appreciated in Figure 7.11, leads to the fact that the transition from the pre-yield line to the post yield line is smooth, complicating the interpretation of $\sigma_p c$. While the post-yield line uses multiple points to fit, allowing to identify outliers, there are few points capable of fitting the pre-yield line. Some of these points present poor readings and high disturbance, as during the consolidation test the sample is still adapting to the external ring. The combination of these factors could produce high variability in the pre-yield line and, therefore, lead to inaccurate values of σ_{pc}.

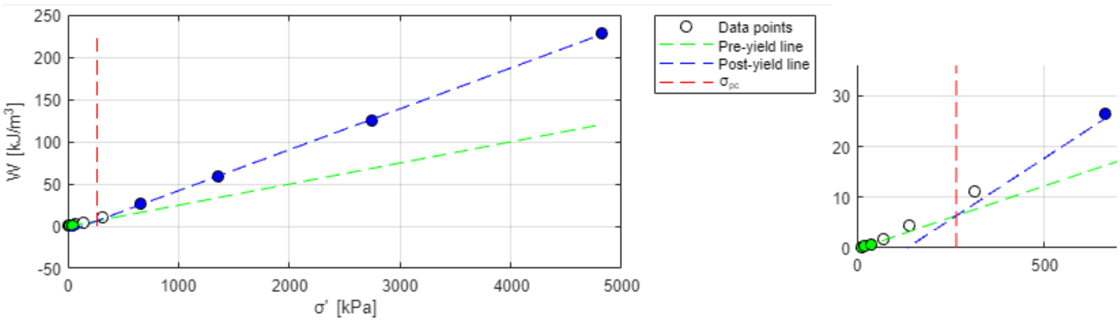

Figure 7.11. Results from pre-consolidation stress analysis of Tests B3T1 (left) and B2T1 (right)

7.3 Soil disturbance

Interpretation of Janbu's method in Section 7.1 leads to the idea that soil samples could be highly disturbed in the part prior, and surrounding, the pre-consolidation stress. This can be confirmed following Karlsrud's recommendation of using a criterion proposed by [Lunne and Strandvik, 1997] in which sample quality is assessed based on the normalized change in void ratios, $\Delta e/e_0$; and a criterion proposed by Karlsrud correlating sample quality with the ratio M_0/M_L. These criteria are summarized in Table 7.2.

Implementation of Karlsrud and Lunne criteria to the soil data used in this thesis can be seen in Figure 7.3. According to it, all samples are highly disturbed. If true, this fact makes interpretation of $sigma_{pc}$ unreliable, specially for methods that, like Janbu's, focus on the study of the over-consolidated state of the soil. This includes Becker's method, which uses this data to conform the pre-yield line, as well as Akai's method. Jacobsen and Pacheco Silva methods are still expected to present high correlation even with a disturbed sample, as both take the shape of the $log_{10}(\sigma) - \epsilon$ curve as a basis, and both are inspired by the original Casagrande's graphical method.

However, it does not seem possible to confirm the variation of the values of σ_{pc} obtained in this thesis from the ones obtained from the values obtained in an undisturbed sample.

Sample quality	$\Delta e/e_0$	M_0/M_L
Very good to excellent	0–0.04	>2
Good to fair	0.04–0.07	1.5-2
Poor	0.07–0.14	1-1.5
Very Poor	>0.14	<1

Table 7.2. Criteria to assess sample quality based on Lunne and Karlsrud reccomendations.

Test	Lunne		Karlsrud	
	$\Delta e/e_0$	Quality	M_0/M_L	Quality
B0T1	0.21651	Very Poor	<1	Very Poor
B0T2	0.25021	Very Poor	<1	Very Poor
B0T3	0.40301	Very Poor	<1	Very Poor
B0T4	0.32913	Very Poor	<1	Very Poor
B1T1	0.42275	Very Poor	1.1	Poor
B1T2	0.41927	Very Poor	1.16	Poor
B1T3	0.60289	Very Poor	1.1	Poor
B1T4	0.24652	Very Poor	1.43	Poor
B2T1	0.30215	Very Poor	<1	Very Poor
B3T1	0.49841	Very Poor	<1	Very Poor
B3T2	0.28468	Very Poor	<1	Very Poor

Table 7.3. Quality of consolidation tests according to Karlsrud and Lunne criteria.

Conclusion 8

8.1 Strain separation methods

Several particularities appear during this analysis, hampering the interpretation.

First, it seems that most of the tests were performed with variable and, in some cases, extremely low values of load increment ratios. This has as a consequence the difficulty and, in some cases, impossibility, to use strain separation methods. Brinch Hansen's method seems specially affected by this issue, being impossible to obtain solutions for certain steps. Additionally, this circumstance questions the validity of some of the parameters, specifically the coefficient of consolidation, as the consolidation process may not be fully occurring in some steps.

Second, the properties of the settlement curves of some tests questions the traditional determination of initial consolidation strain, as it can mislead the deformation prediction during the start of the consolidation process. Instead, an alternative is proposed in which the initial consolidation strain is obtained from the data set; and the consolidation process experiments a time delay over a prediction done with Terzaghi's theory.

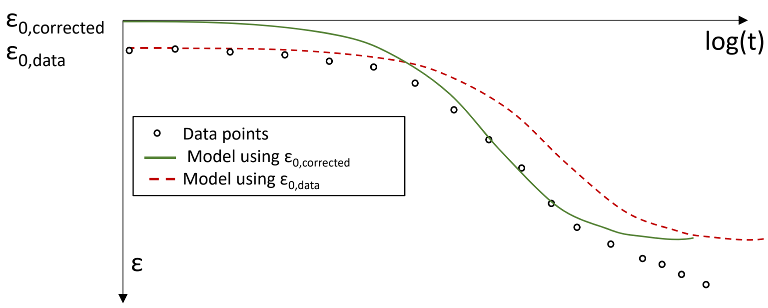

Figure 8.1. Model variation produced by the different criterion to define the initial consolidation settlement

Finally, there is a conceptual difference in the definition of secondary compression index between Brinch Hansen's method and ANACONDA. While Brinch Hansen defines it as the slope of the settlement tail and expects that this slope is constant, ANACONDA treats the secondary compression index as an asymptote to which the settlement curve tends.

From a practical point of view, after running all 4 methods on multiple test, it can not be said that there is a "better" method, but rather that each method works better under certain set of circumstances. While, for example, Brinch Hansen and ANACONDA lead to more complete results, both require a significant amount of time dedicated to each time step, while 24h or Taylor methods can offer results much faster. Main characteristics have been summarized as follows:

- 24h
  - Objective: Determination of the stress-strain curve and tangent modulus. Oriented to calculation of pre-consolidation stress and stress-strain analysis.
  - Advantages: Fast and automatic.
  - Limitations: Unable to obtain consolidation or creep parameters.
  - Source of errors: Tests that take long time to consolidate can lead to wrong results and spikes in the stress-strain curve.
- Taylor
  - Objective: Determination of consolidation parameters. Oriented to soils that do not present a significant amount of creep.
  - Advantages: Simple and intuitive. Allows to obtain consolidation parameters even if the consolidation curve is not completely finished. Works with tests of short duration.
  - Limitations: Unable to obtain creep parameters. Highly sensitive to noise in the area surrounding the end of consolidation.
  - Source of errors: Fitting line can be difficult to establish if the data does not form a clear straight section.
- Brinch Hansen
  - Objective: Determination of consolidation and creep parameters. Oriented to soils that present significant creep.
  - Advantages: Intuitive and easy to set up looking at the consolidation curve.
  - Limitations: Tests with insufficient data or low LIR values can prevent the method from working. Requires long duration tests to accurately define creep. Otherwise is very sensitive to data noise and errors in the tail of the curve.
  - Source of errors: Consolidation fitting line can be difficult to define if the data does not form a clear straight section. Creep fitting line can be difficult to define if the test does not run for enough time to get multiple creep data points.
- ANACONDA
  - Objective: Determination of consolidation and creep parameters. Oriented to soils that present significant creep, especially where study of long-term creep is essential.
  - Advantages: Model allows for prediction of long term creep. It can offer solutions even with bad quality data.
  - Limitations: Requires long duration tests to accurately define creep.
  - Source of errors: Interpretation is complex, solution is not intuitive. Requires a process of trial and error to find the best solution.

However, the analysis performed presents several limitations. The low LIR values of most tests makes the evaluation of the consolidation parameters, specifically the consolidation coefficient, inaccurate.

8.2 Pre-consolidation stress methods

From the study concerning the analysis of the pre-consolidation stress, evidence suggests that soil data could present disturbance, hampering the interpretation of different methods and questioning the validity of the results obtained.

Janbu's method seems incapable to offer a solution in this situation, having been discarded from the comparative analysis. The rest of the methods are still able to offer solutions that are, to a point, concordant between themselves. The exception is Becker's method in specific cases of low curvature in the test. Akai, Pacheco Silva and Jacobsen method offer similar results for most situations.

A new comparative analysis with less disturbed samples could improve the determination of σ_{pc} and lead to better results. It has been proved by multiple research papers, e.g. [Becker et al., 1987], [Paniagua, 2016] or [Boone, 2010] the high correlation of these methods when working with high quality samples. This analysis gives an insight on the issues and limitations these methods can run into when applied to more disturbed samples and when performed by someone less experienced.

In practice, there does not seem to exist a more precise method. Determination of σ_{pc} should be done by comparing several methods to obtain a consistent, shared value. An important element of the analysis is that an iterative approach significantly improves convergence between different methods and reduces user error. Methods should not be used in an isolated way, but under constant comparison with the rest of them to find the solution that satisfies most of them.

Bibliography

Akai, 1960. K. Akai. *De strukturellen Eigenschaften von Schluft Mitteilugen (in German)*. 1960.

ASTM International, 2011. ASTM International. *ASTM D2435 - Standard Test Methods for One-Dimensional Consolidation Properties of Soils Using Incremental Loading*. 2011.

Becker et al., 1987. D.E Becker, J.H.A. Crooks, K.Been and M.G. Jefferies. *Work as a criterion for determining in situ and yield stresses in clays*. 1987.

Boone, 2010. S.J. Boone. *A critical reapraisal of preconsolidation pressure interpretations using the oedometer test*. 2010.

Brinch Hansen, 1961a. J. Brinch Hansen. *A model law for simultaneous primary and secondary consolidation*. 1961.

Brinch Hansen, 1961b. J. Brinch Hansen. *Rapport no.6, Aalborg Limfjordsforbindelse. Bundundersøgelser*, 1961b.

Casagrande, 1936. A. Casagrande. *The determination of the Pre-Consolidation Load and its practical significance*. 1936.

Google, 2018. Google. *Google Earth Pro*, 2018.

Grønbech et al. G.L. Grønbech, L.B. Ibsen and B.N. Nielsen. *Interpretation of Consolidation test on Tertiary Clay*.

Holtz and Kovacs, 1982. Robert D. Holtz and William D. Kovacs. *An introduction to geotechnical engineering*. ISBN: 0-13-484394-0, Handbook. Prentice Hall, 1982.

Jacobsen, 1992. H.M. Jacobsen. *Bestemmelse af forbelastningstryk i laboratoriet (in Danish)*. 1992.

Janbu, 1963. N. Janbu. *Soil compressibility as determined by oedometer and triaxial tests*. 1963.

Kjell Karlsrud and Hernandez-Martinez, 2013. K. Kjell Karlsrud and F.G. Hernandez-Martinez. *Strength and deformation properties of Norwegian clays from laboratory tests on high-quality block samples*. 2013.

Lunne and Strandvik, 1997. Berre T. Lunne, T. and S. Strandvik. *Sample disturbance effects in soft low plastic Norwegian clays*. 1997.

Pacheco Silva, 1970. F. Pacheco Silva. *A new graphical construction for determination of the pre-consolidation stress of a soil sample*. 1970.

Paniagua, 2016. P. Paniagua. *Study on the practices for preconsolidation stress evaluation from oedometer tests*. 2016.

Taylor, 1948. D.W. Taylor. *Fundamentals of Soil Mechanics*. 1948.

Thorsen, 2006. Grete Thorsen. *Nørre Lyngby. Konsolideringsforsøg*, 2006.

Vestergaard, 2007. Kenneth Vestergaard. *Excel spreadsheet calculator for ANACONDA [untitled]*, 2007.

A Results from strain separation analysis

In this appendix the raw data obtained from the strain separation analysis is shown, distributed along the different tests. Each test shows the analysis outcome in an initial picture and data tables for each of the methods used.

A.1 Superficial samples

A.1.1 Test B0T1

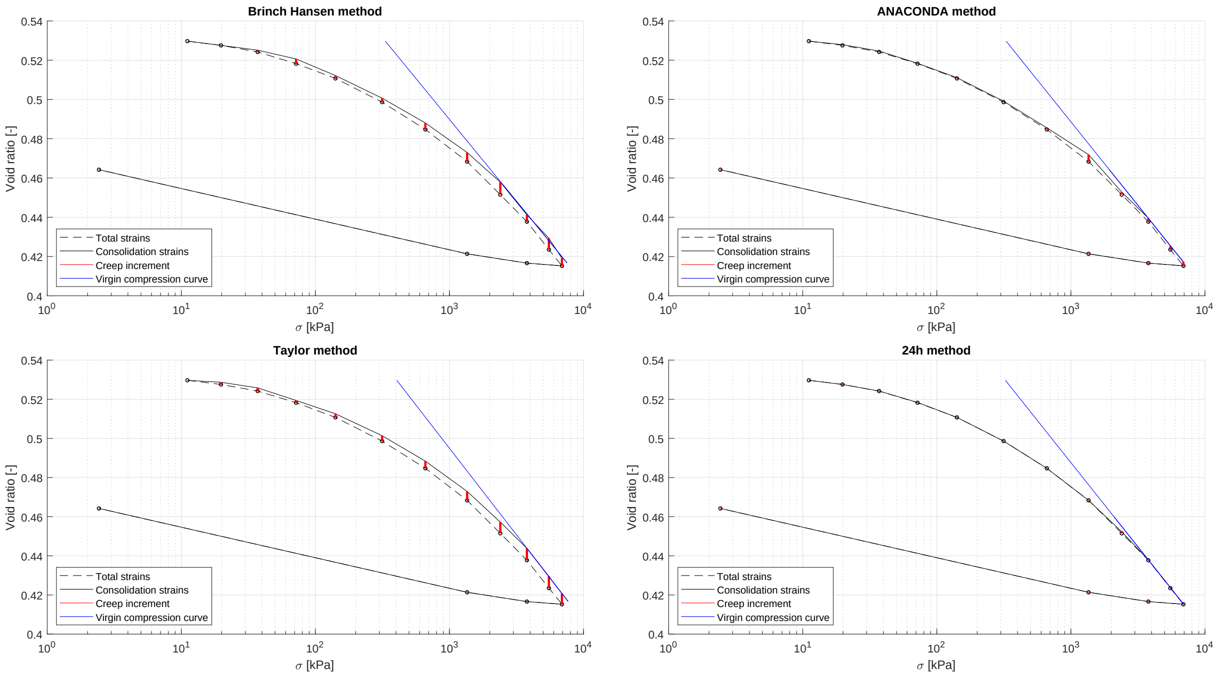

Figure A.1. Results from analysis of test B0T1.

	σ $[kPa]$	e_t [-]	e_{100} [-]	ϵ_{cr} [%]	c_v $[m^2/s]$	$c_{\alpha,\epsilon}$ [%]	M [kPa]
1	11.1	0.52969	0.52969	-3.4694 10^{-18}	0.00029298	-1.3793 10^{-18}	55313.1179
2	19.78	0.52755	0.52755	-2.7756 10^{-17}	2.3961 10^{-05}	-6.3174 10^{-18}	6199.6599
3	37.12	0.52419	0.52511	0.060381	2.9465 10^{-06}	0.0292	10862.1585
4	71.82	0.51822	0.52062	0.169	2.7561 10^{-05}	0.046952	11833.99
5	141.21	0.51072	0.51216	0.09417	5.4211 10^{-06}	0.037946	12548.5328
6	314.69	0.49863	0.50066	0.13217	7.4001 10^{-06}	0.050996	23069.4567
7	661.65	0.48471	0.48802	0.21848	1.2363 10^{-05}	0.077106	41995.7693
8	1355.56	0.46834	0.47296	0.30211	2.2787 10^{-05}	0.10152	70526.5224
9	2396.44	0.45151	0.45791	0.42371	1.772 10^{-05}	0.12291	105779.1605
10	3784.27	0.43774	0.44119	0.21459	4.182 10^{-06}	0.090152	127021.76
11	5519.06	0.42351	0.42932	0.36999	9.1733 10^{-06}	0.13288	223639.1525
12	6906.89	0.41525	0.41908	0.23863	3.5986 10^{-06}	0.10319	207235.4451
13	3784.27	0.41663	-	-	-	-	-
14	1355.56	0.42137	-	-	-	-	-
15	2.43	0.46421	-	-	-	-	-

Table A.1. Results from analysis of test B0T1 using Brinch Hansen method.

	σ [kPa]	e_t [-]	e_{100} [-]	ϵ_{cr} [%]	c_v [m^2/s]	$c_{\alpha,\epsilon}$ [%]	M [kPa]
1	11.1	0.52969	0.52969	-1.0786 10^{-17}	0.00041384	-3.7154 10^{-15}	55500
2	19.78	0.52755	0.52791	0.024496	5.0041 10^{-06}	0.066334	7430.1807
3	37.12	0.52419	0.52467	0.028097	1.3084 10^{-05}	0.057585	8196.7881
4	71.82	0.51822	0.51843	0.022562	9.9065 10^{-06}	0.063703	8503.8747
5	141.21	0.51072	0.5111	0.026377	1.0031 10^{-05}	0.079484	14493.9644
6	314.69	0.49863	0.49913	0.033161	1.977 10^{-05}	0.055155	22168.9518
7	661.65	0.48471	0.48555	0.054998	1.7257 10^{-05}	0.13692	39102.8445
8	1355.56	0.46834	0.47187	0.23002	3.0799 10^{-05}	0.10389	77587.1477
9	2396.44	0.45151	0.4528	0.088577	8.1476 10^{-06}	0.24838	83515.0434
10	3784.27	0.43774	0.43951	0.11293	8.0454 10^{-06}	0.23898	159744.0893
11	5519.06	0.42351	0.42539	0.12161	4.3589 10^{-06}	0.34904	187957.582
12	6906.89	0.41525	0.41732	0.13174	1.5458 10^{-06}	0.30123	263107.0918
13	3784.27	0.41663	-	-	-	-	-
14	1355.56	0.42137	-	-	-	-	-
15	2.43	0.46421	-	-	-	-	-

Table A.2. Results from analysis of test B0T1 using ANACONDA method.

	σ [kPa]	e_t [-]	e_{100} [-]	ϵ_{cr} [%]	c_v [m^2/s]	$c_{\alpha,\epsilon}$ [%]	M [kPa]
1	11.1	0.52969	0.52966	-0.0022222	4.7118 10^{-05}	-	49949.9387
2	19.78	0.52755	0.52867	0.073335	1.6348 10^{-05}	-	13469.3502
3	37.12	0.52419	0.52581	0.10631	1.8152 10^{-05}	-	9271.5114
4	71.82	0.51822	0.51938	0.075824	2.5365 10^{-07}	-	8252.3369
5	141.21	0.51072	0.51257	0.12082	1.2998 10^{-06}	-	15593.1167
6	314.69	0.49863	0.50138	0.17917	2.5871 10^{-06}	-	23710.7958
7	661.65	0.48471	0.48838	0.23965	2.8491 10^{-06}	-	40842.0627
8	1355.56	0.46834	0.47291	0.29874	3.4039 10^{-06}	-	68642.1464
9	2396.44	0.45151	0.45722	0.37338	1.7331 10^{-06}	-	101513.3789
10	3784.27	0.43774	0.44381	0.39659	4.8086 10^{-06}	-	158284.7549
11	5519.06	0.42351	0.42952	0.39265	1.5784 10^{-06}	-	185750.6683
12	6906.89	0.41525	0.42067	0.35429	7.2493 10^{-06}	-	239956.1997
13	3784.27	0.41663	-	-	-	-	-
14	1355.56	0.42137	-	-	-	-	-
15	2.43	0.46421	-	-	-	-	-

Table A.3. Results from analysis of test B0T1 using Taylor method.

	σ	e_t	e_{100}	ϵ_{cr}	c_v	$c_{\alpha,\epsilon}$	M
	$[kPa]$	[-]	[-]	[%]	$[m^2/s]$	[%]	[kPa]
1	11.1	0.52969	0.52969	0	$2.0415\ 10^{-14}$	-	55500
2	19.78	0.52755	0.52755	$1.9429\ 10^{-16}$	$2.0394\ 10^{-14}$	-	6200
3	37.12	0.52419	0.52419	0	$2.0329\ 10^{-14}$	-	7881.8182
4	71.82	0.51822	0.51837	0.01	$2.0223\ 10^{-14}$	-	9131.5789
5	141.21	0.51072	0.51072	$-1.9984\ 10^{-15}$	$2.0051\ 10^{-14}$	-	13878
6	314.69	0.49863	0.49863	$-8.8818\ 10^{-16}$	$1.9826\ 10^{-14}$	-	21959.4937
7	661.65	0.48471	0.48471	$2.6645\ 10^{-15}$	$1.9497\ 10^{-14}$	-	38127.4725
8	1355.56	0.46834	0.46834	0	$1.912\ 10^{-14}$	-	64851.4019
9	2396.44	0.45151	0.45228	0.05	$1.8702\ 10^{-14}$	-	99131.4286
10	3784.27	0.43774	0.43789	0.01	$1.829\ 10^{-14}$	-	147641.4894
11	5519.06	0.42351	0.42382	0.02	$1.7941\ 10^{-14}$	-	188564.1304
12	6906.89	0.41525	0.4154	0.01	$1.7623\ 10^{-14}$	-	252332.7273
13	3784.27	0.41663	-	-	-	-	-
14	1355.56	0.42137	-	-	-	-	-
15	2.43	0.46421	-	-	-	-	-

Table A.4. Results from analysis of test B0T1 using 24h method.

A.1.2 Test B0T2

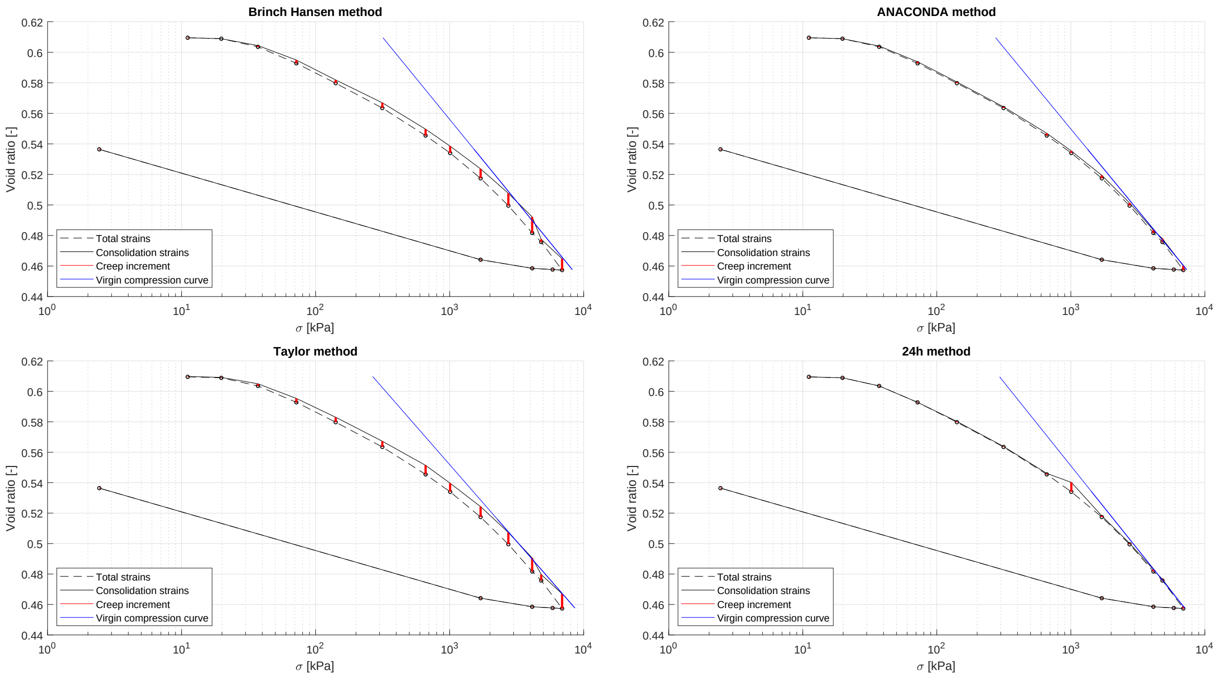

Figure A.2. Results from analysis of test B0T2.

	σ $[kPa]$	e_t [-]	e_{100} [-]	ϵ_{cr} [%]	c_v $[m^2/s]$	$c_{\alpha,\epsilon}$ [%]	M [kPa]
1	11.1	0.60952	0.60952	-4.8572 10^{-17}	6.6203 10^{-06}	-2.0174 10^{-17}	29097.0726
2	19.78	0.60887	0.60887	1.3878 10^{-17}	1.8323 10^{-05}	6.9892 10^{-18}	21687.6115
3	37.12	0.60356	0.60438	0.052924	6.3115 10^{-06}	0.020949	6216.3925
4	71.82	0.59277	0.5949	0.13208	1.1837 10^{-05}	0.047102	5891.4285
5	141.21	0.57973	0.58187	0.13299	8.0297 10^{-06}	0.043499	8576.4689
6	314.69	0.56347	0.56691	0.21399	1.9023 10^{-05}	0.064995	18669.422
7	661.65	0.54544	0.54963	0.26154	1.7294 10^{-05}	0.080039	32331.7047
8	1008.61	0.53401	0.53852	0.2806	9.2414 10^{-06}	0.088728	50246.0892
9	1702.52	0.51743	0.52362	0.38474	2.3519 10^{-05}	0.11293	74986.891
10	2743.4	0.49955	0.50763	0.50559	2.9138 10^{-05}	0.14461	104831.7681
11	4131.23	0.48168	0.49216	0.65602	3.8525 10^{-05}	0.17167	144396.0046
12	4825.14	0.47573	0.4775	0.10627	1.7672 10^{-07}	0.08126	76203.1083
13	6906.89	0.45737	0.46479	0.42369	1.7764 10^{-05}	0.12629	263801.6321
14	5866.02	0.45769	-	-	-	-	-
15	4131.23	0.4585	-	-	-	-	-
16	1702.52	0.46413	-	-	-	-	-
17	2.43	0.53642	-	-	-	-	-

Table A.5. Results from analysis of test B0T2 using Brinch Hansen method.

	σ	e_t	e_{100}	ϵ_{cr}	c_v	$c_{\alpha,\epsilon}$	M
	$[kPa]$	[-]	[-]	[%]	$[m^2/s]$	[%]	[kPa]
1	11.1	0.60952	0.60952	-4.8326 10^{-17}	6.0759 10^{-07}	-3.7204 10^{-17}	37000
2	19.78	0.60887	0.60887	3.072 10^{-17}	1.8694 10^{-07}	2.8049 10^{-17}	21700
3	37.12	0.60356	0.60409	0.036805	1.1127 10^{-05}	0.069743	5832.7393
4	71.82	0.59277	0.59377	0.064835	3.6189 10^{-05}	0.1214	5417.3692
5	141.21	0.57973	0.5805	0.04785	1.5315 10^{-05}	0.13257	8413.129
6	314.69	0.56347	0.56427	0.052708	1.7638 10^{-05}	0.14508	17216.0913
7	661.65	0.54544	0.54691	0.09296	1.7606 10^{-05}	0.23924	32181.4009
8	1008.61	0.53401	0.53535	0.084279	3.037 10^{-06}	0.24059	48304.849
9	1702.52	0.51743	0.51941	0.12462	8.1876 10^{-06}	0.17085	70104.1482
10	2743.4	0.49955	0.50134	0.11683	5.3765 10^{-06}	0.30845	92729.2775
11	4131.23	0.48168	0.48349	0.11417	2.435 10^{-06}	0.33022	125172.2848
12	4825.14	0.47573	0.47799	0.14266	7.894 10^{-07}	0.3523	203086.6308
13	6906.89	0.45737	0.46012	0.16615	2.2726 10^{-06}	0.4331	187590.1123
14	5866.02	0.45769	-	-	-	-	-
15	4131.23	0.4585	-	-	-	-	-
16	1702.52	0.46413	-	-	-	-	-
17	2.43	0.53642	-	-	-	-	-

Table A.6. Results from analysis of test B0T2 using ANACONDA method.

	σ	e_t	e_{100}	ϵ_{cr}	c_v	$c_{\alpha,\epsilon}$	M
	$[kPa]$	[-]	[-]	[%]	$[m^2/s]$	[%]	[kPa]
1	11.1	0.60952	0.60978	0.016207	4.7134 10^{-06}	-	29260.1771
2	19.78	0.60887	0.60916	0.017778	5.8862 10^{-07}	-	22587.131
3	37.12	0.60356	0.60497	0.087565	1.5798 10^{-06}	-	6663.7767
4	71.82	0.59277	0.59533	0.15901	2.6827 10^{-06}	-	5797.335
5	141.21	0.57973	0.58297	0.20136	2.0622 10^{-06}	-	9039.2123
6	314.69	0.56347	0.56724	0.2339	2.0832 10^{-06}	-	17748.0248
7	661.65	0.54544	0.55138	0.36921	6.3893 10^{-06}	-	35235.7118
8	1008.61	0.53401	0.53965	0.35026	3.5185 10^{-06}	-	47596.9553
9	1702.52	0.51743	0.52424	0.4235	3.3345 10^{-06}	-	72526.9124
10	2743.4	0.49955	0.50728	0.47961	3.1013 10^{-06}	-	98765.795
11	4131.23	0.48168	0.49056	0.55148	2.9862 10^{-06}	-	133684.8474
12	4825.14	0.47573	0.47967	0.24484	9.9574 10^{-07}	-	102553.4771
13	6906.89	0.45737	0.46695	0.59477	2.7822 10^{-06}	-	263489.1293
14	5866.02	0.45769	-	-	-	-	-
15	4131.23	0.4585	-	-	-	-	-
16	1702.52	0.46413	-	-	-	-	-
17	2.43	0.53642	-	-	-	-	-

Table A.7. Results from analysis of test B0T2 using Taylor method.

	σ [kPa]	e_t [-]	e_{100} [-]	ϵ_{cr} [%]	c_v [m^2/s]	$c_{\alpha,\epsilon}$ [%]	M [kPa]
1	11.1	0.60952	0.60952	0	$2.0414\ 10^{-14}$	-	37000
2	19.78	0.60887	0.60887	$-2.7756\ 10^{-16}$	$2.04\ 10^{-14}$	-	21700
3	37.12	0.60356	0.60356	$1.4433\ 10^{-15}$	$2.0354\ 10^{-14}$	-	5254.5455
4	71.82	0.59277	0.59277	$6.6613\ 10^{-16}$	$2.0186\ 10^{-14}$	-	5179.1045
5	141.21	0.57973	0.58022	0.03	$1.9903\ 10^{-14}$	-	8896.1538
6	314.69	0.56347	0.56379	0.02	$1.9557\ 10^{-14}$	-	17007.8431
7	661.65	0.54544	0.54608	0.04	$1.9147\ 10^{-14}$	-	31541.8182
8	1008.61	0.53401	0.54021	0.385	$1.878\ 10^{-14}$	-	95057.5342
9	1702.52	0.51743	0.51823	0.05	$1.8443\ 10^{-14}$	-	50835.8974
10	2743.4	0.49955	0.5002	0.04	$1.8033\ 10^{-14}$	-	92935.7143
11	4131.23	0.48168	0.48297	0.08	$1.7611\ 10^{-14}$	-	129703.7383
12	4825.14	0.47573	0.47653	0.05	$1.7262\ 10^{-14}$	-	173477.5
13	6906.89	0.45737	0.45866	0.08	$1.7057\ 10^{-14}$	-	187545.045
14	5866.02	0.45769	-	-	-	-	-
15	4131.23	0.4585	-	-	-	-	-
16	1702.52	0.46413	-	-	-	-	-
17	2.43	0.53642	-	-	-	-	-

Table A.8. Results from analysis of test B0T2 using 24h method.

A.1.3 Test B0T3

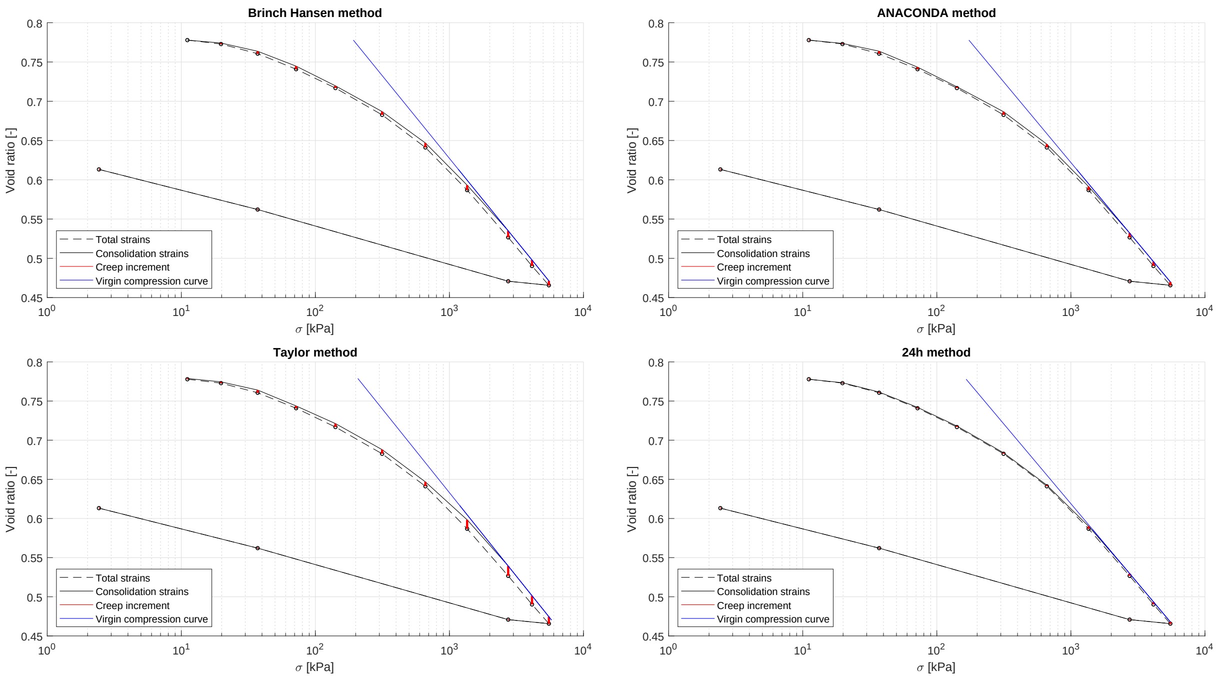

Figure A.3. Results from analysis of test B0T3.

	σ $[kPa]$	e_t [-]	e_{100} [-]	ϵ_{cr} [%]	c_v $[m^2/s]$	$c_{\alpha,\epsilon}$ [%]	M [kPa]
1	11.1	0.77786	0.77787	$1.9429\ 10^{-16}$	$1.7647\ 10^{-07}$	$1.5255\ 10^{-16}$	11111.0801
2	19.78	0.77288	0.77414	0.080297	$8.8609\ 10^{-08}$	0.066439	4148.082
3	37.12	0.7606	0.76366	0.17182	$1.0044\ 10^{-07}$	0.17265	2944.2536
4	71.82	0.74084	0.74472	0.21797	$1.029\ 10^{-07}$	0.21511	3261.6988
5	141.21	0.71681	0.71961	0.15705	$8.4404\ 10^{-08}$	0.1407	4918.1269
6	314.69	0.68263	0.68687	0.23781	$9.9073\ 10^{-08}$	0.23379	9432.0687
7	661.65	0.64116	0.64688	0.32169	$1.0724\ 10^{-07}$	0.29904	15445.3135
8	1355.56	0.58687	0.59313	0.34213	$1.0607\ 10^{-07}$	0.24495	22978.4132
9	2743.4	0.52671	0.53505	0.47685	$1.2636\ 10^{-07}$	0.34715	42536.7584
10	4131.23	0.49022	0.49793	0.43323	$1.0706\ 10^{-07}$	0.32423	66541.6661
11	5519.06	0.46565	0.47121	0.31238	$8.7224\ 10^{-08}$	0.26866	92468.8068
12	2743.4	0.47081	-	-	-	-	-
13	37.12	0.56213	-	-	-	-	-
14	2.43	0.61321	-	-	-	-	-

Table A.9. Results from analysis of test B0T3 using Brinch Hansen method.

	σ [kPa]	e_t [-]	e_{100} [-]	ϵ_{cr} [%]	c_v [m^2/s]	$c_{\alpha,\epsilon}$ [%]	M [kPa]
1	11.1	0.77786	0.77786	0.0026205	$1.7425\ 10^{-07}$	0.0061708	9249.0307
2	19.78	0.77288	0.77363	0.044069	$5.238\ 10^{-08}$	0.13463	3652.0367
3	37.12	0.7606	0.76377	0.17761	$6.5253\ 10^{-08}$	0.19554	3128.8934
4	71.82	0.74084	0.74342	0.14315	$5.4924\ 10^{-08}$	0.34173	3034.9783
5	141.21	0.71681	0.71839	0.087042	$4.9343\ 10^{-08}$	0.24086	4935.7417
6	314.69	0.68263	0.68665	0.23247	$6.6496\ 10^{-08}$	0.49083	9727.943
7	661.65	0.64116	0.64538	0.23848	$6.8031\ 10^{-08}$	0.52323	14963.9795
8	1355.56	0.58687	0.59136	0.25063	$6.7692\ 10^{-08}$	0.52901	22867.0974
9	2743.4	0.52671	0.53219	0.32352	$7.0493\ 10^{-08}$	0.71576	41745.5283
10	4131.23	0.49022	0.49575	0.32359	$5.573\ 10^{-08}$	0.75115	67797.3284
11	5519.06	0.46565	0.46998	0.24957	$4.418\ 10^{-08}$	0.65543	95878.4648
12	2743.4	0.47081	-	-	-	-	-
13	37.12	0.56213	-	-	-	-	-
14	2.43	0.61321	-	-	-	-	-

Table A.10. Results from analysis of test B0T3 using ANACONDA method.

	σ [kPa]	e_t [-]	e_{100} [-]	ϵ_{cr} [%]	c_v [m^2/s]	$c_{\alpha,\epsilon}$ [%]	M [kPa]
1	11.1	0.77786	0.77885	0.055397	$2.322\ 10^{-07}$	-	17181.8741
2	19.78	0.77288	0.77451	0.091516	$2.5716\ 10^{-08}$	-	3559.1068
3	37.12	0.7606	0.76403	0.19294	$2.4721\ 10^{-08}$	-	2946.073
4	71.82	0.74084	0.74374	0.16297	$1.5718\ 10^{-08}$	-	3043.9453
5	141.21	0.71681	0.72121	0.24704	$1.9264\ 10^{-08}$	-	5481.3365
6	314.69	0.68263	0.68795	0.29878	$2.2625\ 10^{-08}$	-	9285.673
7	661.65	0.64116	0.64677	0.31531	$2.1427\ 10^{-08}$	-	14997.3992
8	1355.56	0.58687	0.59831	0.64293	$2.8565\ 10^{-08}$	-	25489.0862
9	2743.4	0.52671	0.53942	0.71416	$2.9417\ 10^{-08}$	-	41944.3001
10	4131.23	0.49022	0.50122	0.61821	$2.6496\ 10^{-08}$	-	64671.9301
11	5519.06	0.46565	0.47461	0.50338	$2.6318\ 10^{-08}$	-	92841.8211
12	2743.4	0.47081	-	-	-	-	-
13	37.12	0.56213	-	-	-	-	-
14	2.43	0.61321	-	-	-	-	-

Table A.11. Results from analysis of test B0T3 using Taylor method.

	σ	e_t	e_{100}	ϵ_{cr}	c_v	$c_{\alpha,\epsilon}$	M
	$[kPa]$	[-]	[-]	[%]	$[m^2/s]$	[%]	[kPa]
1	11.1	0.77786	0.77786	$1.1102\ 10^{-16}$	$2.0404\ 10^{-14}$	-	9250
2	19.78	0.77288	0.77341	0.03	$2.0342\ 10^{-14}$	-	3472
3	37.12	0.7606	0.76149	0.05	$2.0189\ 10^{-14}$	-	2588.0597
4	71.82	0.74084	0.74191	0.06	$1.9868\ 10^{-14}$	-	3154.5455
5	141.21	0.71681	0.71806	0.07	$1.9404\ 10^{-14}$	-	5178.3582
6	314.69	0.68263	0.68388	0.07	$1.8811\ 10^{-14}$	-	9035.4167
7	661.65	0.64116	0.64258	0.08	$1.8031\ 10^{-14}$	-	14955.1724
8	1355.56	0.58687	0.59007	0.18	$1.7087\ 10^{-14}$	-	23522.3729
9	2743.4	0.52671	0.52973	0.17	$1.5936\ 10^{-14}$	-	40939.233
10	4131.23	0.49022	0.49342	0.18	$1.4856\ 10^{-14}$	-	68030.8824
11	5519.06	0.46565	0.46797	0.13	$1.4201\ 10^{-14}$	-	97051.049
12	2743.4	0.47081	-	-	-	-	-
13	37.12	0.56213	-	-	-	-	-
14	2.43	0.61321	-	-	-	-	-

Table A.12. Results from analysis of test B0T3 using 24h method.

A.1.4 Test B0T4

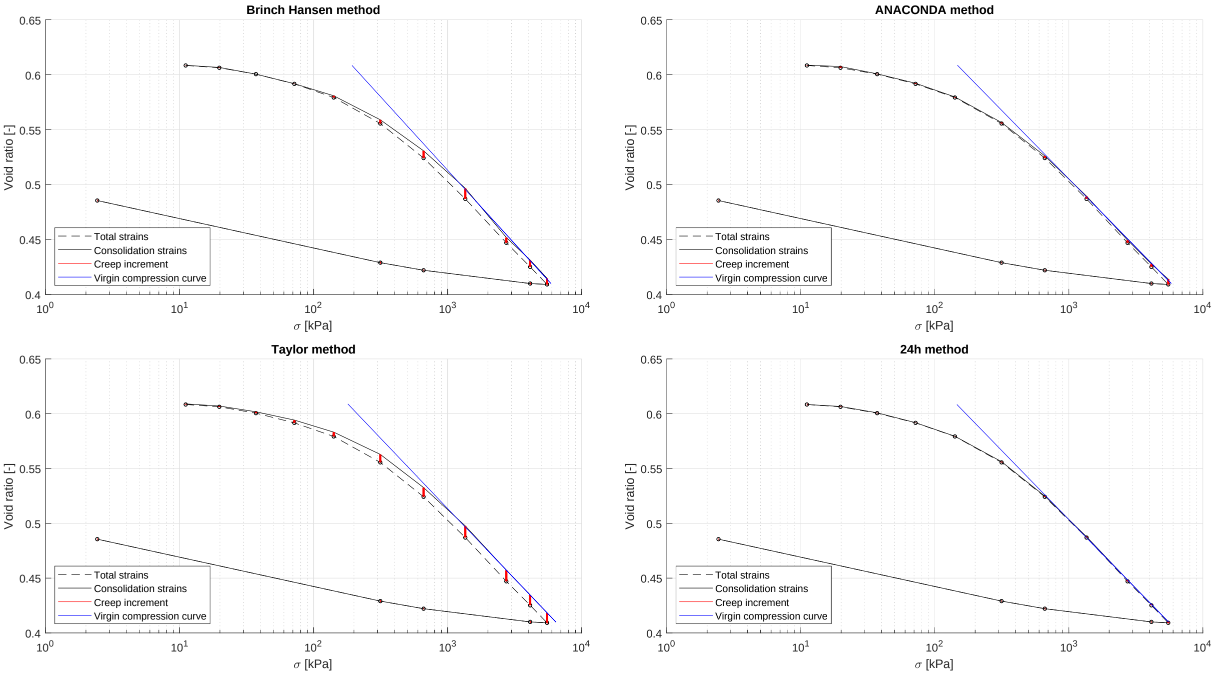

Figure A.4. Results from analysis of test B0T4.

	σ [kPa]	e_t [-]	e_{100} [-]	ϵ_{cr} [%]	c_v [m^2/s]	$c_{\alpha,\epsilon}$ [%]	M [kPa]
1	11.1	0.60839	0.60855	5.6899 10^{-16}	2.9636 10^{-06}	2.7001 10^{-16}	15263.1088
2	19.78	0.6063	0.60662	6.1062 10^{-16}	4.6199 10^{-07}	3.7182 10^{-16}	7234.119
3	37.12	0.6005	0.6005	3.6637 10^{-15}	4.4653 10^{-07}	1.873 10^{-15}	4563.1266
4	71.82	0.59165	0.59181	1.3323 10^{-14}	4.2498 10^{-06}	5.0745 10^{-15}	6426.0827
5	141.21	0.57925	0.58083	0.10017	4.1408 10^{-06}	0.041146	10176.1071
6	314.69	0.55558	0.55896	0.21278	5.247 10^{-06}	0.07424	12772.7491
7	661.65	0.52419	0.53077	0.41088	1.4742 10^{-05}	0.12816	19818.0781
8	1355.56	0.487	0.49665	0.61004	1.2433 10^{-05}	0.19587	32743.3818
9	2743.4	0.44707	0.45191	0.301	9.0506 10^{-07}	0.13663	49940.803
10	4131.23	0.42517	0.4314	0.38689	2.4301 10^{-06}	0.15546	108925.2503
11	5519.06	0.40923	0.41485	0.33556	7.9179 10^{-07}	0.17037	135012.6806
12	4131.23	0.41004	-	-	-	-	-
13	661.65	0.42211	-	-	-	-	-
14	314.69	0.42904	-	-	-	-	-
15	2.43	0.48555	-	-	-	-	-

Table A.13. Results from analysis of test B0T4 using Brinch Hansen method.

	σ [kPa]	e_t [-]	e_{100} [-]	ϵ_{cr} [%]	c_v [m^2/s]	$c_{\alpha,\epsilon}$ [%]	M [kPa]
1	11.1	0.60839	0.60868	0.010164	$6.9117\ 10^{-06}$	0.026282	13560.7302
2	19.78	0.6063	0.60741	0.060449	$1.9885\ 10^{-05}$	0.17811	11012.5382
3	37.12	0.6005	0.60078	0.01855	$5.5239\ 10^{-06}$	0.055003	4209.9551
4	71.82	0.59165	0.5922	0.03545	$9.4648\ 10^{-06}$	0.081233	6510.467
5	141.21	0.57925	0.57975	0.03045	$9.3496\ 10^{-06}$	0.079367	8971.427
6	314.69	0.55558	0.55649	0.059542	$1.1749\ 10^{-05}$	0.1743	12009.1839
7	661.65	0.52419	0.52613	0.1281	$1.123\ 10^{-05}$	0.30484	18401.9089
8	1355.56	0.487	0.4895	0.16488	$1.3919\ 10^{-05}$	0.37701	30498.518
9	2743.4	0.44707	0.44956	0.16383	$1.6124\ 10^{-05}$	0.36071	55933.79
10	4131.23	0.42517	0.42783	0.16846	$2.5567\ 10^{-06}$	0.39418	102840.8731
11	5519.06	0.40923	0.41409	0.30338	$2.3696\ 10^{-06}$	0.23289	162670.0982
12	4131.23	0.41004	-	-	-	-	-
13	661.65	0.42211	-	-	-	-	-
14	314.69	0.42904	-	-	-	-	-
15	2.43	0.48555	-	-	-	-	-

Table A.14. Results from analysis of test B0T4 using ANACONDA method.

	σ [kPa]	e_t [-]	e_{100} [-]	ϵ_{cr} [%]	c_v [m^2/s]	$c_{\alpha,\epsilon}$ [%]	M [kPa]
1	11.1	0.60839	0.60896	0.035262	$1.3797\ 10^{-06}$	-	23427.4769
2	19.78	0.6063	0.60703	0.045405	$1.5659\ 10^{-07}$	-	7241.9433
3	37.12	0.6005	0.60174	0.076916	$3.2698\ 10^{-07}$	-	5278.7262
4	71.82	0.59165	0.5942	0.15852	$1.8071\ 10^{-06}$	-	7408.2016
5	141.21	0.57925	0.58319	0.24476	$3.2396\ 10^{-06}$	-	10148.3774
6	314.69	0.55558	0.56284	0.4509	$3.6086\ 10^{-06}$	-	13726.2244
7	661.65	0.52419	0.53259	0.52206	$1.6824\ 10^{-06}$	-	18466.7048
8	1355.56	0.487	0.49761	0.65928	$3.2129\ 10^{-06}$	-	31936.4092
9	2743.4	0.44707	0.45724	0.63171	$1.6183\ 10^{-06}$	-	55346.1152
10	4131.23	0.42517	0.43461	0.58627	$1.1671\ 10^{-06}$	-	98746.7171
11	5519.06	0.40923	0.41831	0.56349	$1.2902\ 10^{-06}$	-	137032.7443
12	4131.23	0.41004	-	-	-	-	-
13	661.65	0.42211	-	-	-	-	-
14	314.69	0.42904	-	-	-	-	-
15	2.43	0.48555	-	-	-	-	-

Table A.15. Results from analysis of test B0T4 using Taylor method.

	σ	e_t	e_{100}	ϵ_{cr}	c_v	$c_{\alpha,\epsilon}$	M
	$[kPa]$	[-]	[-]	[%]	$[m^2/s]$	[%]	[kPa]
1	11.1	0.60839	0.60839	0	$2.0406\ 10^{-14}$	-	11100
2	19.78	0.6063	0.60662	0.02	$2.0362\ 10^{-14}$	-	7890.9091
3	37.12	0.6005	0.60082	0.02	$2.0291\ 10^{-14}$	-	4816.6667
4	71.82	0.59165	0.59181	0.01	$2.0122\ 10^{-14}$	-	6196.4286
5	141.21	0.57925	0.57941	0.01	$1.9877\ 10^{-14}$	-	9011.6883
6	314.69	0.55558	0.55623	0.04	$1.9501\ 10^{-14}$	-	12047.2222
7	661.65	0.52419	0.52483	0.04	$1.8872\ 10^{-14}$	-	17792.8205
8	1355.56	0.487	0.4878	0.05	$1.808\ 10^{-14}$	-	30170
9	2743.4	0.44707	0.44836	0.08	$1.7191\ 10^{-14}$	-	56646.5306
10	4131.23	0.42517	0.42614	0.06	$1.6372\ 10^{-14}$	-	100567.3913
11	5519.06	0.40923	0.4102	0.06	$1.5914\ 10^{-14}$	-	140184.8485
12	4131.23	0.41004	-	-	-	-	-
13	661.65	0.42211	-	-	-	-	-
14	314.69	0.42904	-	-	-	-	-
15	2.43	0.48555	-	-	-	-	-

Table A.16. Results from analysis of test B0T4 using 24h method.

A.2 Borehole B1

A.2.1 Test B1T1

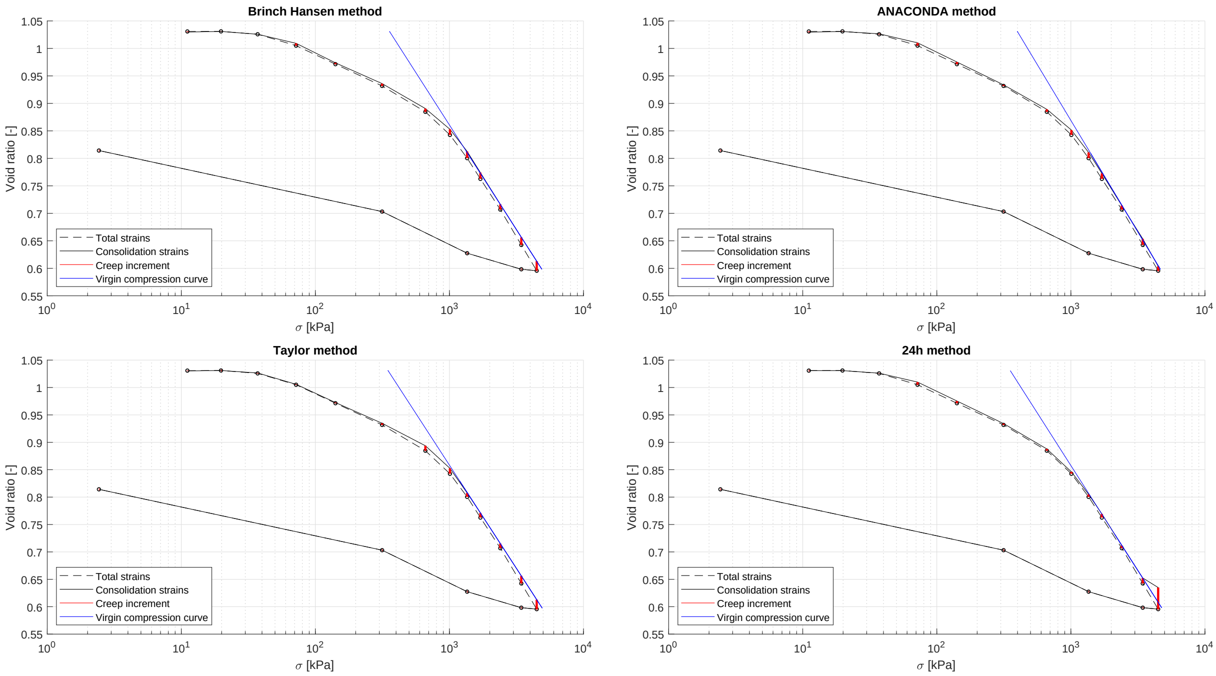

Figure A.5. Results from analysis of test B1T1.

	σ	e_t	e_{100}	ϵ_{cr}	c_v	$c_{\alpha,\epsilon}$	M
	$[kPa]$	[-]	[-]	[%]	$[m^2/s]$	[%]	[kPa]
1	11.1	1.0308	1.0298	2.0817 10^{-17}	1.4671 10^{-05}	9.482 10^{-18}	32449.1048
2	19.78	1.031	1.0308	-4.8572 10^{-17}	4.8941 10^{-07}	-3.1033 10^{-17}	-17361.0125
3	37.12	1.0257	1.0257	-1.1102 10^{-16}	2.7491 10^{-08}	-2.0463 10^{-16}	6940.2079
4	71.82	1.005	1.0093	0.2081	2.2567 10^{-08}	0.37773	4273.9208
5	141.21	0.97133	0.97372	0.11986	2.5916 10^{-08}	0.14937	3963.8531
6	314.69	0.93175	0.93597	0.20775	6.6668 10^{-08}	0.14831	9327.8426
7	661.65	0.88465	0.89058	0.29192	8.3539 10^{-08}	0.23436	15518.2987
8	1008.61	0.84263	0.8529	0.50578	7.3533 10^{-08}	0.55777	18692.6097
9	1355.56	0.80041	0.81259	0.60004	5.5251 10^{-08}	0.71561	17472.1493
10	1702.52	0.76265	0.77402	0.56021	3.8598 10^{-08}	0.66056	18262.6904
11	2396.44	0.70682	0.71637	0.62405	4.3949 10^{-08}	0.66536	24435.4532
12	3437.31	0.64247	0.65615	0.67381	3.816 10^{-08}	0.63997	35086.3417
13	4478.18	0.59558	0.61305	0.87803	2.5717 10^{-08}	0.5262	49020.539
14	3437.31	0.59822	-	-	-	-	-
15	1355.56	0.62745	-	-	-	-	-
16	314.69	0.70317	-	-	-	-	-
17	2.43	0.81421	-	-	-	-	-

Table A.17. Results from analysis of test B1T1 using Brinch Hansen method.

	σ [kPa]	e_t [-]	e_{100} [-]	ϵ_{cr} [%]	c_v [m^2/s]	$c_{\alpha,\epsilon}$ [%]	M [kPa]
1	11.1	1.0308	1.0296	-0.05798	1.4588 10^{-06}	-0.081897	57746.0652
2	19.78	1.031	1.0307	-0.010565	1.5129 10^{-08}	-0.023307	-16156.3553
3	37.12	1.0257	1.0266	0.043017	2.3987 10^{-08}	0.11195	8483.893
4	71.82	1.005	1.0102	0.251	1.4422 10^{-08}	0.68567	4297.7363
5	141.21	0.97133	0.97526	0.19306	1.6997 10^{-08}	0.18033	4035.8521
6	314.69	0.93175	0.93372	0.099997	3.4752 10^{-08}	0.22991	8478.8349
7	661.65	0.88465	0.88917	0.23205	4.6629 10^{-08}	0.52836	15809.7562
8	1008.61	0.84263	0.85151	0.4403	3.8542 10^{-08}	1.145	18699.992
9	1355.56	0.80041	0.81076	0.51793	2.8409 10^{-08}	1.4114	17284.1894
10	1702.52	0.76265	0.77262	0.48633	1.9952 10^{-08}	1.2784	18464.7581
11	2396.44	0.70682	0.71409	0.48729	2.1484 10^{-08}	1.2276	24067.5968
12	3437.31	0.64247	0.65361	0.54499	1.865 10^{-08}	0.92553	34936.3585
13	4478.18	0.59558	0.60362	0.40404	6.7778 10^{-09}	1.0127	42269.9154
14	3437.31	0.59822	-	-	-	-	-
15	1355.56	0.62745	-	-	-	-	-
16	314.69	0.70317	-	-	-	-	-
17	2.43	0.81421	-	-	-	-	-

Table A.18. Results from analysis of test B1T1 using ANACONDA method.

	σ [kPa]	e_t [-]	e_{100} [-]	ϵ_{cr} [%]	c_v [m^2/s]	$c_{\alpha,\epsilon}$ [%]	M [kPa]
1	11.1	1.0308	1.0302	-0.030833	5.7709 10^{-08}	-	-121091.9723
2	19.78	1.031	1.031	-1.3531 10^{-15}	2.5996 10^{-09}	-	-21257.101
3	37.12	1.0257	1.0265	0.038403	7.8761 10^{-09}	-	7825.0052
4	71.82	1.005	1.0058	0.037194	3.196 10^{-09}	-	3397.9338
5	141.21	0.97133	0.97255	0.059854	4.7888 10^{-09}	-	4237.9708
6	314.69	0.93175	0.93472	0.14633	1.2345 10^{-08}	-	9309.2273
7	661.65	0.88465	0.89372	0.44675	1.8976 10^{-08}	-	17179.864
8	1008.61	0.84263	0.85254	0.48801	1.4159 10^{-08}	-	17102.1974
9	1355.56	0.80041	0.80752	0.35047	7.806 10^{-09}	-	15645.7487
10	1702.52	0.76265	0.77112	0.41734	6.2376 10^{-09}	-	19349.4158
11	2396.44	0.70682	0.71521	0.41309	7.334 10^{-09}	-	25194.521
12	3437.31	0.64247	0.65631	0.68153	6.7861 10^{-09}	-	35872.6819
13	4478.18	0.59558	0.61285	0.85049	4.9863 10^{-09}	-	48615.3137
14	3437.31	0.59822	-	-	-	-	-
15	1355.56	0.62745	-	-	-	-	-
16	314.69	0.70317	-	-	-	-	-
17	2.43	0.81421	-	-	-	-	-

Table A.19. Results from analysis of test B1T1 using Taylor method.

	σ	e_t	e_{100}	ϵ_{cr}	c_v	$c_{\alpha,\epsilon}$	M
	$[kPa]$	[-]	[-]	[%]	$[m^2/s]$	[%]	[kPa]
1	11.1	1.0308	1.0308	0	$2.0421\ 10^{-14}$	-	-27750
2	19.78	1.031	1.0308	-0.01	$2.0433\ 10^{-14}$	-	$1.250919832498429\ 10^{20}$
3	37.12	1.0257	1.0261	0.02	$2.0413\ 10^{-14}$	-	7539.1304
4	71.82	1.005	1.0099	0.24	$2.0252\ 10^{-14}$	-	4337.5
5	141.21	0.97133	0.97539	0.2	$1.9771\ 10^{-14}$	-	4081.7647
6	314.69	0.93175	0.93418	0.12	$1.9073\ 10^{-14}$	-	8545.8128
7	661.65	0.88465	0.8879	0.16	$1.8279\ 10^{-14}$	-	15217.5439
8	1008.61	0.84263	0.84608	0.17	$1.7418\ 10^{-14}$	-	16842.7184
9	1355.56	0.80041	0.80508	0.23	$1.6651\ 10^{-14}$	-	17175.7426
10	1702.52	0.76265	0.76935	0.33	$1.5921\ 10^{-14}$	-	19713.6364
11	2396.44	0.70682	0.71149	0.23	$1.517\ 10^{-14}$	-	24348.0702
12	3437.31	0.64247	0.65242	0.49	$1.4204\ 10^{-14}$	-	35768.7285
13	4478.18	0.59558	0.63501	1.9425	$1.3335\ 10^{-14}$	-	121384.2566
14	3437.31	0.59822	-	-	-	-	-
15	1355.56	0.62745	-	-	-	-	-
16	314.69	0.70317	-	-	-	-	-
17	2.43	0.81421	-	-	-	-	-

Table A.20. Results from analysis of test B1T1 using 24h method.

A.2.2 Test B1T2

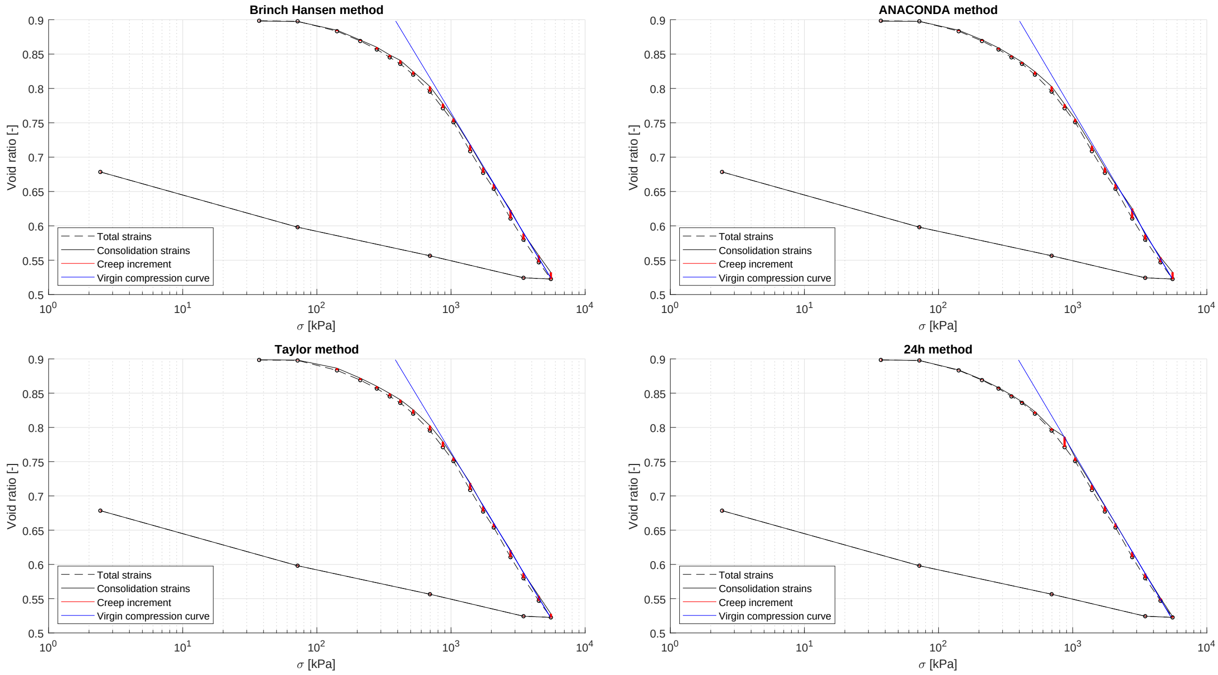

Figure A.6. Results from analysis of test B1T2.

	σ $[kPa]$	e_t [-]	e_{100} [-]	ϵ_{cr} [%]	c_v $[m^2/s]$	$c_{\alpha,\epsilon}$ [%]	M [kPa]
1	37.12	0.89848	0.8981	$2.7756\ 10^{-16}$	0.00010571	$1.1032\ 10^{-16}$	37093.3382
2	71.82	0.89772	0.89734	$-1.9429\ 10^{-16}$	$2.3932\ 10^{-05}$	$-6.4183\ 10^{-17}$	86742.6352
3	141.21	0.88328	0.88474	0.076953	$1.0978\ 10^{-07}$	0.071809	10467.5564
4	210.6	0.86903	0.87043	0.073734	$7.4351\ 10^{-08}$	0.071977	9212.7679
5	279.99	0.85668	0.85994	0.17517	$8.4019\ 10^{-08}$	0.15868	12569.454
6	349.39	0.84528	0.84873	0.18415	$7.8258\ 10^{-08}$	0.15263	11755.6517
7	418.78	0.83578	0.84086	0.28668	$1.4604\ 10^{-07}$	0.20905	16758.6912
8	522.87	0.82001	0.82451	0.23696	$4.9749\ 10^{-08}$	0.22968	12099.3617
9	696.34	0.79531	0.80284	0.39622	$7.4756\ 10^{-08}$	0.37656	15206.5994
10	869.82	0.77118	0.77774	0.34126	$3.3973\ 10^{-08}$	0.3873	13131.9864
11	1043.3	0.75085	0.7563	0.28677	$2.9569\ 10^{-08}$	0.3953	15374.0221
12	1390.26	0.70867	0.71759	0.46932	$3.7219\ 10^{-08}$	0.51574	17029.1446
13	1737.22	0.67713	0.68504	0.40884	$2.6131\ 10^{-08}$	0.50517	20255.3479
14	2084.18	0.65395	0.6608	0.35301	$2.6447\ 10^{-08}$	0.47438	27188.9171
15	2778.09	0.61063	0.62294	0.64781	$3.9512\ 10^{-08}$	0.66623	34826.1899
16	3472.01	0.57985	0.5889	0.47644	$2.9462\ 10^{-08}$	0.52076	38737.4962
17	4512.88	0.54698	0.55678	0.51588	$4.296\ 10^{-08}$	0.65257	61569.5897
18	5553.75	0.52266	0.53231	0.50801	$7.3839\ 10^{-08}$	0.60323	80822.0528
19	3472.01	0.52437	-	-	-	-	-
20	696.34	0.55648	-	-	-	-	-
21	71.82	0.59809	-	-	-	-	-
22	2.43	0.67846	-	-	-	-	-

Table A.21. Results from analysis of test B1T2 using Brinch Hansen method.

	σ [kPa]	e_t [-]	e_{100} [-]	ϵ_{cr} [%]	c_v [m^2/s]	$c_{\alpha,\epsilon}$ [%]	M [kPa]
1	37.12	0.89848	0.8979	-0.028452	2.1721 10^{-05}	-0.055054	33524.4856
2	71.82	0.89772	0.89761	0.0024185	4.5945 10^{-06}	0.0031115	228367.4541
3	141.21	0.88328	0.88467	0.072544	6.6134 10^{-08}	0.17174	10192.1358
4	210.6	0.86903	0.8708	0.11039	4.7903 10^{-08}	0.24169	9506.7027
5	279.99	0.85668	0.85896	0.125	4.0891 10^{-08}	0.31337	11127.497
6	349.39	0.84528	0.84785	0.14189	3.3149 10^{-08}	0.38647	11870.2755
7	418.78	0.83578	0.83835	0.14854	3.2723 10^{-08}	0.38391	13877.1147
8	522.87	0.82001	0.82448	0.2379	3.4653 10^{-08}	0.47434	14262.538
9	696.34	0.79531	0.80281	0.39478	3.7436 10^{-08}	0.45896	15207.0231
10	869.82	0.77118	0.77711	0.31275	1.9569 10^{-08}	0.78492	12827.2762
11	1043.3	0.75085	0.75572	0.25641	1.4088 10^{-08}	0.79577	15407.8316
12	1390.26	0.70867	0.71648	0.41674	1.922 10^{-08}	1.1726	16802.0166
13	1737.22	0.67713	0.68478	0.40153	1.4596 10^{-08}	1.1449	20794.2955
14	2084.18	0.65395	0.66081	0.36002	1.4498 10^{-08}	1.0628	27496.4385
15	2778.09	0.61063	0.62517	0.76676	2.3051 10^{-08}	0.72653	36992.7792
16	3472.01	0.57985	0.5873	0.4014	1.5347 10^{-08}	1.1245	34822.0514
17	4512.88	0.54698	0.55426	0.38914	2.1596 10^{-08}	1.1543	59851.598
18	5553.75	0.52266	0.53251	0.51565	3.933 10^{-08}	0.87765	90937.2951
19	3472.01	0.52437	-	-	-	-	-
20	696.34	0.55648	-	-	-	-	-
21	71.82	0.59809	-	-	-	-	-
22	2.43	0.67846	-	-	-	-	-

Table A.22. Results from analysis of test B1T2 using ANACONDA method.

	σ [kPa]	e_t [-]	e_{100} [-]	ϵ_{cr} [%]	c_v [m^2/s]	$c_{\alpha,\epsilon}$ [%]	M [kPa]
1	37.12	0.89848	0.89873	0.013334	$4.7099\ 10^{-05}$	-	55680.6281
2	71.82	0.89772	0.89825	0.027777	$4.705\ 10^{-05}$	-	135775.1554
3	141.21	0.88328	0.88644	0.1665	$2.6663\ 10^{-08}$	-	11168.8914
4	210.6	0.86903	0.87195	0.15371	$1.9724\ 10^{-08}$	-	9096.9475
5	279.99	0.85668	0.86004	0.17695	$1.6935\ 10^{-08}$	-	11071.0962
6	349.39	0.84528	0.84957	0.22566	$1.884\ 10^{-08}$	-	12588.6841
7	418.78	0.83578	0.8404	0.24298	$2.8088\ 10^{-08}$	-	14375.9222
8	522.87	0.82001	0.82574	0.3018	$1.5628\ 10^{-08}$	-	13497.4836
9	696.34	0.79531	0.8025	0.37845	$1.4228\ 10^{-08}$	-	14179.9171
10	869.82	0.77118	0.7792	0.42186	$9.6502\ 10^{-09}$	-	14143.331
11	1043.3	0.75085	0.75605	0.2737	$5.5457\ 10^{-09}$	-	14241.1085
12	1390.26	0.70867	0.7188	0.53323	$7.8239\ 10^{-09}$	-	17697.7839
13	1737.22	0.67713	0.68472	0.39965	$5.0758\ 10^{-09}$	-	19344.5687
14	2084.18	0.65395	0.65958	0.29657	$4.5281\ 10^{-09}$	-	26223.6488
15	2778.09	0.61063	0.62087	0.53892	$6.8486\ 10^{-09}$	-	34054.5297
16	3472.01	0.57985	0.58738	0.39655	$5.0748\ 10^{-09}$	-	39374.2533
17	4512.88	0.54698	0.55417	0.37845	$7.4816\ 10^{-09}$	-	59542.6696
18	5553.75	0.52266	0.52794	0.27774	$8.7881\ 10^{-09}$	-	75386.7358
19	3472.01	0.52437	-	-	-	-	-
20	696.34	0.55648	-	-	-	-	-
21	71.82	0.59809	-	-	-	-	-
22	2.43	0.67846	-	-	-	-	-

Table A.23. Results from analysis of test B1T2 using Taylor method.

	σ [kPa]	e_t [-]	e_{100} [-]	ϵ_{cr} [%]	c_v [m^2/s]	$c_{\alpha,\epsilon}$ [%]	M [kPa]
1	37.12	0.89848	0.89848	0	2.0409 10^{-14}	-	46400
2	71.82	0.89772	0.89772	0	2.0383 10^{-14}	-	86750
3	141.21	0.88328	0.88385	0.03	2.0293 10^{-14}	-	9505.4795
4	210.6	0.86903	0.86979	0.04	1.9987 10^{-14}	-	9377.027
5	279.99	0.85668	0.85801	0.07	1.9698 10^{-14}	-	11191.9355
6	349.39	0.84528	0.84718	0.1	1.9446 10^{-14}	-	12175.4386
7	418.78	0.83578	0.8373	0.08	1.9216 10^{-14}	-	13344.2308
8	522.87	0.82001	0.82305	0.16	1.8994 10^{-14}	-	13878.6667
9	696.34	0.79531	0.79873	0.18	1.8624 10^{-14}	-	13552.3438
10	869.82	0.77118	0.78619	0.79	1.8182 10^{-14}	-	26284.8485
11	1043.3	0.75085	0.75598	0.27	1.7669 10^{-14}	-	10910.6918
12	1390.26	0.70867	0.71608	0.39	1.7165 10^{-14}	-	16521.9048
13	1737.22	0.67713	0.68492	0.41	1.6397 10^{-14}	-	21156.0976
14	2084.18	0.65395	0.65984	0.31	1.5826 10^{-14}	-	26284.8485
15	2778.09	0.61063	0.61842	0.41	1.5305 10^{-14}	-	31830.7339
16	3472.01	0.57985	0.58669	0.36	1.4562 10^{-14}	-	41552.0958
17	4512.88	0.54698	0.55078	0.2	1.3984 10^{-14}	-	55072.4868
18	5553.75	0.52266	0.52399	0.07	1.3432 10^{-14}	-	73820.5674
19	3472.01	0.52437	-	-	-	-	-
20	696.34	0.55648	-	-	-	-	-
21	71.82	0.59809	-	-	-	-	-
22	2.43	0.67846	-	-	-	-	-

Table A.24. Results from analysis of test B1T2 using 24h method.

A.2.3 Test B1T3

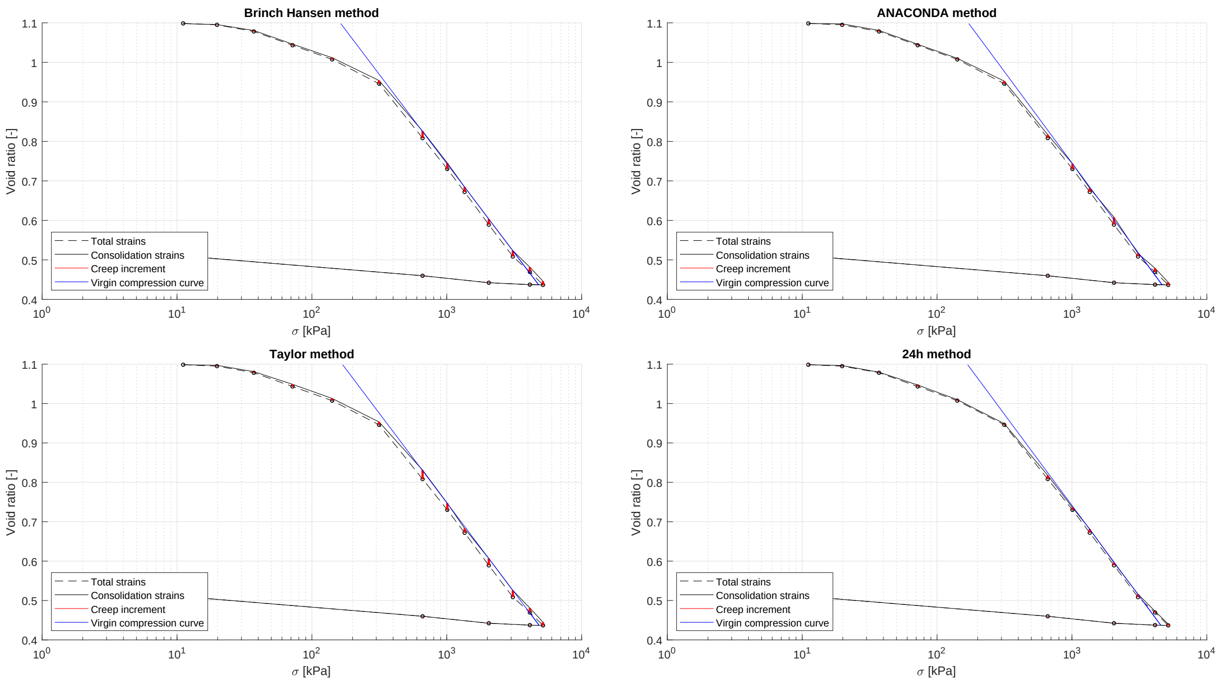

Figure A.7. Results from analysis of test B1T3.

	σ [kPa]	e_t [-]	e_{100} [-]	ϵ_{cr} [%]	c_v [m^2/s]	$c_{\alpha,\epsilon}$ [%]	M [kPa]
1	11.1	1.0985	1.0979	$5.5511\ 10^{-17}$	$1.1664\ 10^{-05}$	$3.0102\ 10^{-17}$	20464.7567
2	19.78	1.095	1.0956	$-9.4369\ 10^{-16}$	$6.8786\ 10^{-08}$	$-7.3208\ 10^{-16}$	7901.9803
3	37.12	1.0782	1.0806	0.11615	$4.6399\ 10^{-08}$	0.17704	2425.3044
4	71.82	1.0433	1.0462	0.13184	$4.2801\ 10^{-08}$	0.11859	2120.9035
5	141.21	1.0074	1.0117	0.20697	$6.3093\ 10^{-08}$	0.17984	4223.9463
6	314.69	0.94607	0.95403	0.379	$1.2282\ 10^{-07}$	0.30126	6314.8758
7	661.65	0.80831	0.82602	0.84309	$8.1744\ 10^{-08}$	0.60922	5691.7244
8	1008.61	0.73019	0.74559	0.73307	$5.6952\ 10^{-08}$	0.79448	9058.9106
9	1355.56	0.67202	0.68464	0.60069	$3.1033\ 10^{-08}$	0.63713	11953.9844
10	2049.48	0.58928	0.60313	0.65952	$4.2145\ 10^{-08}$	0.66792	17879.1462
11	3090.35	0.50864	0.52336	0.70111	$5.322\ 10^{-08}$	0.55171	27402.6919
12	4131.23	0.46958	0.48166	0.57501	$5.7873\ 10^{-08}$	0.55503	52408.7589
13	5172.1	0.43682	0.44612	0.44196	$4.27\ 10^{-08}$	0.44635	61511.9718
14	4131.23	0.43745	-	-	-	-	-
15	2049.48	0.44228	-	-	-	-	-
16	661.65	0.45992	-	-	-	-	-
17	2.43	0.52859	-	-	-	-	-

Table A.25. Results from analysis of test B1T3 using Brinch Hansen method.

	σ [kPa]	e_t [-]	e_{100} [-]	ϵ_{cr} [%]	c_v [m^2/s]	$c_{\alpha,\epsilon}$ [%]	M [kPa]
1	11.1	1.0985	1.0981	-0.022736	5.8976 10^{-05}	-0.059626	12116.4418
2	19.78	1.095	1.0974	0.12628	1.5427 10^{-07}	0.3656	26707.6731
3	37.12	1.0782	1.0808	0.12919	2.8407 10^{-08}	0.38185	2194.8651
4	71.82	1.0433	1.0457	0.10821	2.642 10^{-08}	0.34909	2075.6917
5	141.21	1.0074	1.0102	0.13481	3.6203 10^{-08}	0.35209	4105.6628
6	314.69	0.94607	0.95257	0.31492	6.5304 10^{-08}	0.62384	6320.5131
7	661.65	0.80831	0.81696	0.40537	4.0859 10^{-08}	1.1968	5373.1047
8	1008.61	0.73019	0.74343	0.64096	3.0672 10^{-08}	1.6505	9908.8073
9	1355.56	0.67202	0.68126	0.44292	1.5996 10^{-08}	1.3074	11720.1835
10	2049.48	0.58928	0.60797	0.88724	2.7133 10^{-08}	0.69814	19881.7705
11	3090.35	0.50864	0.51609	0.35127	2.5614 10^{-08}	1.0913	23789.1932
12	4131.23	0.46958	0.47897	0.44317	3.2642 10^{-08}	0.88611	58888.8122
13	5172.1	0.43682	0.44339	0.31484	1.8512 10^{-08}	0.8966	61432.1598
14	4131.23	0.43745	-	-	-	-	-
15	2049.48	0.44228	-	-	-	-	-
16	661.65	0.45992	-	-	-	-	-
17	2.43	0.52859	-	-	-	-	-

Table A.26. Results from analysis of test B1T3 using ANACONDA method.

	σ [kPa]	e_t [-]	e_{100} [-]	ϵ_{cr} [%]	c_v [m^2/s]	$c_{\alpha,\epsilon}$ [%]	M [kPa]
1	11.1	1.0985	1.0984	-0.0041558	3.8062 10^{-05}	-	14968.495
2	19.78	1.095	1.097	0.096787	3.6609 10^{-08}	-	12569.2845
3	37.12	1.0782	1.081	0.13498	1.031 10^{-08}	-	2276.156
4	71.82	1.0433	1.0489	0.26492	9.9228 10^{-09}	-	2267.8975
5	141.21	1.0074	1.013	0.26781	1.4396 10^{-08}	-	4064.7484
6	314.69	0.94607	0.95341	0.34944	2.3635 10^{-08}	-	6111.9593
7	661.65	0.80831	0.83116	1.0879	1.7117 10^{-08}	-	5959.9672
8	1008.61	0.73019	0.74703	0.8017	1.1602 10^{-08}	-	8660.5199
9	1355.56	0.67202	0.68289	0.51752	5.6685 10^{-09}	-	11359.8225
10	2049.48	0.58928	0.60661	0.82539	1.013 10^{-08}	-	19105.0613
11	3090.35	0.50864	0.52563	0.80881	1.0961 10^{-08}	-	26989.4676
12	4131.23	0.46958	0.48089	0.53834	1.1343 10^{-08}	-	48856.7367
13	5172.1	0.43682	0.44488	0.38364	6.6584 10^{-09}	-	60702.6774
14	4131.23	0.43745	-	-	-	-	-
15	2049.48	0.44228	-	-	-	-	-
16	661.65	0.45992	-	-	-	-	-
17	2.43	0.52859	-	-	-	-	-

Table A.27. Results from analysis of test B1T3 using Taylor method.

	σ [kPa]	e_t [-]	e_{100} [-]	ϵ_{cr} [%]	c_v [m^2/s]	$c_{\alpha,\epsilon}$ [%]	M [kPa]
1	11.1	1.0985	1.0985	0	$2.041\ 10^{-14}$	-	15857.1429
2	19.78	1.095	1.0964	0.07	$2.0378\ 10^{-14}$	-	8680
3	37.12	1.0782	1.0796	0.07	$2.0241\ 10^{-14}$	-	2167.5
4	71.82	1.0433	1.0471	0.18	$1.9845\ 10^{-14}$	-	2238.7097
5	141.21	1.0074	1.0099	0.12	$1.9171\ 10^{-14}$	-	3920.339
6	314.69	0.94607	0.94901	0.14	$1.8385\ 10^{-14}$	-	5982.069
7	661.65	0.80831	0.81776	0.45	$1.6963\ 10^{-14}$	-	5551.36
8	1008.61	0.73019	0.73607	0.28	$1.4838\ 10^{-14}$	-	8919.2802
9	1355.56	0.67202	0.68126	0.44	$1.3664\ 10^{-14}$	-	13293.1034
10	2049.48	0.58928	0.596	0.32	$1.265\ 10^{-14}$	-	17091.6256
11	3090.35	0.50864	0.51599	0.35	$1.1425\ 10^{-14}$	-	27319.4226
12	4131.23	0.46958	0.47294	0.16	$1.0413\ 10^{-14}$	-	50774.6341
13	5172.1	0.43682	0.44039	0.17	$9.8994\ 10^{-15}$	-	67152.9032
14	4131.23	0.43745	-	-	-	-	-
15	2049.48	0.44228	-	-	-	-	-
16	661.65	0.45992	-	-	-	-	-
17	2.43	0.52859	-	-	-	-	-

Table A.28. Results from analysis of test B1T3 using 24h method.

A.2.4 Test B1T4

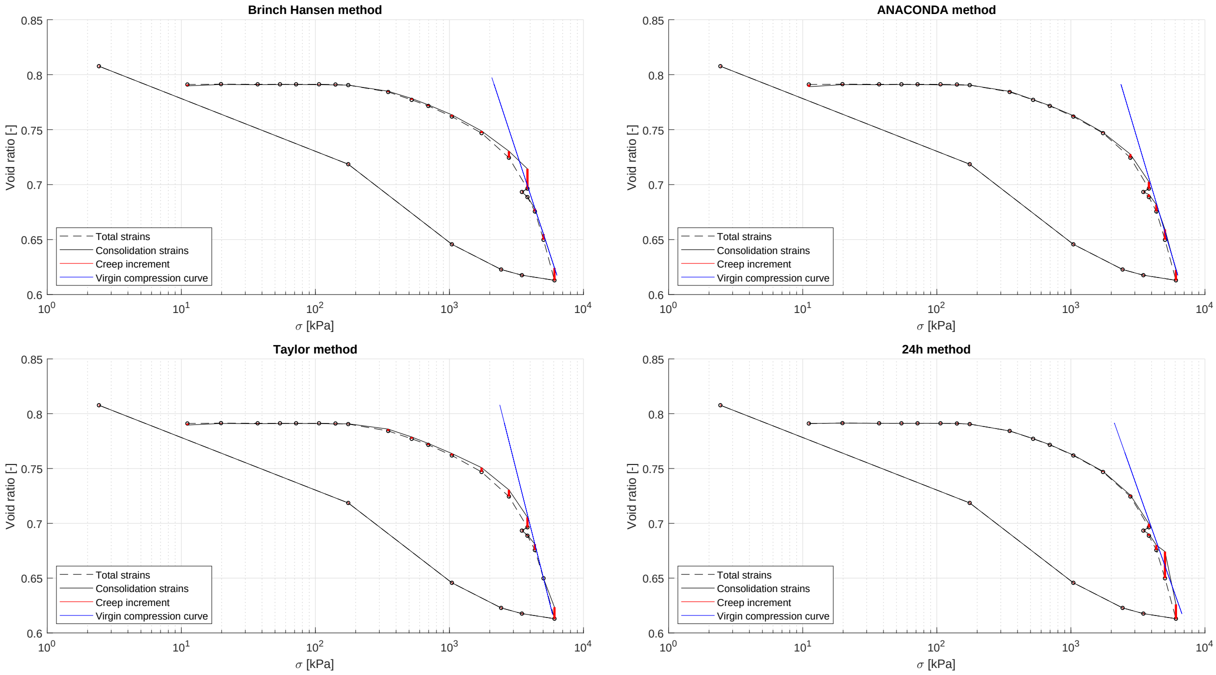

Figure A.8. Results from analysis of test B1T4.

	σ	e_t	e_{100}	ϵ_{cr}	c_v	$c_{\alpha,\epsilon}$	M
	$[kPa]$	[-]	[-]	[%]	$[m^2/s]$	[%]	[kPa]
1	11.1	0.79107	0.78982	1.0408 10^{-17}	0.00029201	5.8759 10^{-18}	110253.7301
2	19.78	0.79143	0.79107	1.3878 10^{-17}	0.00029242	6.7513 10^{-18}	-12400
3	37.12	0.79125	0.79089	-2.7756 10^{-17}	2.7949 10^{-05}	-2.1612 10^{-17}	173332.1162
4	54.47	0.79125	0.79107	-1.3878 10^{-17}	5.8803 10^{-05}	-1.2805 10^{-17}	-173254.3546
5	71.82	0.79125	0.79107	7.6328 10^{-17}	0.00029242	3.3584 10^{-17}	169071846.7455
6	106.52	0.79125	0.79089	-3.4694 10^{-17}	0.00013047	-1.396 10^{-17}	346246.7252
7	141.21	0.79107	0.79071	-2.0817 10^{-17}	2.6109 10^{-05}	-7.652 10^{-18}	347721.9016
8	175.91	0.79054	0.79054	-5.5511 10^{-17}	4.8865 10^{-05}	-3.074 10^{-17}	346885.6384
9	349.39	0.78427	0.78495	0.037263	7.9093 10^{-07}	0.022942	55611.5815
10	522.87	0.77711	0.77835	0.073677	5.8971 10^{-07}	0.038456	47051.9827
11	696.34	0.77156	0.77255	0.061566	3.4151 10^{-07}	0.040102	53486.14
12	1043.3	0.7619	0.7635	0.089939	5.807 10^{-07}	0.050629	68668.5892
13	1737.22	0.74686	0.74882	0.11239	4.5812 10^{-07}	0.061193	84571.1192
14	2778.09	0.72449	0.73044	0.33456	3.7007 10^{-07}	0.21126	101370.3904
15	3818.96	0.69638	0.71437	1.0051	3.9896 10^{-07}	0.6229	115985.2458
16	3472.01	0.69334	-	-	-	-	-
17	3818.96	0.68869	-	-	-	-	-
18	4339.4	0.67562	0.67823	0.135	1.528 10^{-08}	0.35678	87562.9162
19	5033.32	0.64984	0.65511	0.28688	1.5984 10^{-08}	0.69238	53729.9739
20	6074.19	0.61297	0.62419	0.62758	1.9989 10^{-08}	0.74572	60266.5822
21	3472.01	0.61762	-	-	-	-	-
22	2431.13	0.62281	-	-	-	-	-
23	1043.3	0.64573	-	-	-	-	-
24	175.91	0.71858	-	-	-	-	-
25	2.43	0.80772	-	-	-	-	-

Table A.29. Results from analysis of test B1T4 using Brinch Hansen method.

	σ [kPa]	e_t [-]	e_{100} [-]	ϵ_{cr} [%]	c_v [m^2/s]	$c_{\alpha,\epsilon}$ [%]	M [kPa]
1	11.1	0.79107	0.78905	-0.10904	$2.7263\ 10^{-05}$	-0.18227	20976.535
2	19.78	0.79143	0.79095	-0.023485	$3.664\ 10^{-05}$	-0.040433	-8207.0491
3	37.12	0.79125	0.79088	-0.016669	$1.5481\ 10^{-05}$	-0.025341	505163.7893
4	54.47	0.79125	0.79112	-0.006014	$1.4328\ 10^{-05}$	-0.0096312	-133108.0292
5	71.82	0.79125	0.79098	-0.014332	$1.4996\ 10^{-05}$	-0.025883	232430.3855
6	106.52	0.79125	0.79077	-0.024409	$1.2161\ 10^{-05}$	-0.040566	286259.4235
7	141.21	0.79107	0.79063	-0.024977	$2.8937\ 10^{-06}$	-0.051852	467692.0188
8	175.91	0.79054	0.79056	0.0038772	$9.2969\ 10^{-07}$	0.011464	873549.3273
9	349.39	0.78427	0.78481	0.030596	$6.168\ 10^{-07}$	0.066245	53936.3169
10	522.87	0.77711	0.77729	0.010621	$2.7798\ 10^{-07}$	0.033053	41301.0001
11	696.34	0.77156	0.77185	0.023306	$1.7639\ 10^{-07}$	0.068695	57059.3233
12	1043.3	0.7619	0.76272	0.049953	$3.4845\ 10^{-07}$	0.13172	68072.5105
13	1737.22	0.74686	0.74741	0.037389	$2.7369\ 10^{-07}$	0.1003	81120.3479
14	2778.09	0.72449	0.72768	0.18552	$1.6732\ 10^{-07}$	0.46125	94424.4223
15	3818.96	0.69638	0.70262	0.35093	$5.1401\ 10^{-08}$	1.063	74339.9158
16	3472.01	0.69334	-	-	-	-	-
17	3818.96	0.68869	-	-	-	-	-
18	4339.4	0.67562	0.68186	0.34682	$1.8155\ 10^{-08}$	1.1022	101608.3208
19	5033.32	0.64984	0.65927	0.52592	$1.3407\ 10^{-08}$	1.6834	54999.3612
20	6074.19	0.61297	0.62234	0.5252	$9.4862\ 10^{-09}$	1.5666	50438.0023
21	3472.01	0.61762	-	-	-	-	-
22	2431.13	0.62281	-	-	-	-	-
23	1043.3	0.64573	-	-	-	-	-
24	175.91	0.71858	-	-	-	-	-
25	2.43	0.80772	-	-	-	-	-

Table A.30. Results from analysis of test B1T4 using ANACONDA method.

	σ	e_t	e_{100}	ϵ_{cr}	c_v	$c_{\alpha,\epsilon}$	M
	$[kPa]$	[-]	[-]	[%]	$[m^2/s]$	[%]	[kPa]
1	11.1	0.79107	0.78964	-0.08	$6.2303\ 10^{-06}$	-	$-3.999196469105\ 10^{19}$
2	19.78	0.79143	0.79107	-0.02	$1.6777\ 10^{-05}$	-	-10850
3	37.12	0.79125	0.79089	-0.02	$1.5598\ 10^{-06}$	-	173400
4	54.47	0.79125	0.79103	-0.012454	$1.0466\ 10^{-05}$	-	-229937.6464
5	71.82	0.79125	0.79107	-0.010046	$1.1546\ 10^{-05}$	-	-720256.6101
6	106.52	0.79125	0.79103	-0.012222	$4.7193\ 10^{-05}$	-	1594114.3534
7	141.21	0.79107	0.79067	-0.02283	$2.1754\ 10^{-07}$	-	168336.7088
8	175.91	0.79054	0.79082	0.015949	$8.5889\ 10^{-06}$	-	-395253.5189
9	349.39	0.78427	0.78595	0.093822	$2.2958\ 10^{-07}$	-	63749.5632
10	522.87	0.77711	0.77873	0.090655	$1.1737\ 10^{-07}$	-	43029.3029
11	696.34	0.77156	0.77281	0.069918	$6.5288\ 10^{-08}$	-	52449.4978
12	1043.3	0.7619	0.76367	0.09887	$1.0044\ 10^{-07}$	-	67891.9081
13	1737.22	0.74686	0.7508	0.22012	$1.4452\ 10^{-07}$	-	96545.2072
14	2778.09	0.72449	0.73052	0.33711	$6.2394\ 10^{-08}$	-	91868.1348
15	3818.96	0.69638	0.70558	0.5136	$2.2114\ 10^{-08}$	-	74693.8427
16	3472.01	0.69334	-	-	-	-	-
17	3818.96	0.68869	-	-	-	-	-
18	4339.4	0.67562	0.681	0.3005	$6.7797\ 10^{-09}$	-	113647.6238
19	5033.32	0.64984	0.64973	-0.00611	$1.8287\ 10^{-09}$	-	39729.4948
20	6074.19	0.61297	0.62344	0.58515	$3.707\ 10^{-09}$	-	70868.2098
21	3472.01	0.61762	-	-	-	-	-
22	2431.13	0.62281	-	-	-	-	-
23	1043.3	0.64573	-	-	-	-	-
24	175.91	0.71858	-	-	-	-	-
25	2.43	0.80772	-	-	-	-	-

Table A.31. Results from analysis of test B1T4 using Taylor method.

	σ [kPa]	e_t [-]	e_{100} [-]	ϵ_{cr} [%]	c_v [m^2/s]	$c_{\alpha,\epsilon}$ [%]	M [kPa]
1	11.1	0.79107	0.79107	0	2.0423 10^{-14}	-	-18500
2	19.78	0.79143	0.79143	0	2.0446 10^{-14}	-	-43400
3	37.12	0.79125	0.79125	0	2.0451 10^{-14}	-	173400
4	54.47	0.79125	0.79125	0	2.0445 10^{-14}	-	Inf
5	71.82	0.79125	0.79125	0	2.0445 10^{-14}	-	Inf
6	106.52	0.79125	0.79125	0	2.0448 10^{-14}	-	Inf
7	141.21	0.79107	0.79107	0	2.0444 10^{-14}	-	346900
8	175.91	0.79054	0.79054	0	2.0438 10^{-14}	-	115666.6667
9	349.39	0.78427	0.78427	-2.7756 10^{-16}	2.0393 10^{-14}	-	49565.7143
10	522.87	0.77711	0.77729	0.01	2.025 10^{-14}	-	44482.0513
11	696.34	0.77156	0.77174	0.01	2.0093 10^{-14}	-	55958.0645
12	1043.3	0.7619	0.76226	0.02	1.9946 10^{-14}	-	65464.1509
13	1737.22	0.74686	0.7474	0.03	1.9699 10^{-14}	-	83604.8193
14	2778.09	0.72449	0.72574	0.07	1.9327 10^{-14}	-	86022.314
15	3818.96	0.69638	0.69961	0.18	1.8813 10^{-14}	-	71292.4658
16	3472.01	0.69334	-	-	-	-	-
17	3818.96	0.68869	-	-	-	-	-
18	4339.4	0.67562	0.68009	0.25	1.8125 10^{-14}	-	91305.2632
19	5033.32	0.64984	0.67419	1.3602	1.7883 10^{-14}	-	210420.6624
20	6074.19	0.61297	0.62604	0.73	1.722 10^{-14}	-	38690.8518
21	3472.01	0.61762	-	-	-	-	-
22	2431.13	0.62281	-	-	-	-	-
23	1043.3	0.64573	-	-	-	-	-
24	175.91	0.71858	-	-	-	-	-
25	2.43	0.80772	-	-	-	-	-

Table A.32. Results from analysis of test B1T4 using 24h method.

A.3 Borehole B2

A.3.1 Test B2T1

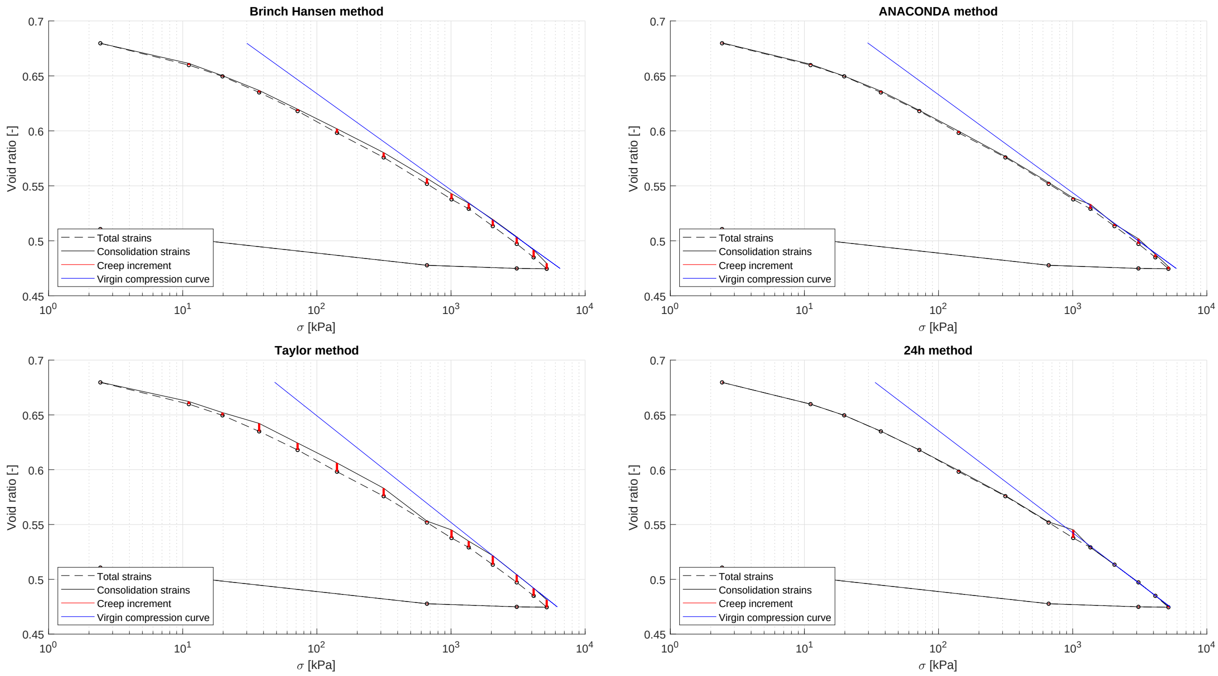

Figure A.9. Results from analysis of test B2T1.

	σ [kPa]	e_t [-]	e_{100} [-]	ϵ_{cr} [%]	c_v [m^2/s]	$c_{\alpha,\epsilon}$ [%]	M [kPa]
1	2.43	0.67966	0.67966	0	7.0205 10^{-05}	0	5493.9578
2	11.1	0.65984	0.66138	0.096627	2.9238 10^{-06}	0.066439	796.6775
3	19.78	0.64959	0.65017	0.0362	2.3038 10^{-06}	0.025129	1301.4173
4	37.12	0.63498	0.63676	0.089861	7.6167 10^{-06}	0.045076	2170.8676
5	71.82	0.61801	0.6197	0.096634	9.5391 10^{-06}	0.045076	3418.0554
6	141.21	0.59818	0.60187	0.19042	1.0939 10^{-05}	0.07241	6536.843
7	314.69	0.57584	0.58023	0.27041	1.5101 10^{-05}	0.10319	13471.7448
8	661.65	0.55182	0.55681	0.3013	1.3318 10^{-05}	0.11752	24888.9648
9	1008.61	0.5377	0.54285	0.30065	1.3907 10^{-05}	0.10861	41746.4368
10	1355.56	0.52914	0.53413	0.29717	2.4384 10^{-05}	0.11664	66812.6806
11	2049.48	0.51334	0.51942	0.36423	3.2341 10^{-05}	0.13523	79275.0436
12	3090.35	0.49722	0.50362	0.38292	5.2015 10^{-05}	0.13288	110691.2818
13	4131.23	0.48495	0.49164	0.38126	4.8169 10^{-05}	0.13288	145919.7681
14	5172.1	0.47454	0.47953	0.30147	4.932 10^{-06}	0.12575	144441.9615
15	3090.35	0.47487	-	-	-	-	-
16	661.65	0.47773	-	-	-	-	-
17	2.43	0.51066	-	-	-	-	-

Table A.33. Results from analysis of test B2T1 using Brinch Hansen method.

	σ [kPa]	e_t [-]	e_{100} [-]	ϵ_{cr} [%]	c_v [m^2/s]	$c_{\alpha,\epsilon}$ [%]	M [kPa]
1	2.43	0.67966	0.68008	0.024839	$2.6798\ 10^{-07}$	0.070085	-51395.2688
2	11.1	0.65984	0.66057	0.045633	$1.9324\ 10^{-06}$	0.11903	746.5557
3	19.78	0.64959	0.64983	0.016234	$1.4378\ 10^{-06}$	0.037605	1358.3971
4	37.12	0.63498	0.63616	0.064439	$2.895\ 10^{-06}$	0.18603	2130.3892
5	71.82	0.61801	0.61865	0.038565	$4.0253\ 10^{-06}$	0.10083	3328.8137
6	141.21	0.59818	0.5997	0.07013	$5.6297\ 10^{-06}$	0.18446	6152.8971
7	314.69	0.57584	0.57667	0.052439	$8.3002\ 10^{-06}$	0.14389	12653.9193
8	661.65	0.55182	0.55304	0.07578	$1.4488\ 10^{-05}$	0.23127	24665.8318
9	1008.61	0.5377	0.53895	0.065336	$3.7615\ 10^{-06}$	0.20088	41365.9992
10	1355.56	0.52914	0.5332	0.24596	$3.1203\ 10^{-05}$	0.14149	101467.9598
11	2049.48	0.51334	0.51511	0.10766	$1.1296\ 10^{-05}$	0.25519	64425.3649
12	3090.35	0.49722	0.50188	0.2774	$3.7383\ 10^{-05}$	0.13308	132238.9992
13	4131.23	0.48495	0.48763	0.15901	$1.1858\ 10^{-05}$	0.46165	122697.1838
14	5172.1	0.47454	0.47649	0.10942	$2.1152\ 10^{-06}$	0.25794	157012.0248
15	3090.35	0.47487	-	-	-	-	-
16	661.65	0.47773	-	-	-	-	-
17	2.43	0.51066	-	-	-	-	-

Table A.34. Results from analysis of test B2T1 using ANACONDA method.

	σ [kPa]	e_t [-]	e_{100} [-]	ϵ_{cr} [%]	c_v [m^2/s]	$c_{\alpha,\epsilon}$ [%]	M [kPa]
1	2.43	0.67966	0.67983	0.0099544	$2.306\ 10^{-05}$	-	24189.6505
2	11.1	0.65984	0.66222	0.14179	$6.3742\ 10^{-07}$	-	827.1573
3	19.78	0.64959	0.65209	0.14872	$7.9192\ 10^{-07}$	-	1439.3143
4	37.12	0.63498	0.64225	0.43281	$3.776\ 10^{-06}$	-	2959.4896
5	71.82	0.61801	0.62438	0.37911	$3.2102\ 10^{-06}$	-	3262.2034
6	141.21	0.59818	0.60617	0.47525	$4.3221\ 10^{-06}$	-	6402.1141
7	314.69	0.57584	0.58312	0.43363	$4.5473\ 10^{-06}$	-	12647.7899
8	661.65	0.55182	0.55312	0.077418	$7.0833\ 10^{-08}$	-	19424.3803
9	1008.61	0.5377	0.54504	0.43685	$7.3448\ 10^{-06}$	-	72198.3626
10	1355.56	0.52914	0.5348	0.33742	$1.9871\ 10^{-05}$	-	56930.3128
11	2049.48	0.51334	0.52158	0.49014	$1.6924\ 10^{-05}$	-	88140.6357
12	3090.35	0.49722	0.50428	0.42037	$9.4261\ 10^{-06}$	-	101077.7518
13	4131.23	0.48495	0.49196	0.41717	$1.561\ 10^{-05}$	-	141965.187
14	5172.1	0.47454	0.48123	0.39834	$9.7827\ 10^{-06}$	-	162932.5682
15	3090.35	0.47487	-	-	-	-	-
16	661.65	0.47773	-	-	-	-	-
17	2.43	0.51066	-	-	-	-	-

Table A.35. Results from analysis of test B2T1 using Taylor method.

	σ	e_t	e_{100}	ϵ_{cr}	c_v	$c_{\alpha,\epsilon}$	M
	$[kPa]$	[-]	[-]	[%]	$[m^2/s]$	[%]	[kPa]
1	2.43	0.67966	0.67966	0	$8.1659\ 10^{-14}$	-	12150
2	11.1	0.65984	0.65984	0	$8.1165\ 10^{-14}$	-	734.7458
3	19.78	0.64959	0.64959	0	$7.9473\ 10^{-14}$	-	1422.9508
4	37.12	0.63498	0.63514	0.01	$7.8405\ 10^{-14}$	-	2016.2791
5	71.82	0.61801	0.61801	$4.4409\ 10^{-16}$	$7.6959\ 10^{-14}$	-	3401.9608
6	141.21	0.59818	0.59919	0.06	$7.5311\ 10^{-14}$	-	6195.5357
7	314.69	0.57584	0.57634	0.03	$7.3402\ 10^{-14}$	-	12755.8824
8	661.65	0.55182	0.55232	0.03	$7.1319\ 10^{-14}$	-	24262.9371
9	1008.61	0.5377	0.54518	0.445	$6.952\ 10^{-14}$	-	81637.6471
10	1355.56	0.52914	0.52914	0	$6.8239\ 10^{-14}$	-	36329.8429
11	2049.48	0.51334	0.51334	$-5.3291\ 10^{-15}$	$6.7309\ 10^{-14}$	-	73821.2766
12	3090.35	0.49722	0.49722	0	$6.5915\ 10^{-14}$	-	108423.9583
13	4131.23	0.48495	0.48495	0	$6.4608\ 10^{-14}$	-	142586.3014
14	5172.1	0.47454	0.47554	0.06	$6.3603\ 10^{-14}$	-	185869.6429
15	3090.35	0.47487	-	-	-	-	-
16	661.65	0.47773	-	-	-	-	-
17	2.43	0.51066	-	-	-	-	-

Table A.36. Results from analysis of test B2T1 using 24h method.

A.4 Borehole B3

A.4.1 Test B3T1

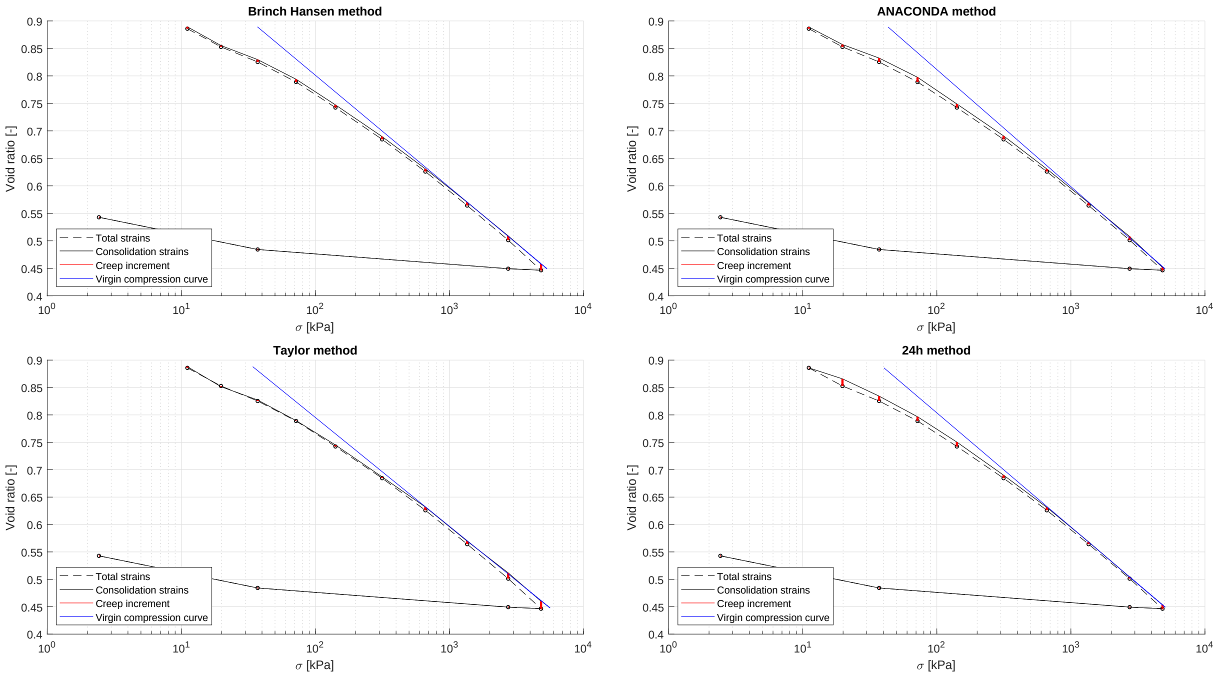

Figure A.10. Results from analysis of test B3T1.

	σ $[kPa]$	e_t [-]	e_{100} [-]	ϵ_{cr} [%]	c_v $[m^2/s]$	$c_{\alpha,\epsilon}$ [%]	M [kPa]
1	11.1	0.88584	0.88924	-2.0817 10^{-17}	7.3386 10^{-05}	-8.4657 10^{-18}	27712.6178
2	19.78	0.85277	0.85516	0.12676	1.0114 10^{-08}	0.27367	481.3974
3	37.12	0.82536	0.82963	0.21548	1.3933 10^{-08}	0.46968	1283.2658
4	71.82	0.78889	0.79387	0.2639	1.768 10^{-08}	0.60145	1834.3956
5	141.21	0.74239	0.74727	0.25802	2.0695 10^{-08}	0.38822	2813.9682
6	314.69	0.68456	0.68957	0.26499	2.6351 10^{-08}	0.39868	5682.2695
7	661.65	0.62597	0.63086	0.2587	2.791 10^{-08}	0.31017	11169.6671
8	1355.56	0.56416	0.57015	0.31671	3.6112 10^{-08}	0.36463	21603.7154
9	2743.4	0.50123	0.50894	0.40824	5.638 10^{-08}	0.44469	42854.8461
10	4825.14	0.44642	0.4577	0.61764	6.1341 10^{-08}	0.35047	76780.0833
11	2743.4	0.44925	-	-	-	-	-
12	37.12	0.48422	-	-	-	-	-
13	2.43	0.54281	-	-	-	-	-

Table A.37. Results from analysis of test B3T1 using Brinch Hansen method.

	σ [kPa]	e_t [-]	e_{100} [-]	ϵ_{cr} [%]	c_v [m^2/s]	$c_{\alpha,\epsilon}$ [%]	M [kPa]
1	11.1	0.88584	0.88892	0.16076	$2.3529\ 10^{-06}$	0.44529	19378.4064
2	19.78	0.85277	0.85706	0.23547	$7.5629\ 10^{-09}$	0.64563	514.945
3	37.12	0.82536	0.83241	0.36946	$1.0132\ 10^{-08}$	0.98425	1329.7141
4	71.82	0.78889	0.79744	0.46145	$1.3713\ 10^{-08}$	1.3191	1875.1413
5	141.21	0.74239	0.74885	0.3452	$1.4066\ 10^{-08}$	0.88367	2699.0485
6	314.69	0.68456	0.69088	0.34194	$1.9148\ 10^{-08}$	0.89504	5655.7867
7	661.65	0.62597	0.63064	0.25261	$1.8927\ 10^{-08}$	0.67851	10885.8712
8	1355.56	0.56416	0.56926	0.27436	$2.215\ 10^{-08}$	0.74208	21368.1946
9	2743.4	0.50123	0.50778	0.35442	$3.1018\ 10^{-08}$	0.95243	42665.2384
10	4825.14	0.44642	0.45154	0.27162	$2.6026\ 10^{-08}$	0.58388	69956.9332
11	2743.4	0.44925	-	-	-	-	-
12	37.12	0.48422	-	-	-	-	-
13	2.43	0.54281	-	-	-	-	-

Table A.38. Results from analysis of test B3T1 using ANACONDA method.

	σ [kPa]	e_t [-]	e_{100} [-]	ϵ_{cr} [%]	c_v [m^2/s]	$c_{\alpha,\epsilon}$ [%]	M [kPa]
1	11.1	0.88584	0.88805	0.11683	$1.5483\ 10^{-07}$	-	9461.1528
2	19.78	0.85277	0.85148	-0.068151	$1.5534\ 10^{-09}$	-	448.5823
3	37.12	0.82536	0.82719	0.096577	$2.512\ 10^{-09}$	-	1349.1312
4	71.82	0.78889	0.78958	0.036883	$2.9087\ 10^{-09}$	-	1743.9868
5	141.21	0.74239	0.7451	0.14324	$3.7145\ 10^{-09}$	-	2948.1934
6	314.69	0.68456	0.68688	0.12284	$4.6484\ 10^{-09}$	-	5631.7364
7	661.65	0.62597	0.63192	0.31489	$6.3847\ 10^{-09}$	-	11931.4474
8	1355.56	0.56416	0.56964	0.28988	$6.9988\ 10^{-09}$	-	21059.4273
9	2743.4	0.50123	0.51176	0.55741	$1.2095\ 10^{-08}$	-	45317.619
10	4825.14	0.44642	0.45995	0.71607	$1.3138\ 10^{-08}$	-	75938.8409
11	2743.4	0.44925	-	-	-	-	-
12	37.12	0.48422	-	-	-	-	-
13	2.43	0.54281	-	-	-	-	-

Table A.39. Results from analysis of test B3T1 using Taylor method.

	σ $[kPa]$	e_t [-]	e_{100} [-]	ϵ_{cr} [%]	c_v $[m^2/s]$	$c_{\alpha,\epsilon}$ [%]	M [kPa]
1	11.1	0.88584	0.88584	0	$2.0394\ 10^{-14}$	-	5045.4545
2	19.78	0.85277	0.86581	0.69	$2.0219\ 10^{-14}$	-	818.8679
3	37.12	0.82536	0.83425	0.47	$1.9522\ 10^{-14}$	-	1038.3234
4	71.82	0.78889	0.79663	0.41	$1.8894\ 10^{-14}$	-	1743.7186
5	141.21	0.74239	0.75033	0.42	$1.8094\ 10^{-14}$	-	2832.2449
6	314.69	0.68456	0.69004	0.29	$1.7092\ 10^{-14}$	-	5438.2445
7	661.65	0.62597	0.63126	0.28	$1.5964\ 10^{-14}$	-	11156.2701
8	1355.56	0.56416	0.56832	0.22	$1.4841\ 10^{-14}$	-	20838.1381
9	2743.4	0.50123	0.50387	0.14	$1.3716\ 10^{-14}$	-	40699.1202
10	4825.14	0.44642	0.4536	0.38	$1.2678\ 10^{-14}$	-	78260.9023
11	2743.4	0.44925	-	-	-	-	-
12	37.12	0.48422	-	-	-	-	-
13	2.43	0.54281	-	-	-	-	-

Table A.40. Results from analysis of test B3T1 using 24h method.

A.4.2 Test B3T2

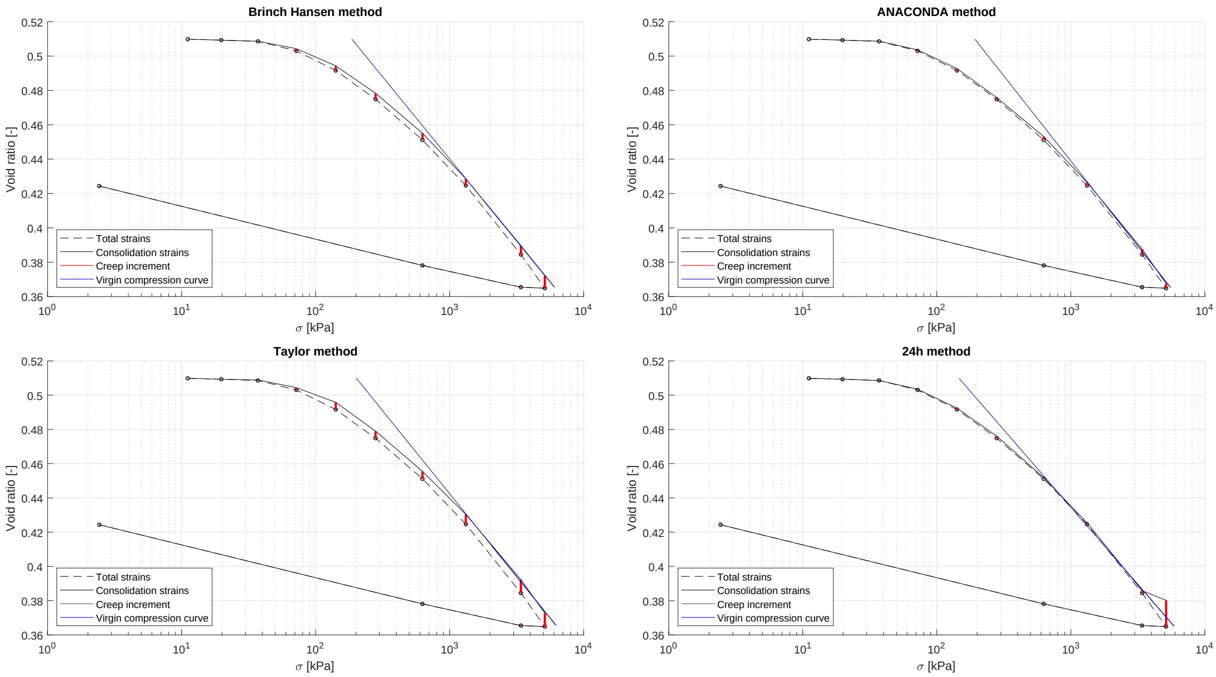

Figure A.11. Results from analysis of test B3T2.

	σ	e_t	e_{100}	ϵ_{cr}	c_v	$c_{\alpha,\epsilon}$	M
	$[kPa]$	[-]	[-]	[%]	$[m^2/s]$	[%]	[kPa]
1	11.1	0.50982	0.50985	-1.7347 10^{-18}	4.7925 10^{-05}	-1.2576 10^{-18}	47422.4345
2	19.78	0.50929	0.50924	-1.3878 10^{-17}	2.9499 10^{-06}	-5.9948 10^{-18}	21695.8477
3	37.12	0.50857	0.50864	5.5511 10^{-17}	1.4423 10^{-06}	3.19 10^{-17}	43359.8829
4	71.82	0.50302	0.50432	0.085818	2.9585 10^{-07}	0.048593	12124.5305
5	141.21	0.49162	0.49433	0.1795	7.2423 10^{-07}	0.087713	10492.3236
6	279.99	0.47486	0.47837	0.23226	1.6282 10^{-06}	0.091981	13126.7264
7	626.95	0.45119	0.45513	0.259	1.7382 10^{-06}	0.11474	22546.3567
8	1320.87	0.42464	0.42854	0.25838	1.99 10^{-07}	0.18962	39408.4626
9	3402.61	0.38444	0.38965	0.34499	2.8174 10^{-07}	0.2107	80816.7494
10	5137.4	0.36486	0.3721	0.47963	2.139 10^{-07}	0.28468	149311.3256
11	3402.61	0.36546	-	-	-	-	-
12	626.95	0.37813	-	-	-	-	-
13	2.43	0.42434	-	-	-	-	-

Table A.41. Results from analysis of test B3T2 using Brinch Hansen method.

	σ [kPa]	e_t [-]	e_{100} [-]	ϵ_{cr} [%]	c_v [m^2/s]	$c_{\alpha,\epsilon}$ [%]	M [kPa]
1	11.1	0.50982	0.50985	-9.2437 10^{-05}	1.3506 10^{-05}	-0.00022586	113091.2821
2	19.78	0.50929	0.5093	0.0041581	5.9691 10^{-06}	0.010277	23604.7636
3	37.12	0.50857	0.50869	0.0078429	9.7168 10^{-07}	0.019286	43009.2928
4	71.82	0.50302	0.50363	0.037714	1.0707 10^{-07}	0.11556	10351.8827
5	141.21	0.49162	0.49276	0.075317	1.9311 10^{-07}	0.1839	9642.5882
6	279.99	0.47486	0.47583	0.067341	1.7042 10^{-07}	0.17665	12380.2142
7	626.95	0.45119	0.45318	0.13162	2.5047 10^{-07}	0.30336	23124.6654
8	1320.87	0.42464	0.42654	0.12253	9.1378 10^{-08}	0.33041	39341.4511
9	3402.61	0.38444	0.38767	0.21577	1.7949 10^{-07}	0.28893	80872.9576
10	5137.4	0.36486	0.36758	0.17746	5.4945 10^{-08}	0.53879	130374.6488
11	3402.61	0.36546	-	-	-	-	-
12	626.95	0.37813	-	-	-	-	-
13	2.43	0.42434	-	-	-	-	-

Table A.42. Results from analysis of test B3T2 using ANACONDA method.

	σ [kPa]	e_t [-]	e_{100} [-]	ϵ_{cr} [%]	c_v [m^2/s]	$c_{\alpha,\epsilon}$ [%]	M [kPa]
1	11.1	0.50982	0.50988	0.0043	1.0947 10^{-05}	-	58742.2232
2	19.78	0.50929	0.50926	-0.0018526	6.5367 10^{-07}	-	21092.1868
3	37.12	0.50857	0.50887	0.019907	5.1607 10^{-07}	-	66082.5734
4	71.82	0.50302	0.50437	0.08883	4.8736 10^{-08}	-	11641.2507
5	141.21	0.49162	0.49582	0.27767	1.2941 10^{-07}	-	12256.1728
6	279.99	0.47486	0.47901	0.27437	4.1284 10^{-08}	-	12465.6819
7	626.95	0.45119	0.45552	0.28689	4.0509 10^{-08}	-	22305.721
8	1320.87	0.42464	0.43035	0.37788	5.1041 10^{-08}	-	41626.5639
9	3402.61	0.38444	0.39231	0.52111	6.6127 10^{-08}	-	82648.8712
10	5137.4	0.36486	0.37268	0.51773	4.849 10^{-08}	-	133406.7866
11	3402.61	0.36546	-	-	-	-	-
12	626.95	0.37813	-	-	-	-	-
13	2.43	0.42434	-	-	-	-	-

Table A.43. Results from analysis of test B3T2 using Taylor method.

	σ [kPa]	e_t [-]	e_{100} [-]	ϵ_{cr} [%]	c_v [m^2/s]	$c_{\alpha,\epsilon}$ [%]	M [kPa]
1	11.1	0.50982	0.50982	0	$2.0415\ 10^{-14}$	-	92500
2	19.78	0.50929	0.50929	0	$2.0408\ 10^{-14}$	-	24800
3	37.12	0.50857	0.50857	0	$2.0393\ 10^{-14}$	-	36125
4	71.82	0.50302	0.50348	0.03	$2.0343\ 10^{-14}$	-	10296.7359
5	141.21	0.49162	0.49244	0.054	$2.0159\ 10^{-14}$	-	9492.4761
6	279.99	0.47486	0.47606	0.079	$1.982\ 10^{-14}$	-	12790.7834
7	626.95	0.45119	0.45187	0.045	$1.9325\ 10^{-14}$	-	21657.9276
8	1320.87	0.42464	0.42549	0.056	$1.8691\ 10^{-14}$	-	39720.664
9	3402.61	0.38444	0.3858	0.09	$1.7928\ 10^{-14}$	-	79213.8508
10	5137.4	0.36486	0.38022	1.017	$1.7136\ 10^{-14}$	-	468862.1622
11	3402.61	0.36546	-	-	-	-	-
12	626.95	0.37813	-	-	-	-	-
13	2.43	0.42434	-	-	-	-	-

Table A.44. Results from analysis of test B3T2 using 24h method.

Results from pre-consolidation stress analysis B

In this appendix the data obtained from the pre-consolidation stress analysis is shown, distributed along the different tests. Each test shows the analysis outcome in an initial picture and numerical information in the corresponding data table.

B.1 Superficial samples

B.1.1 Test B0T1

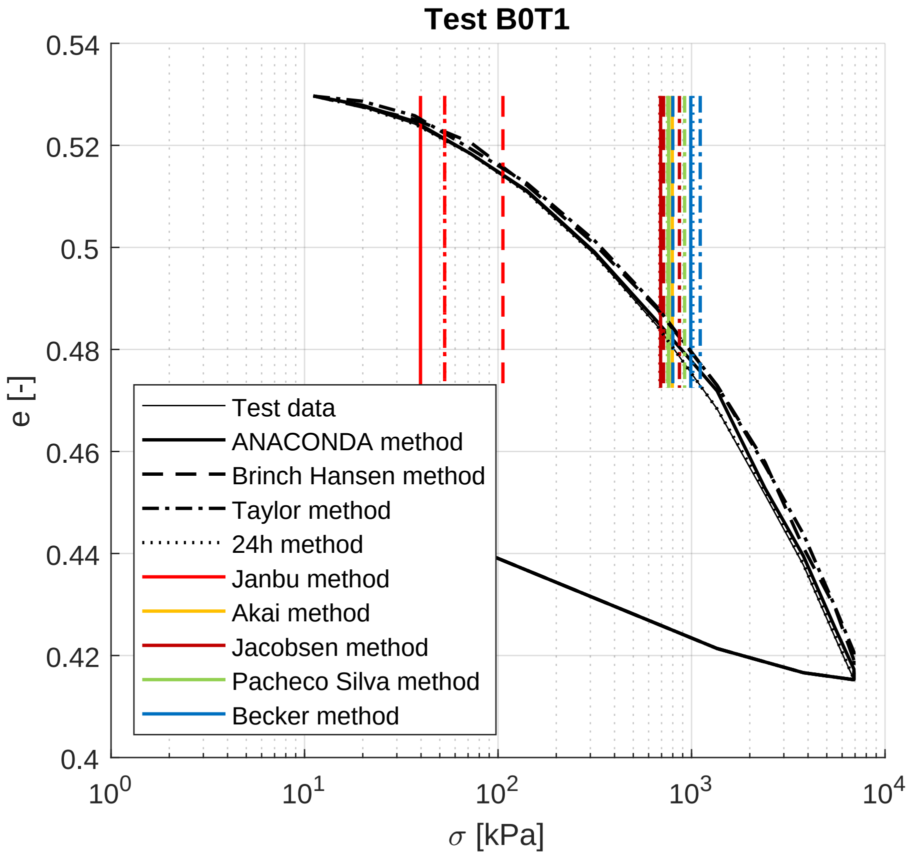

Figure B.1. Results from analysis of test B0T1.

	ANACONDA	Brinch Hansen	Taylor	24h
Janbu	39.7418	105.9783	52.9891	52.9891
Akai	795.2496	795.2496	-	-
Jacobsen	692.0945	716.6307	865.9227	686.3572
Pacheco Silva	761.6542	753.5999	920.9272	750.9162
Becker	991.0898	800.0573	1109.0196	1016.6067

Table B.1. Results from analysis of test B0T1.

B.1.2 Test B0T2

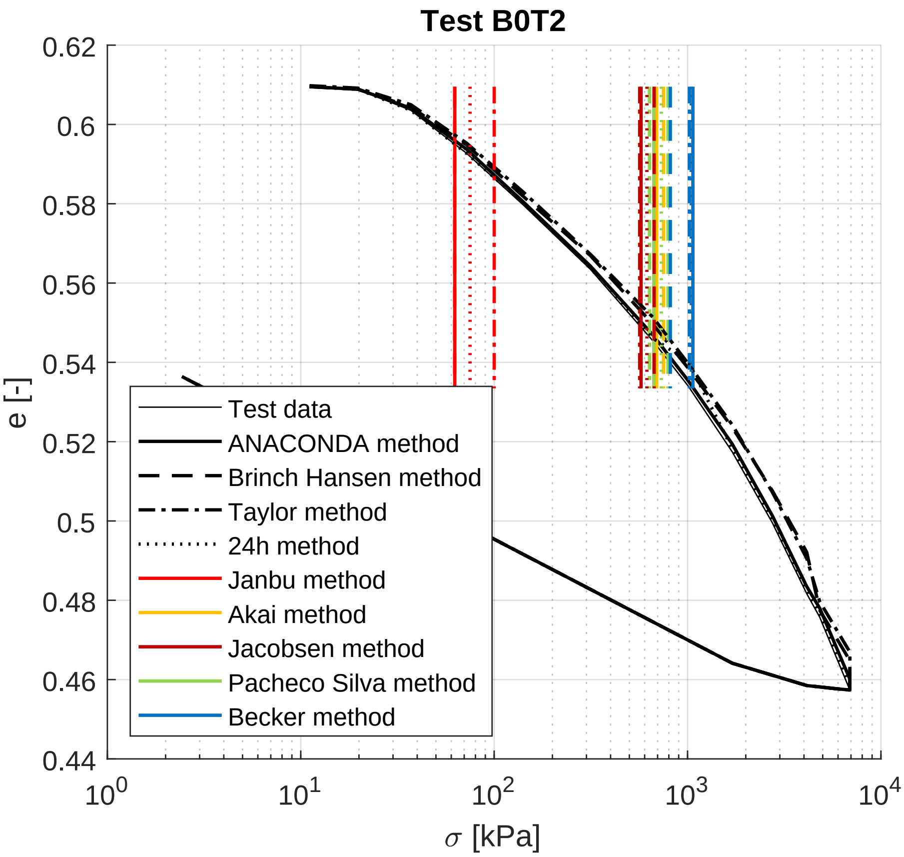

Figure B.2. Results from analysis of test B0T2.

	ANACONDA	Brinch Hansen	Taylor	24h
Janbu	62.5375	62.5375	100.06	75.045
Akai	692.1617	751.0691	-	-
Jacobsen	574.907	672.075	565.3855	616.2889
Pacheco Silva	669.6512	792.4933	635.3117	731.692
Becker	1065.5717	814.5399	1022.1239	1045.5719

Table B.2. Results from analysis of test B0T2.

B.1.3 Test B0T3

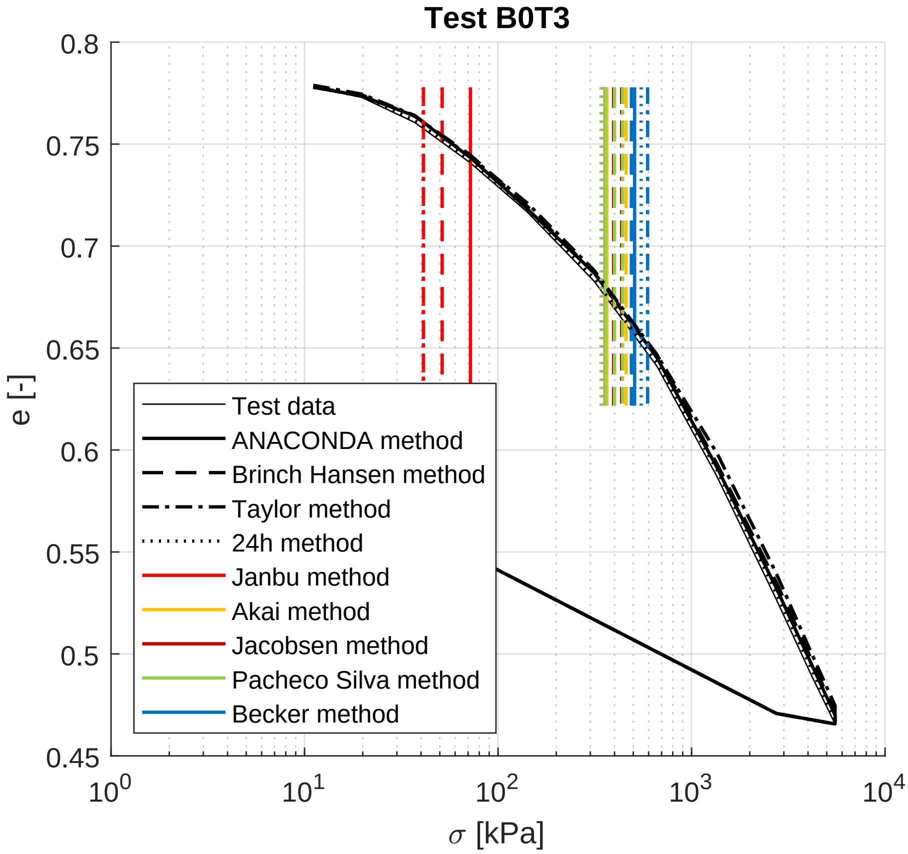

Figure B.3. Results from analysis of test B0T3.

	ANACONDA	Brinch Hansen	Taylor	24h
Janbu	72.0171	51.4408	41.1526	41.1526
Akai	364.7993	458.941	-	-
Jacobsen	357.6219	395.5857	435.3807	341.7527
Pacheco Silva	358.6536	400.2232	440.4637	340.7586
Becker	507.9677	488.6879	592.7987	549.2815

Table B.3. Results from analysis of test B0T3.

B.1.4 Test B0T4

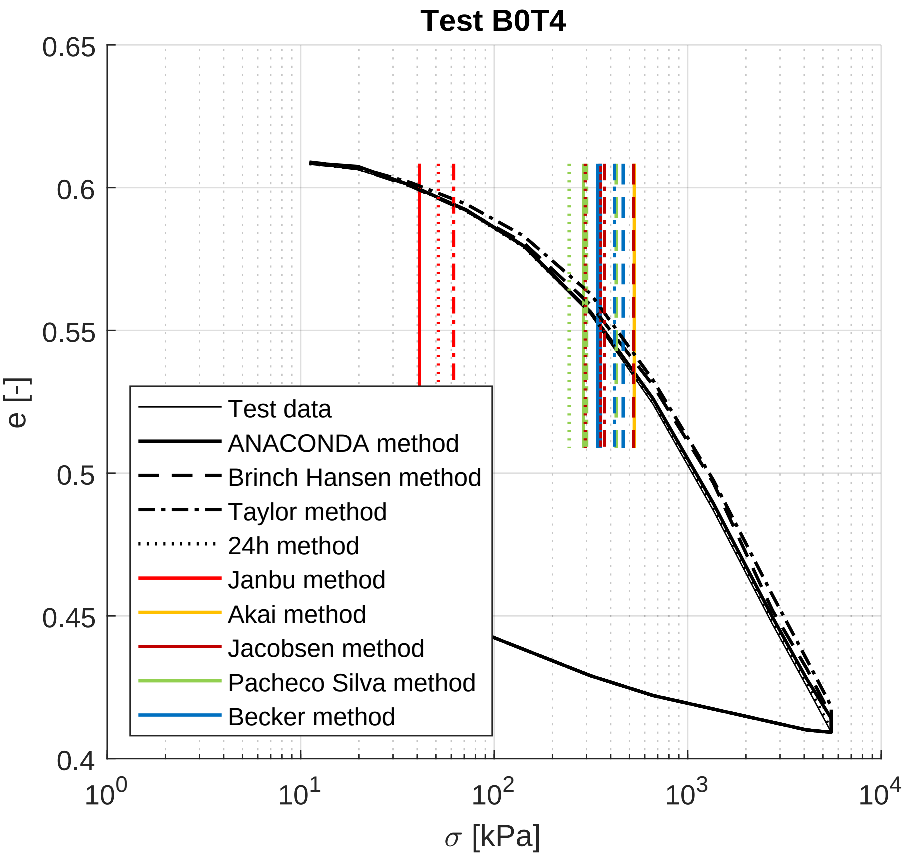

Figure B.4. Results from analysis of test B0T4.

	ANACONDA	Brinch Hansen	Taylor	24h
Janbu	41.1526	41.1526	61.7289	51.4408
Akai	529.5473	529.5473	-	-
Jacobsen	353.2273	525.7127	371.2938	295.6102
Pacheco Silva	289.3813	426.8897	300.5724	243.918
Becker	342.7124	463.8996	418.179	353.1785

Table B.4. Results from analysis of test B0T4.

B.2 Borehole B1

B.2.1 Test B1T1

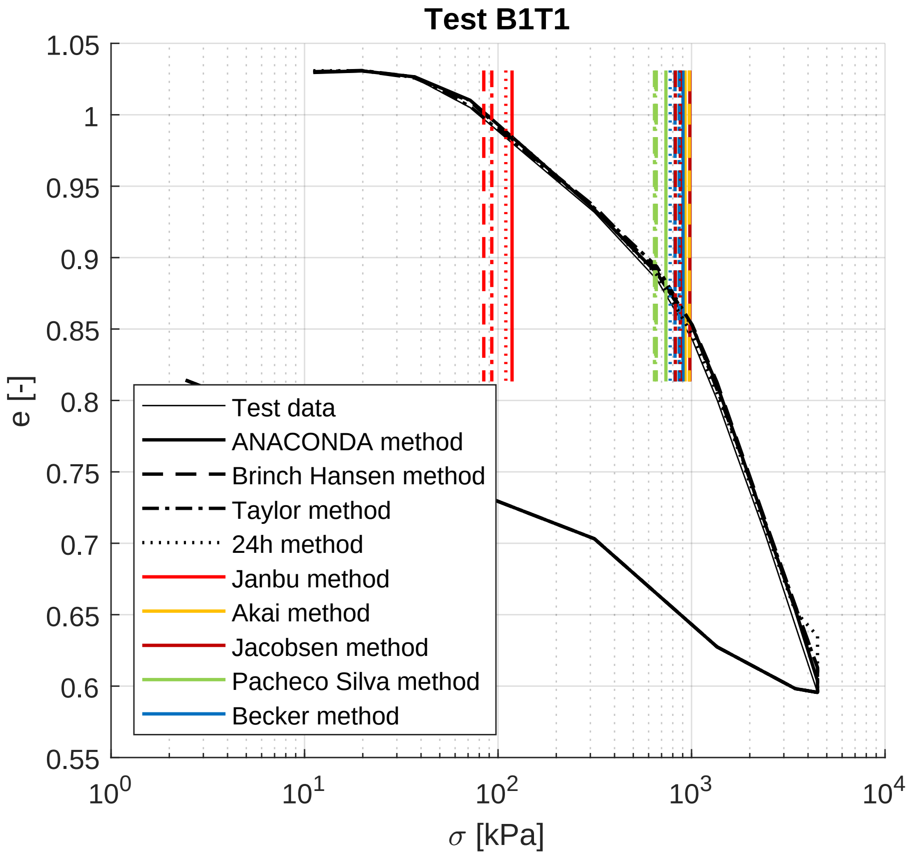

Figure B.5. Results from analysis of test B1T1.

	ANACONDA	Brinch Hansen	Taylor	24h
Janbu	118.1416	84.3869	92.8256	109.703
Akai	926.1907	973.9325	-	-
Jacobsen	979.9363	875.4441	824.785	876.909
Pacheco Silva	737.1826	657.2093	643.4362	651.6103
Becker	903.2651	821.5094	863.0574	775.4938

Table B.5. Results from analysis of test B1T1.

B.2.2 Test B1T2

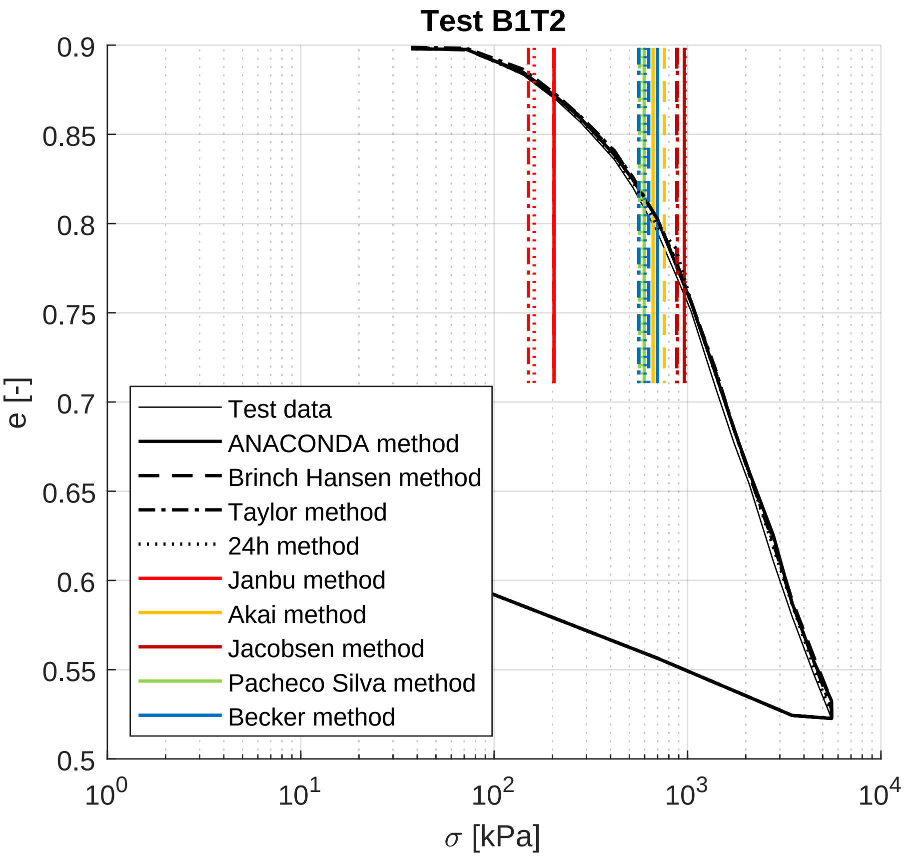

Figure B.6. Results from analysis of test B1T2.

	ANACONDA	Brinch Hansen	Taylor	24h
Janbu	203.9083	203.9083	150.2482	160.9802
Akai	663.1343	757.8678	-	-
Jacobsen	962.2361	879.2283	885.698	969.6824
Pacheco Silva	596.6541	564.1611	561.038	587.2482
Becker	698.0784	629.6653	559.5971	603.1828

Table B.6. Results from analysis of test B1T2.

B.2.3 Test B1T3

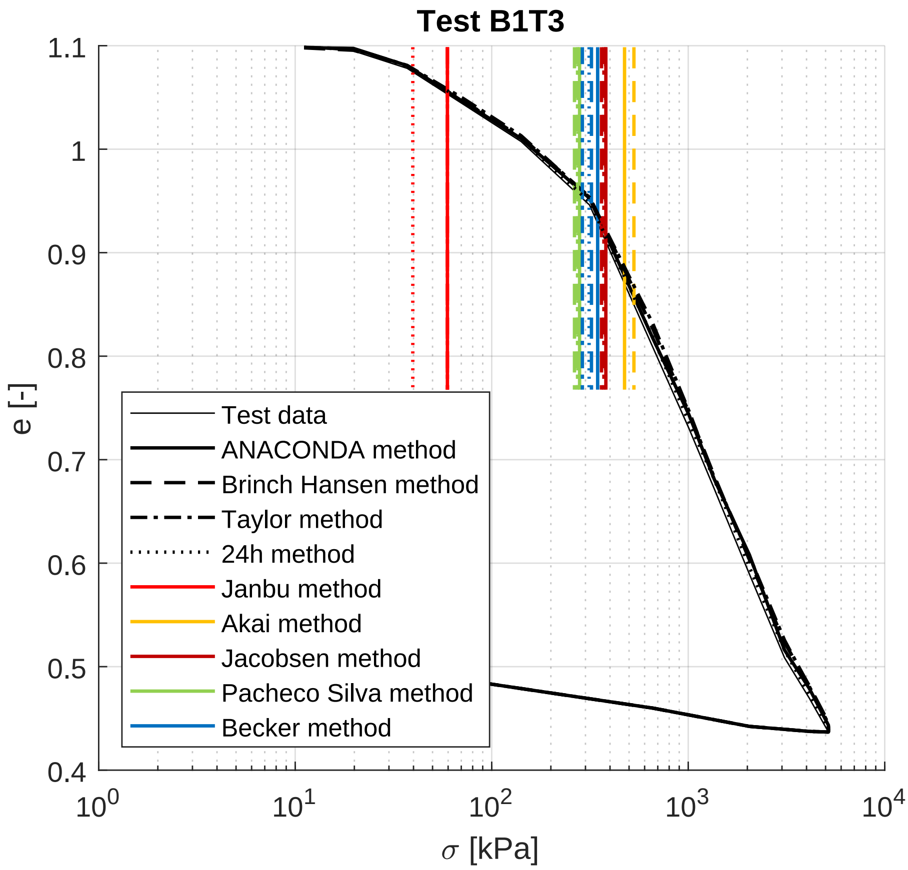

Figure B.7. Results from analysis of test B1T3.

	ANACONDA	Brinch Hansen	Taylor	24h
Janbu	59.5096	59.5096	59.5096	39.673
Akai	474.2011	529.3407	-	-
Jacobsen	380.9373	362.0164	372.2703	379.9607
Pacheco Silva	280.0657	263.799	273.401	274.5654
Becker	346.0824	321.8233	289.3057	313.0487

Table B.7. Results from analysis of test B1T3.

B.3 Borehole B2

B.3.1 Test B2T1

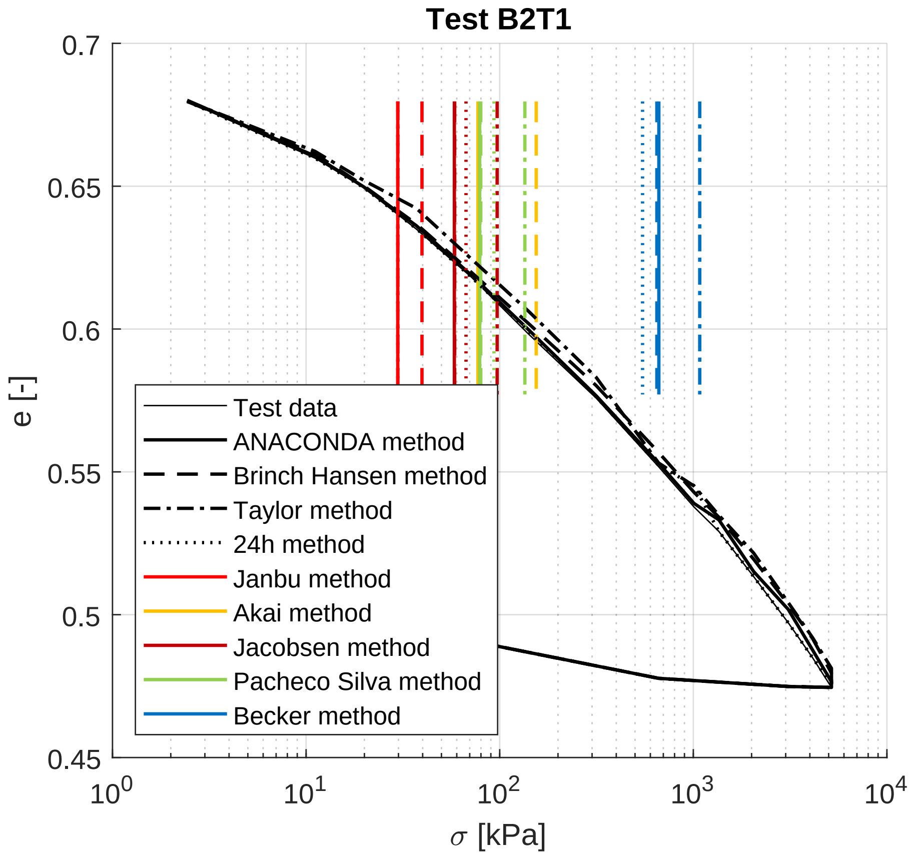

Figure B.8. Results from analysis of test B2T1.

	ANACONDA	Brinch Hansen	Taylor	24h
Janbu	29.7548	39.673	29.7548	29.7548
Akai	77.1955	154.391	-	-
Jacobsen	58.3055	58.5496	97.0018	66.9725
Pacheco Silva	78.8233	79.8341	134.8629	93.3967
Becker	663.6969	648.1864	1079.38	546.8507

Table B.8. Results from analysis of test B2T1.

B.4 Borehole B3

B.4.1 Test B3T1

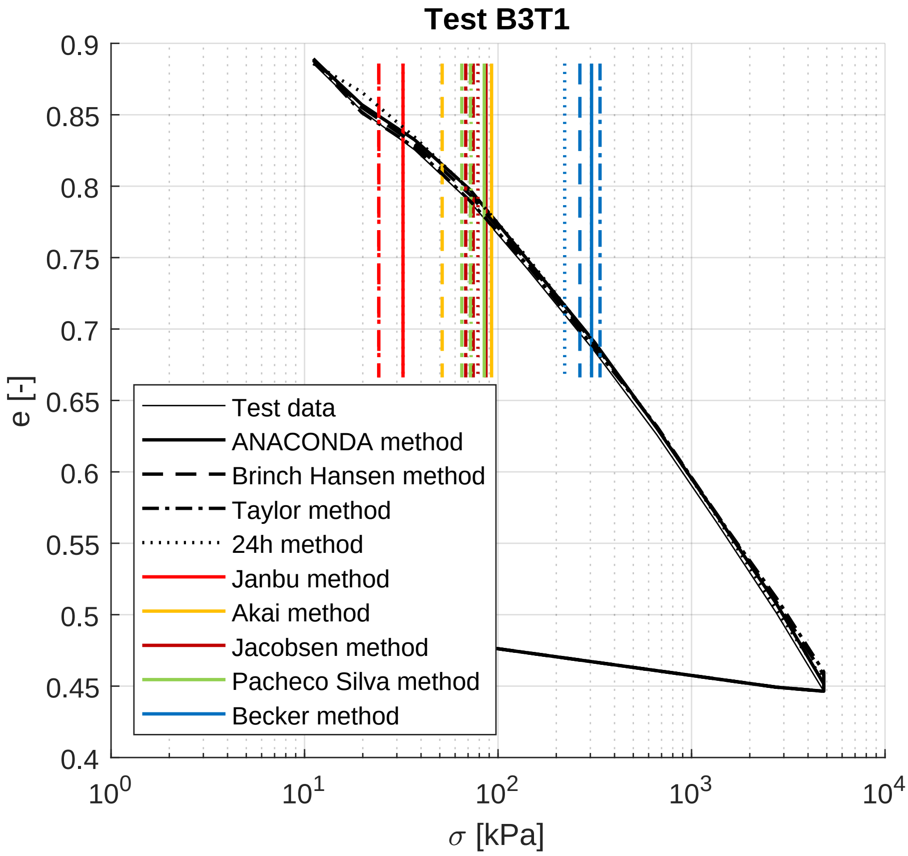

Figure B.9. Results from analysis of test B3T1.

	ANACONDA	Brinch Hansen	Taylor	24h
Janbu	32.2752	24.2064	24.2064	32.2752
Akai	92.5933	51.4407	-	-
Jacobsen	86.6258	74.4188	68.0711	78.6912
Pacheco Silva	84.8922	71.9963	64.974	72.5897
Becker	304.3044	264.8253	336.5617	221.0131

Table B.9. Results from analysis of test B3T1.

B.4.2 Test B3T2

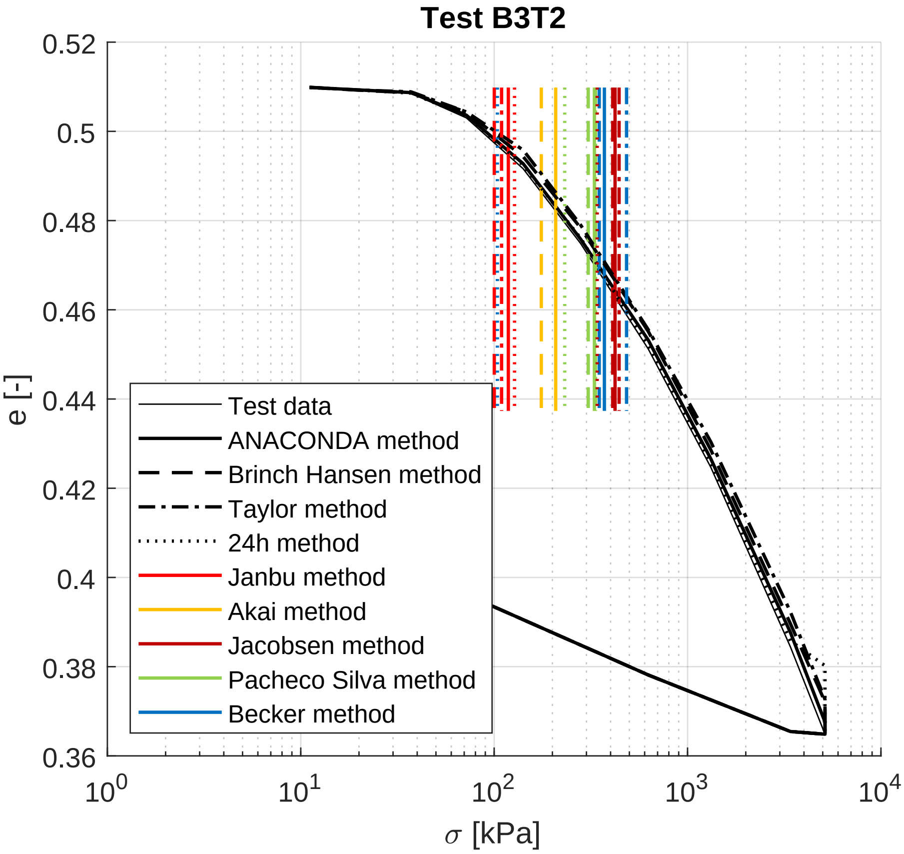

Figure B.10. Results from analysis of test B3T2.

	ANACONDA	Brinch Hansen	Taylor	24h
Janbu	118.3583	100.1494	109.2539	127.4628
Akai	208.1249	175.2631	-	-
Jacobsen	421.8309	410.1121	442.5828	341.0203
Pacheco Silva	329.9592	306.4641	333.9477	231.6915
Becker	371.5149	349.4696	483.7921	103.8953

Table B.10. Results from analysis of test B3T2.